



Search for heavy neutral Higgs bosons produced in association with b -quarks and decaying into b -quarks at $\sqrt{s} = 13$ TeV with the ATLAS detector

The ATLAS Collaboration

A search for heavy neutral Higgs bosons produced in association with one or two b -quarks and decaying to b -quark pairs is presented using 27.8 fb^{-1} of $\sqrt{s} = 13$ TeV proton-proton collision data recorded by the ATLAS detector at the Large Hadron Collider during 2015 and 2016. No evidence of a signal is found. Upper limits on the heavy neutral Higgs boson production cross section times its branching ratio to $b\bar{b}$ are set, ranging from 4.0 to 0.6 pb at 95% confidence level over a Higgs boson mass range of 450 to 1400 GeV. Results are interpreted within the two-Higgs-doublet model and the minimal supersymmetric Standard Model.

Contents

1	Introduction	3
2	The ATLAS detector	4
3	Data and simulated samples	5
3.1	Data	5
3.2	Signal model and background simulations	5
4	Object reconstruction and event selection	8
5	Statistical analysis	12
6	Systematic uncertainties	15
6.1	Systematic uncertainties of the background model	15
6.2	Experimental systematic uncertainties of the signal	16
6.3	Theoretical systematic uncertainties of the signal	17
7	Results	17
7.1	Cross section limits	17
7.2	Model interpretations	18
8	Conclusions	25

1 Introduction

The measured properties of the Higgs boson discovered at the Large Hadron Collider (LHC) by the ATLAS and CMS collaborations [1, 2] with a mass of 125 GeV are consistent with those of the scalar particle that emerges from the mechanism of electroweak symmetry breaking in the Standard Model (SM) with its one doublet of complex scalar fields [3–6]. Alternative electroweak symmetry breaking models which contain a scalar particle with properties similar to the SM Higgs boson remain viable, however. A simple, well-studied and well-motivated extension of the mechanism of electroweak symmetry breaking in the SM is the two-Higgs-doublet model (2HDM), which contains two doublets of complex scalar fields [7, 8]. In the 2HDM there are, assuming negligible CP -violating effects, two CP -even scalar bosons, h and H which satisfy the mass relation $m_h < m_H$, one CP -odd pseudoscalar boson, A , and two electrically charged scalar bosons, H^\pm . The most general renormalizable, electroweak gauge invariant 2HDM contains tree-level Higgs-boson-mediated flavor-changing neutral currents [8] that are in conflict with experimental limits. When symmetries are imposed to naturally suppress flavor changing neutral currents, four model types emerge, distinguished from one another by their Yukawa couplings, as summarized in Table 1 for h , H , and A .

The agreement of SM predictions with measurements of the 125 GeV Higgs boson, assumed in this paper to be the scalar boson h in the 2HDM, is reducing the 2HDM parameter space toward the alignment limit of $\cos(\beta - \alpha) \approx 0$, where $\tan \beta$ is the ratio of the vacuum expectation values of the two scalar doublets and α is the mixing angle of the two CP -even scalar bosons [9]. In the alignment limit, decays of the H and A bosons into gauge boson pairs W^+W^- and ZZ are heavily suppressed, and the fermion coupling pattern simplifies to that of Table 1. The suppression of H/A couplings to W^+W^- and ZZ , along with ATLAS and CMS limits on new particle production, implies that searches for the heavy neutral Higgs bosons of the 2HDM mainly rely on their couplings to third-generation fermions.

Table 1: Tree-level fermion couplings of the 2HDM h , H , and A bosons for model types I, II, X (or lepton-specific), and Y (or flipped). Here U , D , and E refer to up-type quarks, down-type quarks, and charged leptons, respectively, $t_\beta \equiv \tan \beta$ is the ratio of the vacuum expectation values of the two scalar doublets, and $\epsilon = \cos(\beta - \alpha)$ where α is the mixing angle of the two CP -even scalar bosons [9]. The couplings are normalized to the SM Higgs boson couplings $h_{\text{SM}}\bar{U}U$, $h_{\text{SM}}\bar{D}D$, and $h_{\text{SM}}\bar{E}E$ and are given in the alignment limit $\cos(\beta - \alpha) \approx 0$ where the couplings of the light scalar boson h are close to SM expectations.

	$h\bar{U}U$	$h\bar{D}D$	$h\bar{E}E$	$H\bar{U}U$	$H\bar{D}D$	$H\bar{E}E$	$iA\bar{U}\gamma_5 U$	$iA\bar{D}\gamma_5 D$	$iA\bar{E}\gamma_5 E$
I	$1 + \frac{\epsilon}{t_\beta}$	$1 + \frac{\epsilon}{t_\beta}$	$1 + \frac{\epsilon}{t_\beta}$	$-(\frac{1}{t_\beta} - \epsilon)$	$-(\frac{1}{t_\beta} - \epsilon)$	$-(\frac{1}{t_\beta} - \epsilon)$	$-\frac{1}{t_\beta}$	$\frac{1}{t_\beta}$	$\frac{1}{t_\beta}$
II	$1 + \frac{\epsilon}{t_\beta}$	$1 - \epsilon t_\beta$	$1 - \epsilon t_\beta$	$-(\frac{1}{t_\beta} - \epsilon)$	$t_\beta + \epsilon$	$t_\beta + \epsilon$	$-\frac{1}{t_\beta}$	$-t_\beta$	$-t_\beta$
X	$1 + \frac{\epsilon}{t_\beta}$	$1 + \frac{\epsilon}{t_\beta}$	$1 - \epsilon t_\beta$	$-(\frac{1}{t_\beta} - \epsilon)$	$-(\frac{1}{t_\beta} - \epsilon)$	$t_\beta + \epsilon$	$-\frac{1}{t_\beta}$	$\frac{1}{t_\beta}$	$-t_\beta$
Y	$1 + \frac{\epsilon}{t_\beta}$	$1 - \epsilon t_\beta$	$1 + \frac{\epsilon}{t_\beta}$	$-(\frac{1}{t_\beta} - \epsilon)$	$t_\beta + \epsilon$	$-(\frac{1}{t_\beta} - \epsilon)$	$-\frac{1}{t_\beta}$	$-t_\beta$	$\frac{1}{t_\beta}$

The Higgs sector of the minimal supersymmetric Standard Model (MSSM) is a Type II 2HDM, which has motivated searches for heavy neutral Higgs bosons at LEP [10] and the LHC [11, 12]. These searches use decays of heavy neutral Higgs bosons into $\tau^+\tau^-$, and are sensitive to Type II and lepton-specific 2HDMs. They are not sensitive to flipped 2HDMs at large $\tan \beta$, however, and they do not cover the entire MSSM Type II 2HDM parameter space since radiative corrections can significantly increase the ratio of the $b\bar{b}$ and $\tau^+\tau^-$ partial widths beyond the tree-level value of $3m_b^2/m_\tau^2$ [13].

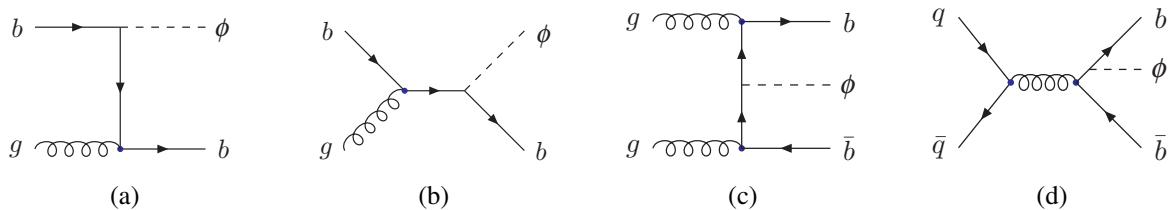


Figure 1: Feynman diagrams for some of the leading-order processes for the production of a heavy neutral Higgs boson (denoted here by ϕ) in association with one or two b -quarks in the 5-flavor scheme. Diagrams (a) and (b) are unique to the 5-flavor scheme, while diagrams (c) and (d) appear in both the 4- and 5-flavor schemes.

This paper presents a search for heavy neutral Higgs bosons produced in association with one or two b -quarks and decaying into b -quark pairs using 27.8 fb^{-1} of $\sqrt{s} = 13 \text{ TeV}$ proton-proton collision data recorded by the ATLAS detector at the LHC during 2015 and 2016. The search is sensitive to the Type II and flipped scenarios of the 2HDM in the regime where $\tan\beta \gg 1$. In the 5-flavor scheme (5FS) [14], processes such as those shown in Figure 1 lead to the production of heavy neutral Higgs bosons in association with one b -quark (Figures 1(a) and 1(b)) or two b -quarks (Figures 1(c) and 1(d)). In practice, the optimal balance between signal efficiency and background rejection is achieved by requiring that signal events contain at least three b -quark-initiated jets. The search is performed for neutral Higgs bosons in the mass range 450–1400 GeV. A similar search was performed by the CMS Collaboration for the mass range 300–1300 GeV [15].

The kinematic distributions for the production and decay of H and A bosons are nearly identical, and therefore this search is insensitive to the CP properties of the two heavy neutral Higgs bosons of the 2HDM. The ϕ boson is used in this paper to represent the CP-even H boson, the CP-odd A boson, or a Higgs boson mass eigenstate with an arbitrary mixture of CP-even and CP-odd eigenstates.

2 The ATLAS detector

The ATLAS experiment [16] at the LHC is a multipurpose particle detector with a forward-backward symmetric cylindrical geometry and a near 4π coverage in solid angle.¹ It consists of an inner tracking detector surrounded by a thin superconducting solenoid providing a 2 T axial magnetic field, electromagnetic and hadronic calorimeters, and a muon spectrometer. The inner tracking detector covers the pseudorapidity range $|\eta| < 2.5$. It consists of silicon pixel, silicon microstrip, and transition radiation tracking detectors. The innermost pixel layer [17, 18] was added before the start of collisions in 2015. Lead/liquid-argon (LAr) sampling calorimeters provide electromagnetic (EM) energy measurements with high granularity. A hadronic steel/scintillator-tile calorimeter covers the central pseudorapidity range $|\eta| < 1.7$. The endcap and forward regions are instrumented with LAr calorimeters for both the EM and hadronic energy measurements up to $|\eta| = 4.9$. The muon spectrometer surrounds the calorimeters and features three large air-core toroid superconducting magnets with eight coils each. The field integral of the toroids ranges from 2.0 to 6.0 T·m across most of the detector. It includes a system of precision tracking chambers and fast

¹ ATLAS uses a right-handed coordinate system with its origin at the nominal interaction point (IP) in the center of the detector and the z -axis coinciding with the axis of the beam pipe. The x -axis points from the IP toward the center of the LHC ring, and the y -axis points upward. Cylindrical coordinates (r, ϕ) are used in the transverse plane, ϕ being the azimuthal angle around the z -axis. The pseudorapidity is defined in terms of the polar angle θ as $\eta = -\ln \tan(\theta/2)$. Angular distance is defined as $\Delta R \equiv \sqrt{(\Delta\eta)^2 + (\Delta\phi)^2}$. Transverse momentum and energy are defined as $p_T = p \sin \theta$ and $E_T = E \sin \theta$, respectively.

detectors for triggering. A two-level trigger system [19] consisting of the level-1 (L1) trigger, implemented in hardware, and the software-based high-level trigger (HLT), selects interesting events. The L1 trigger uses a subset of detector information to reduce the event rate to a design value of at most 100 kHz. The HLT, which can run offline reconstruction algorithms and is used in this analysis for the triggering of b -quark-initiated jets, reduces the event rate to about 1 kHz.

3 Data and simulated samples

3.1 Data

Proton-proton (pp) collision data recorded by the ATLAS detector at the LHC during 2015 and 2016 at a center-of-mass energy of $\sqrt{s} = 13$ TeV were used for the analysis described in this paper. For this data, it is required that the LHC operate with stable beam conditions and that all relevant detector systems be fully functional. The data, corresponding to integrated luminosities of $3.2 \pm 0.1 \text{ fb}^{-1}$ and $24.5 \pm 0.5 \text{ fb}^{-1}$ for 2015 and 2016, respectively, were collected using a combination of HLT triggers, which employ algorithms [19] to identify jets containing b -hadrons (resulting in ‘ b -tagged jets’). Maximum-likelihood algorithms were utilized in 2015, while the offline multivariate classifier MV2c20 [20, 21] was used in 2016. Events were recorded if they passed the L1 single-jet trigger with a transverse energy (E_T) threshold of $E_T = 100$ GeV, and if the HLT identifies either one b -tagged jet with $E_T > 225$ GeV or two b -tagged jets with different thresholds of $E_T = 150$ GeV and $E_T = 50$ GeV. For the single (double) b -tagged jet trigger, the operating points correspond to a b -quark identification efficiency of 79% (72%) in 2015 and 60% (60%) in 2016, as measured with a reference $t\bar{t}$ sample. An inefficiency in the online vertex reconstruction affected a fraction of the data collected during 2016; events from these running periods were not included in the analysis. The efficiency of the combination of the two HLT b -jet triggers is shown in Figure 2 for events passing the final selection described in Section 4 and ranges from 80% for $m_\phi = 450$ GeV to 95% for $m_\phi > 700$ GeV. The efficiency of the double b -tagged jet trigger falls with increasing m_ϕ since the per-jet b -tagging efficiency is dropping with increasing E_T . The single b -tagged jet trigger efficiency increases with increasing m_ϕ because a larger fraction of the second leading jets satisfy $E_T > 225$ GeV.

3.2 Signal model and background simulations

Signal events for the subprocesses $bg \rightarrow b\phi + 0, 1 \text{ jet}$, $gg \rightarrow b\bar{b}\phi$, and $q\bar{q} \rightarrow b\bar{b}\phi$ with $\phi \rightarrow b\bar{b}$ were generated at leading order (LO) for seventeen m_ϕ values from 450 to 1400 GeV using the SHERPA 2.2.0 [22] Monte Carlo (MC) program in the 5FS with the NNPDF30NNLO [23] set of parton distribution functions (PDF). In order to determine the total width at each value of m_ϕ , a specific MSSM scenario tailored for large values of the branching ratio (\mathcal{B}) for $\phi \rightarrow b\bar{b}$ was used in which $\tan\beta = 20$, the higgsino mass parameter $\mu = -800$ GeV, the generic soft-SUSY-breaking mass parameter $M_{\text{SUSY}} = 1000$ GeV, the trilinear Higgs–top–squark coupling $A_t = 2000$ GeV, the $SU(2)$ gaugino mass parameter $M_2 = 800$ GeV, and the $SU(3)$ gaugino mass parameter $M_3 = 1600$ GeV. These parameters suppress ϕ boson decays into top quark pairs, top-squark pairs, and electroweak gauginos, while decays into pairs of b -quarks are enhanced through MSSM radiative corrections [13]. The FeynHiggs program [24] was used to calculate the branching ratios and the cross sections shown in Table 2, where the branching ratio $\mathcal{B}(\phi \rightarrow b\bar{b}) > 85\%$ for all m_ϕ values up to 1400 GeV. Given the large values for $\mathcal{B}(\phi \rightarrow b\bar{b})$ in Table 2, the total widths derived from this set of MSSM parameters also represent the typical total widths in the flipped scenario

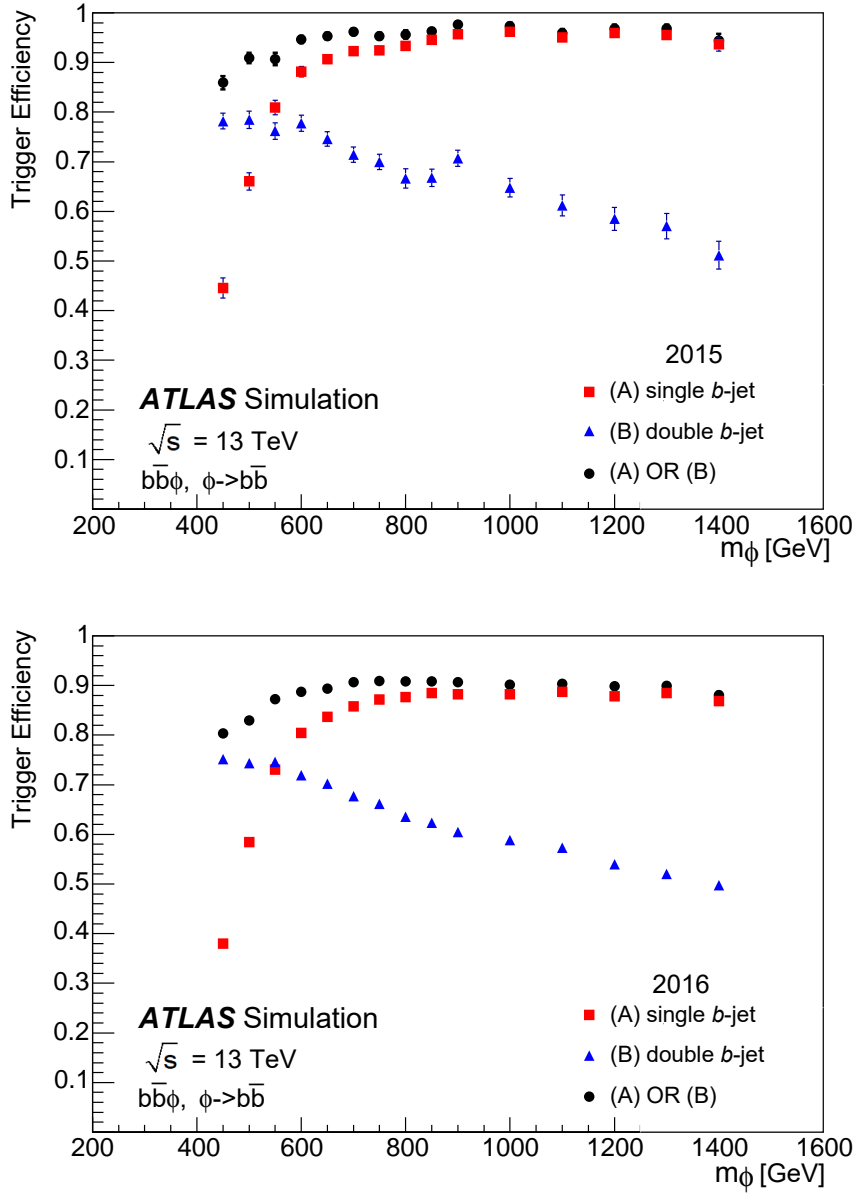


Figure 2: Efficiency of the single b -tagged jet and double b -tagged jet triggers and their logical OR for signal events fulfilling the final selection of Section 4 as a function of the neutral Higgs boson mass for datasets collected in 2015 (top) and 2016 (bottom). The operating points for the single (double) b -tagged jet triggers correspond to b -quark identification efficiencies of 79% (72%) in 2015 and 60% (60%) in 2016.

of the 2HDM in the alignment limit for the same m_ϕ and $\tan\beta$. The values of the total width in Table 2 are much smaller than the 10%–15% experimental $b\bar{b}$ mass resolution. Although several decay modes are present in this MSSM scenario, only the decay mode $\phi \rightarrow b\bar{b}$ is simulated in the generated signal samples. Since they are ignored in the analysis, additional ϕ decay modes that happen to leak into the $\phi \rightarrow b\bar{b}$ acceptance will only make any limits on $\phi \rightarrow b\bar{b}$ more conservative.

Table 2: Mass, total width, and branching ratios of the ϕ boson of the MSSM scenario used for signal event generation where $\tan\beta = 20$, $\mu = -800$ GeV, $M_{\text{SUSY}} = 1000$ GeV, $A_t = 2000$ GeV, $M_2 = 800$ GeV, and $M_3 = 1600$ GeV. The $pp \rightarrow b\bar{b}\phi$ cross section at $\sqrt{s} = 13$ TeV is also shown. Full simulation samples of 300,000 events were produced for each of the mass points. The FeynHiggs program [24] was used to calculate the branching ratios and the cross sections for $pp \rightarrow b\bar{b}\phi$ at $\sqrt{s} = 13$ TeV.

m_ϕ [GeV]	$\Gamma_\phi(\text{total})$ [GeV]	$\mathcal{B}(\phi \rightarrow b\bar{b})$	$\mathcal{B}(\phi \rightarrow \tau^+\tau^-)$	$\mathcal{B}(\phi \rightarrow t\bar{t})$	$\sigma(b\bar{b}\phi)$ [fb]
450	4.7	0.91	0.07	0.02	2792
500	5.1	0.91	0.07	0.02	1694
550	5.5	0.91	0.07	0.02	1066
600	5.9	0.91	0.07	0.02	693
650	6.3	0.91	0.07	0.02	463
700	6.7	0.91	0.07	0.02	317
750	7.1	0.90	0.07	0.02	222
800	7.5	0.90	0.08	0.02	158
850	7.9	0.90	0.08	0.02	115
900	8.3	0.90	0.08	0.02	85
950	8.7	0.90	0.08	0.02	66
1000	9.1	0.90	0.08	0.02	48
1100	9.8	0.90	0.08	0.02	29
1200	10.7	0.89	0.08	0.02	18
1300	11.6	0.87	0.08	0.02	12
1350	12.1	0.87	0.08	0.02	10
1400	12.5	0.86	0.08	0.02	8

The ATLAS detector response to the generated signal events was modeled using the ATLAS full simulation software [25] based on GEANT4 [26]. The impact of multiple pp collisions in the same or nearby bunch crossings (pileup) was simulated by overlaying minimum-bias events on each generated event. The minimum-bias events were generated with PYTHIA 8.186 [27], using the A2 set of tuned parameters [28] and the MSTW2008LO PDF sets [29]. Finally, events were processed using the same reconstruction software as in data.

The background estimate is data-driven, as described in Section 5. Background MC samples (referred to later as ‘multijet MC samples’) served as a guide in developing the background model and consist of a SHERPA 2.1.1 simulation of multiple b -jets, a next-to-leading-order (NLO) POWHEG [30–32] simulation of $t\bar{t}$ production interfaced to PYTHIA 6.428 [33], and an LO MADGRAPH [34] simulation of the subprocess $jj \rightarrow Z jj$, $Z \rightarrow b\bar{b}$ interfaced to PYTHIA 8.205, where j represents a gluon or a u, d, s, c quark/antiquark. The full ATLAS detector simulation software was used for $t\bar{t}$ production. A fast ATLAS detector simulation in which the calorimeter response is parametrized [25, 35] was used for the multiple b -jets and $jj \rightarrow Z jj$ samples.

The dominant background comes from the production of multiple b -jets. In the SHERPA 2.1.1 simulation of multiple b -jets all 2 \rightarrow 2, 3, 4 hard subprocesses with at least one b -quark in the final state were generated at LO. The c - and b -quarks masses are set to their running Yukawa values to properly simulate gluon splitting into heavy quarks.

4 Object reconstruction and event selection

Primary vertex candidates [36] are reconstructed using tracks in the inner detector, and the vertex with the highest sum of the squared transverse momenta of all associated tracks is selected as the hard-scatter primary vertex. Jets are reconstructed using the anti- k_r algorithm [37] with radius parameter $R = 0.4$ from topological clusters of energy in the calorimeter calibrated at the electromagnetic scale [38]. Jets are then calibrated using correction factors derived from simulation and data [39]. In order to suppress jets arising from pileup, jets with transverse momentum $p_T < 60$ GeV and $|\eta| < 2.4$ are removed if they fail to satisfy a requirement imposed by the multivariate jet vertex tagger (JVT) algorithm [40], where the JVT working point provides a 92% selection efficiency for hard-scatter jets. In addition, events with jets consistent with noise in the calorimeter or noncollision backgrounds are vetoed [41].

Jets containing a b -hadron are identified offline using the MV2c20 multivariate classifier [20, 21], which combines information from several algorithms. These algorithms are based on impact parameters of tracks, reconstructed secondary vertices, and a multi-vertex fitter which reconstructs the $b \rightarrow c$ hadron decay chain. A working point with an average b -tagging efficiency of 70%, as determined using simulated $t\bar{t}$ events, is chosen. The corresponding misidentification rates for c -jets and jets originating from light (u, d, s) quarks or gluons is 8.2% and 0.3%, respectively. Jets tagged as b -jets receive an additional energy correction to account for the presence of reconstructed muons in the jet [42].

Event preselection begins by requiring that the event pass the trigger selection and that there be at least three jets with $p_T > 20$ GeV and $|\eta| < 2.4$. The leading and second-leading jets (ordered in p_T) are then required to have $p_{T1} > 160$ GeV and $p_{T2} > 60$ GeV, respectively. The two leading jets must also be b -tagged. Events are considered to be in the signal region, and classified as bbb , if there exists at least one additional b -tagged jet. Events with only two b -tagged jets are considered to be in the control region, and are classified as $bbanti$. For bbb events the “third jet” is defined to be the third-leading b -tagged jet in p_T , while for $bbanti$ events the third jet is the third-leading jet in p_T . The final preselection requirement is that the minimum ΔR between the third jet and the two leading jets must be greater than 0.8. This requirement reduces the background from gluon splitting into $b\bar{b}$ in parton showers and subprocesses such as $bg \rightarrow bg^* \rightarrow bb\bar{b}$.

Events are further classified according to the number of jets. The 3-jet, 4-jet and 5-jet regions are defined, where the last one contains events with five or more jets. A larger number of jets often means that significant final-state radiation (FSR) is present in the ϕ boson decay, making it more difficult to accurately reconstruct m_ϕ from the two highest- p_T jets. For example, the root-mean-square values of the reconstructed signal MC mass distributions for the two highest- p_T jets for the 3-jet, 4-jet and 5-jet regions are 56 GeV, 65 GeV, and 74 GeV, respectively at $m_\phi=600$ GeV, and 163 GeV, 196 GeV, and 210 GeV, respectively at $m_\phi=1200$ GeV. Studies performed with and without jet multiplicity categorization demonstrate improvement in the expected limits from this categorization.

Signal sensitivity is enhanced with a transformation of the kinematic variables p_{T1} , p_{T2} , and the invariant mass of the two leading b -tagged jets, m_{bb} . Two-dimensional distributions of p_{T1} versus m_{bb} and of p_{T2} versus m_{bb} for events with the bbb classification are displayed in Figure 3. As m_ϕ increases the two high- p_T jets from the ϕ boson decay produce additional FSR, but the jet radius parameter remains fixed at $R = 0.4$. As a consequence, the reconstructed mass distribution based on the two highest- p_T jets smears out and it becomes more difficult to distinguish signal from background. However, since FSR occurs stochastically, the ϕ boson decays with little or no FSR in a subset of the signal events, and these have reconstructed

Table 3: The squares of the elements $c_{m_{bb}}$, $c_{p_{T1}}$, and $c_{p_{T2}}$ of the first principal component eigenvectors for the PCAs for $m_\phi = 600, 900, \text{ and } 1200$ GeV and each n -jet region. The eigenvectors are normalized to unity. The principal component is given by $m'_{bb} = c_{m_{bb}}(m_{bb} - \langle m_{bb} \rangle) + c_{p_{T1}}(p_{T1} - \langle p_{T1} \rangle) + c_{p_{T2}}(p_{T2} - \langle p_{T2} \rangle)$, where $\langle m_{bb} \rangle$, $\langle p_{T1} \rangle$, and $\langle p_{T2} \rangle$ are the mean values for m_{bb} , p_{T1} , and p_{T2} , respectively. The transformation into the eigenbasis can provide some physical intuition for the relative contributions of m_{bb} , p_{T1} , and p_{T2} .

m_ϕ [GeV]	3-jet			4-jet			5-jet		
	$c_{m_{bb}}^2$	$c_{p_{T1}}^2$	$c_{p_{T2}}^2$	$c_{m_{bb}}^2$	$c_{p_{T1}}^2$	$c_{p_{T2}}^2$	$c_{m_{bb}}^2$	$c_{p_{T1}}^2$	$c_{p_{T2}}^2$
600	0.74	0.12	0.14	0.76	0.12	0.13	0.82	0.10	0.08
900	0.55	0.20	0.26	0.64	0.16	0.20	0.74	0.14	0.13
1200	0.45	0.25	0.30	0.59	0.20	0.21	0.72	0.15	0.14

masses close to the true m_ϕ (bottom row of Figure 3). If these events can be isolated from the others, they offer a chance to improve the sensitivity via improved mass resolution and signal-to-background ratio.

To isolate events with small FSR and good m_ϕ resolution, a principal component analysis (PCA) [43] is performed on the three-dimensional distribution of the variables m_{bb} , p_{T1} , and p_{T2} using events drawn from the signal MC sample with the bbb classification following preselection. Separate PCAs are performed for each of the seventeen simulated values of m_ϕ and for each of the three n -jet regions. Upon diagonalization of the covariance matrix for m_{bb} , p_{T1} , and p_{T2} , the first, second, and third principal components define the variables m'_{bb} , p'_{T1} , and p'_{T2} , respectively. The point $(m'_{bb}, p'_{T1}, p'_{T2}) = (0, 0, 0)$ corresponds to the vector of mean values for m_{bb} , p_{T1} , and p_{T2} . Two-dimensional distributions of p'_{T1} versus m'_{bb} and of p'_{T2} versus m'_{bb} are shown in Figure 4.

The variables m_{bb} , p_{T1} , and p_{T2} that are used to calculate the PCA variables are reconstructed signal MC quantities, and are subject to the experimental systematic uncertainties, such as jet energy scale uncertainty, discussed in Sec. 6. These uncertainties can lead to jet-multiplicity migration and other effects which alter the event populations in the 3-jet, 4-jet and 5-jet regions and change the PCA variables. Full error propagation is performed to account for these effects, from variation in m_{bb} , p_{T1} , and p_{T2} to jet-multiplicity migration, PCA variable calculation, and, finally, experimental sensitivity to the Higgs boson cross section times branching ratio.

Examples of the relative contributions of m_{bb} , p_{T1} , and p_{T2} to the rotated variable m'_{bb} are shown in Table 3 for the 3-jet region. The largest component of m'_{bb} comes from m_{bb} , regardless of the mass point. However, at larger values of m_ϕ - where there is greater FSR - the p_{T1} and p_{T2} components become more important.

The final event selection requirements are $p'_{T1} > -10$ GeV and $p'_{T2} > -50$ GeV, independent of n -jet and m_ϕ . These requirements reduce the background while retaining a large fraction of the signal events in regions of high signal density in $(m'_{bb}, p'_{T1}, p'_{T2})$ space, as shown in Figure 4. Using m'_{bb} instead of m_{bb} as the final discriminant leads to increased sensitivity, which becomes more pronounced with increasing values of m_ϕ .

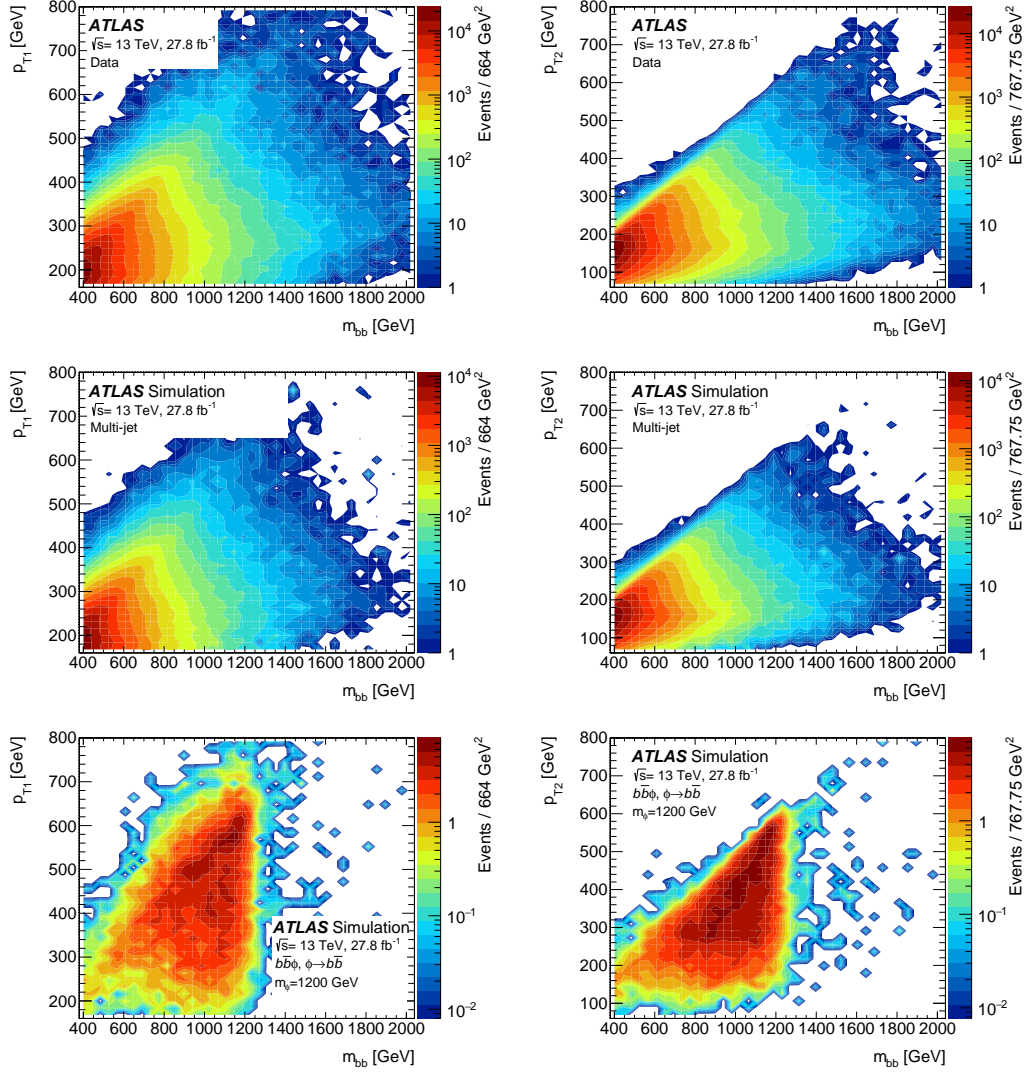


Figure 3: Two-dimensional distributions of p_{T1} versus m_{bb} (left column) and of p_{T2} versus m_{bb} (right column) for events with the bbb classification following preselection, summed over all three n -jet regions. Plots are shown for data (top row), the multijet MC sample (middle row), and the $m_\phi = 1200$ GeV signal MC sample (bottom row). The multijet plots are normalized to an integrated luminosity of 27.8 fb^{-1} based on the cross sections provided by the event generators. The signal plots are normalized to $\sigma(pp \rightarrow b\bar{b}\phi) \times \mathcal{B}(\phi \rightarrow b\bar{b}) = 1 \text{ pb}$.

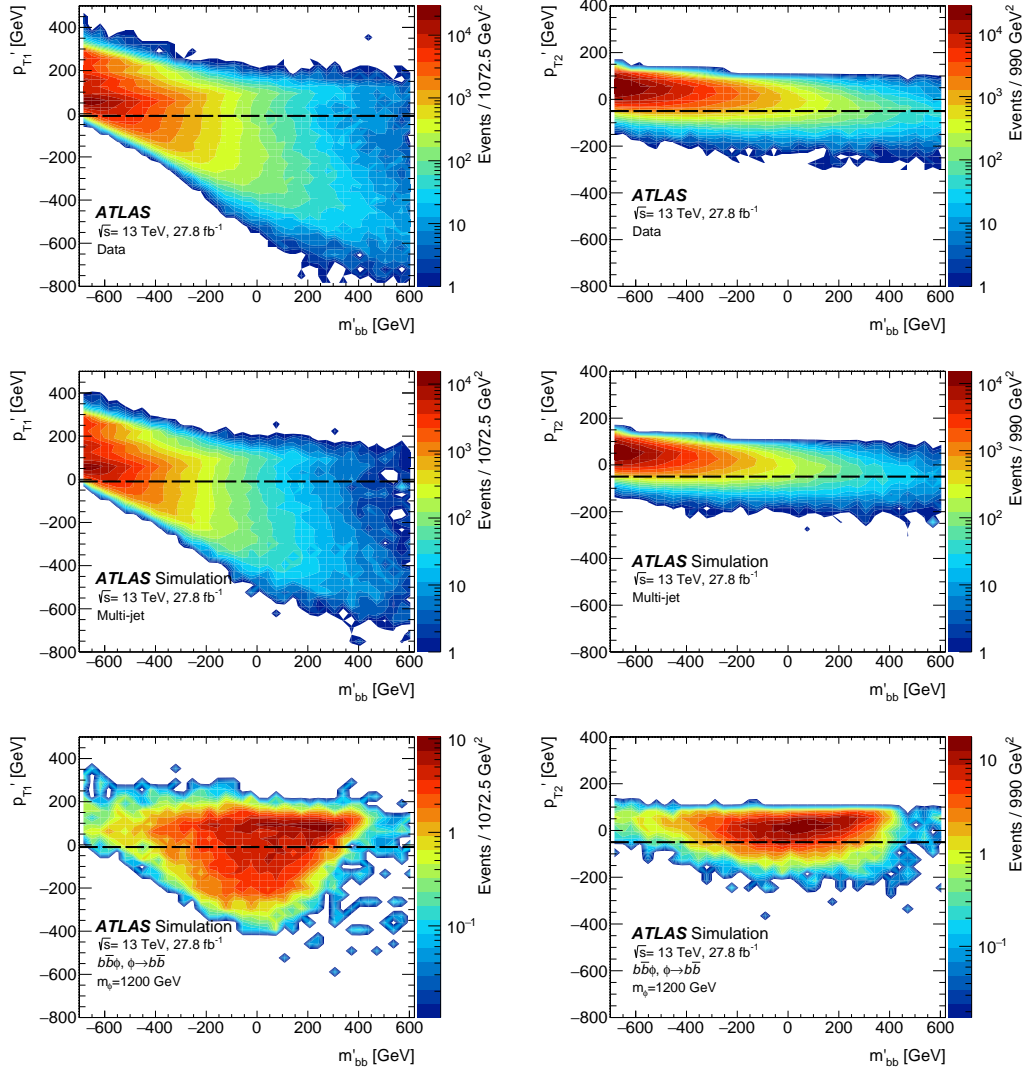


Figure 4: Two-dimensional distributions of p'_{T1} versus m'_{bb} (left column) and of p'_{T2} versus m'_{bb} (right column) for events with the bbb classification following preselection, summed over all three n -jet regions, using the PCA for $m_\phi = 1200$ GeV. Plots are shown for data (top row), the multijet MC sample (middle row), and the $m_\phi = 1200$ GeV signal MC sample (bottom row). The multijet plots are normalized to an integrated luminosity of 27.8 fb^{-1} based on the cross sections provided by the event generators. The signal plots are normalized to $\sigma(pp \rightarrow b\bar{b}\phi) \times \mathcal{B}(\phi \rightarrow b\bar{b}) = 1 \text{ pb}$. The minimum values of p'_{T1} and p'_{T2} in the final event selection are indicated by horizontal lines.

5 Statistical analysis

The presence of a signal is tested with a binned maximum-likelihood fit to the data using m'_{bb} as the final discriminating variable. For each of the considered mass points, a fit is performed simultaneously over six categories corresponding to all combinations of the three jet-multiplicity regions (3-jet, 4-jet, and 5-jet) and of the two b -tag classifications, bbb and $bbanti$. The shapes and normalizations for the different categories consist of a sum of signal and background contributions. The shapes and normalizations of the signal distributions are obtained from signal MC samples, with the exception of a global normalization factor representing the primary variable of interest, the heavy Higgs bosons production cross section times branching ratio $\sigma(pp \rightarrow b\bar{b}\phi) \times \mathcal{B}(\phi \rightarrow b\bar{b})$. The shapes and normalizations of the background distributions are determined by data. The background shapes are free to take any form satisfying the constraint that the bbb and $bbanti$ shapes for a specific jet-multiplicity region be identical modulo a second-order polynomial correction factor. The six background normalization factors float freely in the fit.

Based on the multijet MC sample, the backgrounds for both the bbb and $bbanti$ regions are dominated by the subprocesses $gg \rightarrow gb\bar{b}$ and $gg \rightarrow gg\bar{b}\bar{b}$ (such events enter the bbb region via gluon splitting into $b\bar{b}$ in the parton showering of one of the final-state gluons). However, the subprocesses $gb \rightarrow b\bar{b}\bar{b}$ and $gg \rightarrow b\bar{b}\bar{b}\bar{b}$ uniquely provide a small but non-negligible contribution to the bbb background, and the polynomial correction factor accounts for this and any other differences between the bbb and $bbanti$ regions. The m'_{bb} distributions for both the bbb and $bbanti$ classifications are plotted in Figure 5 for the multijet MC sample along with their ratio. The bbb and $bbanti$ shapes for the 3-jet and 4-jet regions in Figure 5 are nearly identical, while the $bbb/bbanti$ ratio for the 5-jet region appears to have an approximately linear dependence on m'_{bb} . Application of the χ^2 probability test and the F -test [44] to the simulated multijet m'_{bb} distributions over all values of m_ϕ demonstrates that a first-order polynomial is sufficient to describe the ratio of the simulated multijet bbb and $bbanti$ background shapes for signal masses $m_\phi < 1200$ GeV, while a second-order polynomial is needed for $m_\phi \geq 1200$ GeV.

The data bbb and $bbanti$ shapes, as well as their ratio, after applying the selection on p'_{T1} and p'_{T2} are qualitatively similar to the multijet MC distributions, as shown in Figure 6. Applying χ^2 probability and F -test criteria to the data m'_{bb} distributions over all values of m_ϕ , it is found that a first-order polynomial is sufficient for the 3-jet region with masses $m_\phi < 1200$ GeV and for the 4-jet and 5-jet regions with masses $m_\phi < 800$ GeV. For all other jet-category/mass combinations, a second-order polynomial is needed. Potential signal contamination does not affect the results of the tests.

The binned maximum-likelihood fit is performed using the RooFit [45] framework and the HistFactory [46] software tool. A product of Poisson probability terms over the bins of the m'_{bb} distributions involving the numbers of data events $n_{i,j}$ and the sum of expected signal and background yields $\nu_{i,j}$ in each category i and mass bin j forms the binned likelihood function. It accounts for the effects of floating background normalization and systematic uncertainties and is

$$P(\mathbf{n}, \mathbf{a} | \mu, N, \boldsymbol{\gamma}, \boldsymbol{\alpha}) = \prod_{i \in \text{categories}} \prod_{j \in \text{bins}} \text{Pois}(n_{i,j} | \nu_{i,j}) \prod_{p \in \text{sys. nuis. param.}} f_p(a_p | \alpha_p, \sigma_p),$$

$$\nu_{i,j} = N_i \cdot \gamma_{i,j} + \mu \cdot S_{i,j} \cdot \beta_{i,j}(\alpha_p)$$

$$\gamma_{i,j} = \begin{cases} B_{k,j} \cdot (Q_k \cdot P_j + A_k \cdot L_j + 1) , & t = bbb \\ B_{k,j} , & t = bbanti. \end{cases}$$

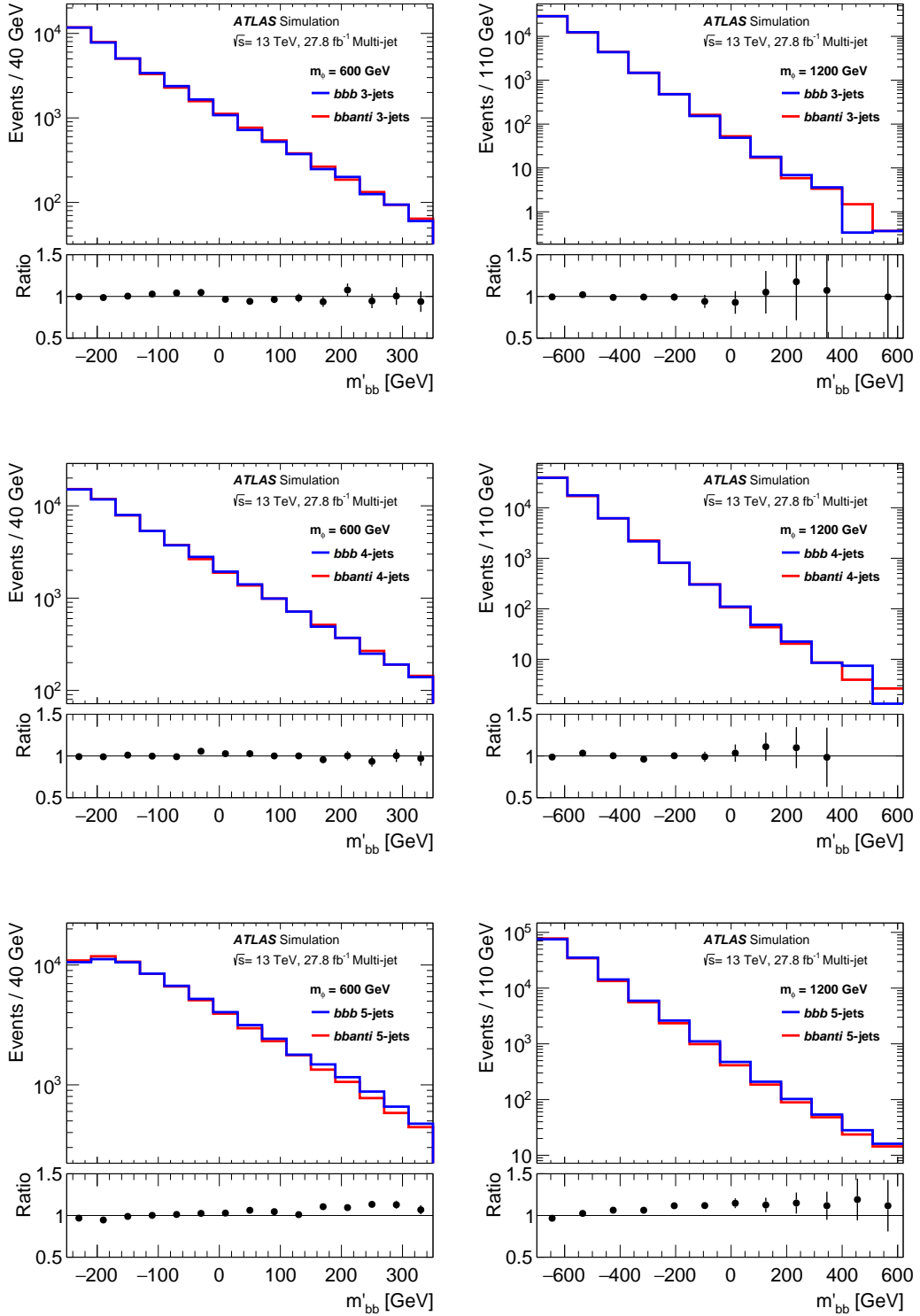


Figure 5: Distributions of m'_{bb} in simulated multijet events with the bbb and $bbanti$ classifications following all selection requirements for the 3-jet (top row), 4-jet (middle row), and 5-jet (bottom row) regions. The definition of the PCA variable m'_{bb} depends on the mass hypothesis m_ϕ and distributions are shown for $m_\phi = 600$ GeV (left column) and $m_\phi = 1200$ GeV (right column). For each case, the $bbanti$ distribution is normalized to an integrated luminosity of 27.8 fb^{-1} based on the cross section provided by the event generator, and the bbb distribution is normalized to the same area as the $bbanti$ distribution. The ratios of bbb to $bbanti$ are also shown.

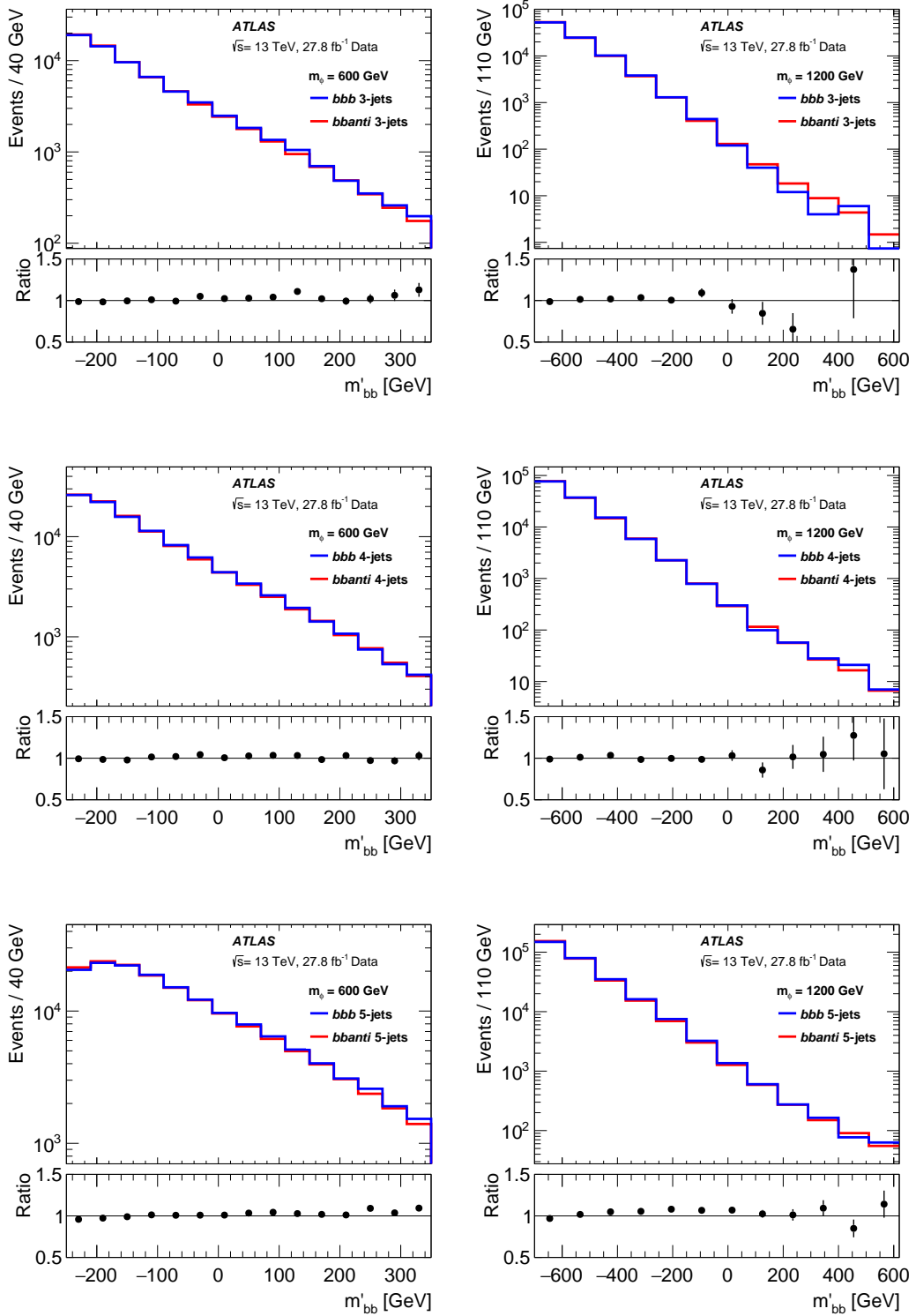


Figure 6: Distributions of m'_{bb} in data with the bbb and $bbanti$ classifications following all selection requirements for the 3-jet (top row), 4-jet (middle row), and 5-jet (bottom row) regions. The definition of the PCA variable m'_{bb} depends on the mass hypothesis m_{ϕ} and distributions are shown for $m_{\phi} = 600$ GeV (left column) and $m_{\phi} = 1200$ GeV (right column). For each case, the bbb distribution is normalized to the $bbanti$ distribution. The ratios of bbb to $bbanti$ are also shown.

The index t runs over the two flavor categories bbb and $bbanti$, k runs over the three jet-multiplicity regions, $i = (t, k)$ runs over the six categories, and p runs over the systematic error nuisance parameters. The boldfaced symbols represent vectors of parameters whereas the symbols of the same type in lightface represent individual parameters (usually containing indices). The template histograms, $S_{i,j}$, are taken directly from signal simulation for the given mass point and are normalized to the event yields expected for a one picobarn signal. Thus, the signal strength parameter μ , which is common to all categories, is $\sigma(pp \rightarrow b\bar{b}\phi) \times \mathcal{B}(\phi \rightarrow b\bar{b})$ in picobarns.

Within the HISTFACTORY framework, the second-order polynomial correction is implemented with the histograms L_j and P_j , which are binned in m'_{bb} and have bin contents given by the bin center value and bin center value squared, respectively. The normalization parameters for these histograms, A_k and Q_k , correspond to the linear and parabolic parameters, respectively, for the jet-multiplicity region k . The signal strength parameter μ , the six background normalization parameters N_i , the background shape parameters $B_{k,j}$, the linear parameters A_k , and the parabolic parameters Q_k , are freely floating parameters in the fit, with the exception that, for a fixed jet-multiplicity region k , the sum over bins j of $B_{k,j}$ is constrained to unity.

The fit model contains nuisance parameters accounting for the statistical uncertainty of the MC signal samples and for systematic variations of the shapes and normalizations of the histogram templates used in the fit, as described in Section 6. The variable $\beta_{i,j}$ represents the systematic variation in the bin content as a function of the nuisance parameters α_p . The nuisance parameters α_p are constrained within the allowed systematic variations by the $f_p(a_p|\alpha_p, \sigma_p)$ terms, where a_p are auxiliary measurements and σ_p denotes the uncertainty in α_p . Individual sources of uncertainties are considered uncorrelated.

The statistical uncertainty related to the size of MC signal samples is estimated with a variation of the Barlow–Beeston method [47]. In this analysis, each bin in each category is given a single Poisson-constrained nuisance parameter associated with the signal MC prediction for the number of events entering the bin and the total statistical uncertainty in that bin.

6 Systematic uncertainties

This analysis relies on the prediction of the shapes and normalizations of the discriminating variable m'_{bb} for the searched signal. The signal uncertainties are divided into two categories: experimental and those related to the theoretical modeling of the signal. The background model is validated through statistical analysis of the data and tests utilizing the multijet MC sample.

6.1 Systematic uncertainties of the background model

The background model is validated through the χ^2 probability and F -test analyses described in Sec. 5. As a cross-check, the fit procedure is applied to a small multijet MC sample with an equivalent integrated luminosity of 6.8 fb^{-1} for eight m_ϕ hypotheses. Events in MC samples are weighted to reflect data-based corrections for pileup, flavor tagging and trigger efficiency. In order to use the data fit procedure without modification, a special unweighted version of the MC sample is produced using acceptance-rejection sampling and the total weight of each event. The results are summarized in Table 4. The eight separate fits should be uncorrelated given the 10%–15% mass resolution for a heavy Higgs boson. With the assumption

of no correlation, the χ^2 per degree of freedom is 1.09 for the eight measurements, indicating that no statistically significant spurious signal is found by the analysis.

Table 4: Best-fit values for $\sigma(pp \rightarrow b\bar{b}\phi) \times \mathcal{B}(\phi \rightarrow b\bar{b})$ in the multijet MC sample with a total uncertainty $\Delta(\sigma \times \mathcal{B})$ for each mass point. The multijet MC sample has an equivalent integrated luminosity of 6.8 fb^{-1} .

Mass [GeV]	$\sigma \times \mathcal{B}$ [pb]	$\Delta(\sigma \times \mathcal{B})$ [pb]
450	-0.99	2.42
550	0.77	1.44
650	-0.75	0.80
750	0.42	0.62
850	-0.31	0.50
1000	-0.24	0.49
1200	0.71	0.35
1400	-0.29	0.20

6.2 Experimental systematic uncertainties of the signal

The dominant experimental systematic uncertainties are related to the calibration of the b -tagging efficiencies in simulation relative to those measured in data for $p_T < 300 \text{ GeV}$. They are extrapolated to $p_T > 300 \text{ GeV}$ using MC simulation taking into account uncertainties in the jet modeling and detector response affecting b -tagging performance. This calibration is performed separately for b -jets, c -jets, and light-flavor jets and as a function of jet p_T and $|\eta|$ [20]. Uncertainties in the cross sections for processes used in the b -tagging calibration, modeling of the jet kinematics and flavor composition in the simulated signal samples, detector simulation, and event reconstruction are included [48–50]. These uncertainties are decomposed into uncorrelated components resulting in three components for b -jets and c -jets, and five components for light-flavor jets.

Simulation-to-data efficiency differences are also corrected for the trigger, specifically for b -tagged jets[51]. Since the background estimation is data-driven, this scaling only affects signal. Scale factors obtained by comparing data and simulated dilepton $t\bar{t}$ events, which are enriched in b -jets, are used to correct simulation-to-data efficiency differences in the b -jet trigger for $p_T < 240 \text{ GeV}$. For $p_T > 240 \text{ GeV}$, due to the limited size of the $t\bar{t}$ data sample, extrapolation based on simulation is used, as described in detail in Ref. [51]. The systematic uncertainties in these scale factors include mismodeling of the fraction of b -jets in simulation, mismodeling of the b -jet trigger efficiency for non- b -jets, simulation statistical uncertainty, data statistical uncertainty for $p_T < 240 \text{ GeV}$, uncertainty in the simulation-based extrapolation to $p_T > 240 \text{ GeV}$, and uncertainties in the dependence of the b -jet trigger efficiency on jet p_T and η . The b -jet trigger was calibrated relative to a set of offline b -tagging operating points to correctly take into account correlations between the b -jet trigger and offline b -tagging.

Systematic uncertainties in the jet energy scale and jet energy resolution are based on measurements with data [39, 52]. All sources of the jet energy scale uncertainty are decomposed into 21 uncorrelated components that are treated as independent.

The uncertainty in the combined 2015+2016 integrated luminosity is 2.1%. It is derived from the calibration of the luminosity scale using x - y beam-separation scans, following a methodology similar to that detailed in Ref. [53], and using the LUCID-2 detector for the baseline luminosity measurements [54].

6.3 Theoretical systematic uncertainties of the signal

The uncertainty related to the choice of generator for the signal hard process and showering model is estimated by comparing the nominal sample with the one obtained by reweighting the nominal sample to the NLO generator MADGRAPH5_aMC@NLO [55, 56] with a 4 flavor scheme (4FS) PDF interfaced to the PYTHIA 8.205 parton showering model. The particle-level Higgs boson mass, Higgs boson p_T , and the p_T values of the two leading b -tagged jets are used for sequential reweighting. The uncertainty from the PDF set used in the nominal sample is computed using the standard-deviation method described in Ref. [23]. Variations in PDF parameters can modify the ϕ boson detection efficiency through changes to the relative contribution of the four Higgs production Feynman diagrams of Figure 1, as well as the distributions of kinematic variables, such as p_T and η for the third b -jet. The PDF uncertainty is likely overestimated, but remains small compared to the statistical uncertainty.

7 Results

The search for a single heavy neutral Higgs boson ϕ produced in association with b -quarks and decaying into a $b\bar{b}$ pair shows no significant excess above the SM background for any of the analyzed mass points. The postfit bbb category distributions of the rotated bb invariant mass m'_{bb} are shown in Figure 7 together with the m'_{bb} distribution extracted from the $bbanti$ region (prefit background).

7.1 Cross section limits

Since no significant excess over the background expectation is observed, upper limits on the production of a single heavy neutral Higgs boson ϕ decaying into a $b\bar{b}$ pair are set. Figure 8 presents the observed and expected limits for $\sigma(pp \rightarrow b\bar{b}\phi) \times \mathcal{B}(\phi \rightarrow b\bar{b})$ at the 95% confidence level (C.L.). The limits at specific mass points are calculated with the C.L._s method [57]. The expected and observed limits between mass points are given by straight lines connecting the mass point limits. Linear interpolations of the PCA parameters for adjacent mass points are used to calculate the observed 95% C.L. limits for masses between the mass points. The straight lines in Figure 8 are consistent with these observed limits to within the accuracy of the method, which grows from 0.00 to 0.56 times the $+1\sigma$ expected limit band as the mass is varied from the mass point itself to a position midway between adjacent mass points.

The leading sources of uncertainty affecting the best-fit value of $\sigma \times \mathcal{B}$ for two of the mass points, 600 and 1200 GeV, are given in Table 5, together with their relative importance. The impact of the given source of uncertainty is obtained by first fixing all the nuisance parameters related to other systematic uncertainties to their best-fit values and then allowing only the nuisance parameters ascribed to the considered source of uncertainty to float in the fit. The uncertainty is dominated by the statistical error, which improves significantly between $m_\phi = 600$ and 1200 GeV due to the sharp drop in the background level. The systematic uncertainties with the largest impact on the sensitivity are related to the flavor-tagging calibration of the offline b -tagging algorithm and b -jet trigger and to jet reconstruction.

Table 5: Grouped contributions to the systematic uncertainty of the best-fit value of $\sigma \times \mathcal{B}$. The best-fit values for $m_\phi = 600$ and 1200 GeV are 0.76 and -0.1 pb, respectively.

Source of uncertainty	$m_\phi = 600$ GeV $\Delta(\sigma \times \mathcal{B})$ [pb]	$m_\phi = 1200$ GeV $\Delta(\sigma \times \mathcal{B})$ [pb]
Total	0.80	0.29
Statistical	0.77	0.26
Systematic	0.20	0.11
Experimental uncertainties		
Jet-related	0.05	0.05
Flavor-tagging	0.12	0.05
Trigger	0.04	0.05
Luminosity	0.02	0.01
Theoretical and modeling uncertainties		
Generator	0.03	0.03
PDF	0.08	0.04
MC statistical	0.09	0.04

7.2 Model interpretations

The two 2HDM scenarios with enhanced $pp \rightarrow b\bar{b}\phi$ production and $\phi \rightarrow b\bar{b}$ decay at large $\tan\beta$ are Type II and Type Y (flipped). The most commonly analyzed scenario is Type II since the Higgs sector of the MSSM is a Type II 2HDM. The results of this search are interpreted in the context of the MSSM for the hMSSM scenario [58] and for the $m_h^{\text{mod}+}$ and $m_h^{\text{mod}-}$ scenarios [59]. The Higgs boson production cross-sections and branching ratios are calculated using the procedures outlined in the LHC Higgs Cross-section Working Group report [60]. The cross-sections for Higgs boson production through $b\bar{b}$ fusion [14] are determined by matching the 5FS [61, 62] and 4FS [63, 64] cross-section calculations. For the hMSSM scenario, the Higgs boson masses and branching ratios are calculated using HDECAY [65, 66]. For the $m_h^{\text{mod}+}$ and $m_h^{\text{mod}-}$ scenarios, the Higgs boson masses and couplings are calculated with FEYNHIGGS [24, 67–70], and the branching ratios are calculated by combining the most precise results from FEYNHIGGS, HDECAY, and PROPHECY4f [71, 72].

The 95% C.L. exclusion limits on $\tan\beta$ as a function of m_A are shown in Figure 9 for the hMSSM benchmark. The hMSSM scenario is well defined and broadly representative of the remaining parameter space with SUSY partners too heavy for direct detection at the LHC. As an indication of the sensitivity variation for different MSSM scenarios, Figure 9 also displays the expected sensitivities for the $m_h^{\text{mod}+}$ and $m_h^{\text{mod}-}$ scenarios, in which top squark mixing parameters are chosen to allow a wide range of $\tan\beta$ values while maintaining compatibility with $m_h = 125$ GeV. The hMSSM limits obtained by this search are comparable to the limits obtained in the charged Higgs boson search in the $H^\pm \rightarrow \tau\nu$ decay channel by ATLAS and CMS Collaborations [73, 74] but not as stringent as the hMSSM limits obtained in the ATLAS and CMS searches for heavy neutral Higgs bosons decaying via $\phi \rightarrow \tau^+\tau^-$ [11, 12].

The 95% C.L. $\tan\beta$ exclusion limits for this search assuming the Type Y (flipped) 2HDM scenario are presented, first in Figure 10 for the specific ϕ mass of 450 GeV as a function of $\cos(\beta - \alpha)$ and then in Figure 11 as a function of m_ϕ in the alignment limit $\cos(\beta - \alpha) = 0$. For these limits, it is assumed that the

flipped 2HDM is CP -conserving with $m_h = 125$ GeV and $m_H = m_{H^\pm} = m_A$. The model grid points are generated using SusHi [62] and 2HDMC [75]. These limits complement the flipped 2HDM limits obtained from the searches for $A \rightarrow Zh$ in ATLAS [76], which exclude regions with $|\cos(\beta - \alpha)| \gtrsim 0.2$ or $\tan \beta \lesssim 4$, and from the search for $A \rightarrow ZH$ in ATLAS [77], which excludes regions with $m_A - m_H \gtrsim 100$ GeV.

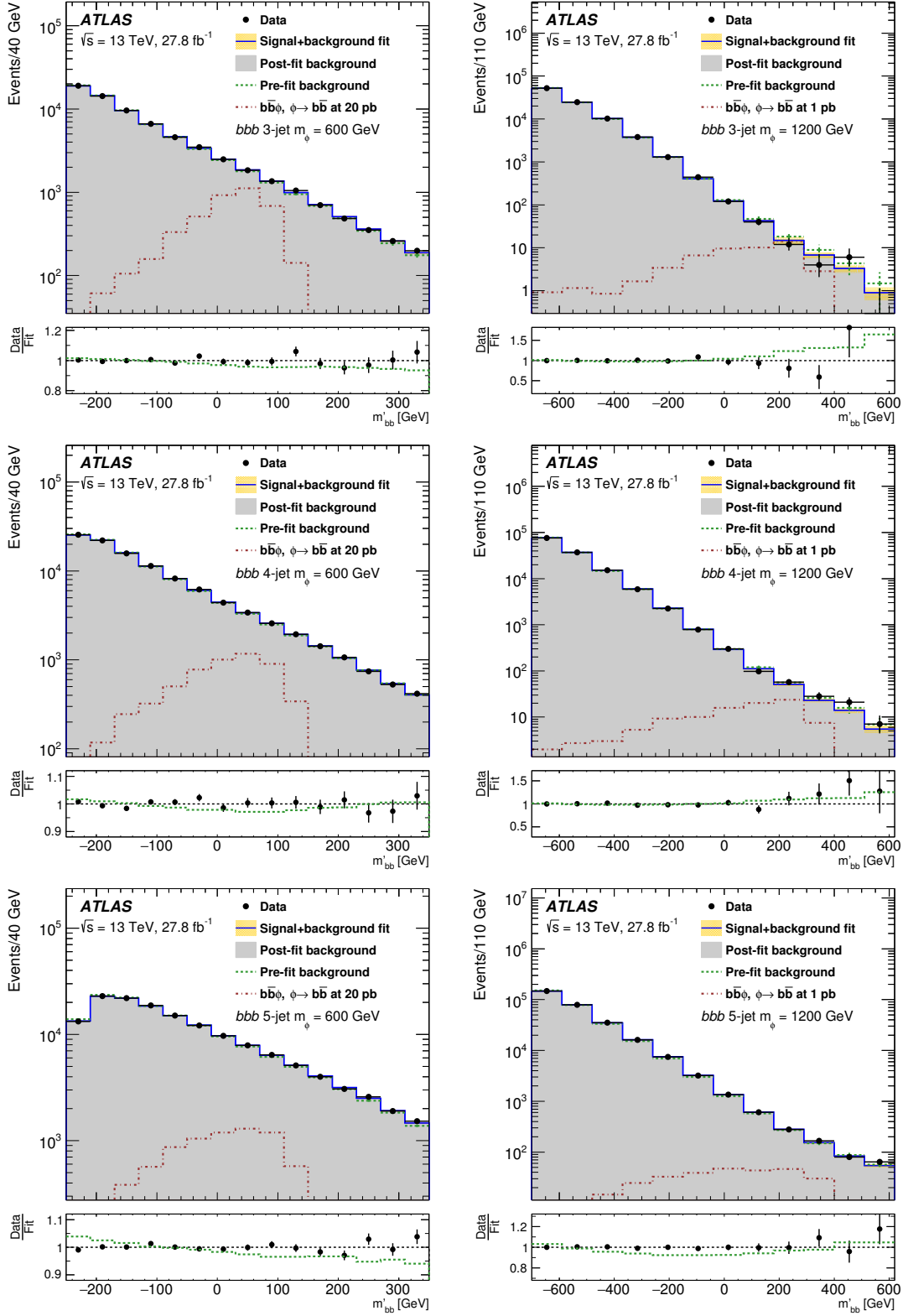


Figure 7: Postfit bbb category distributions of m'_{bb} for the 600 GeV (left) and 1200 GeV (right) mass points in the 3-jet (top), 4-jet (middle), and 5-jet (bottom) categories. The prefit background shape is also shown in the top panels, and its ratio to the postfit shape is shown in the bottom panels (green dashed line). The signal shape (red dashed line) is overlaid for illustration.

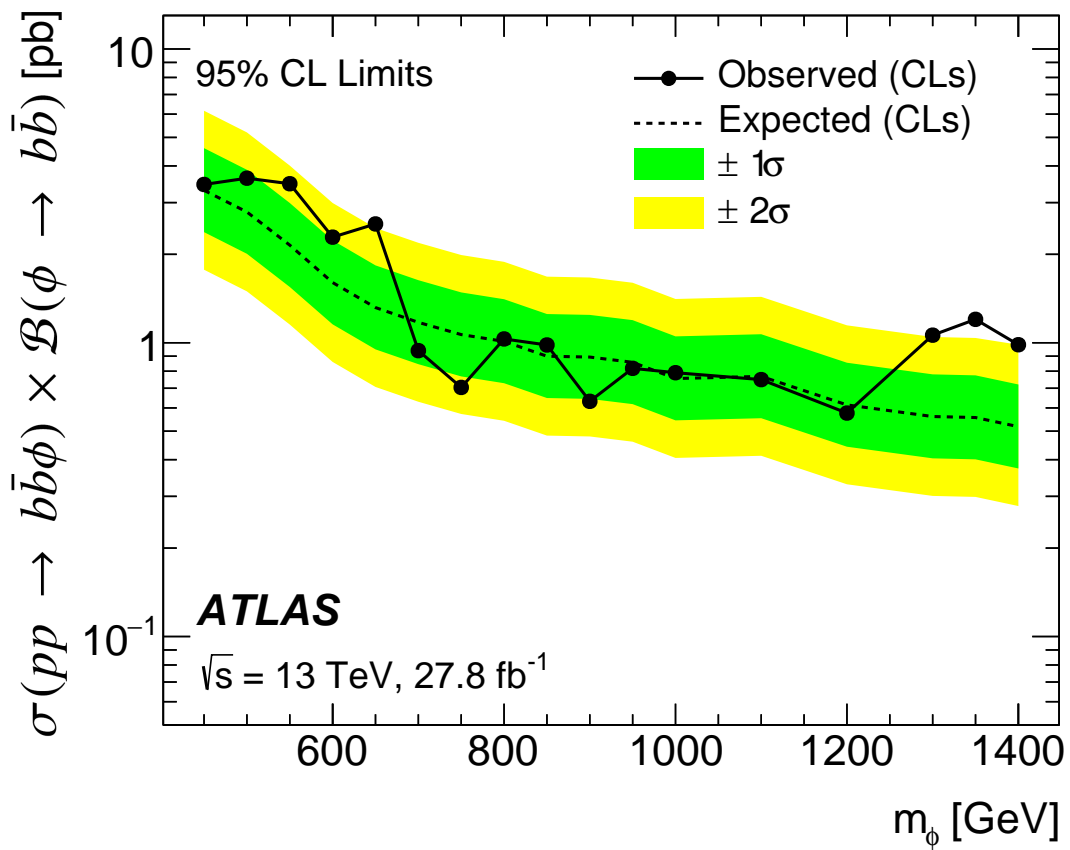


Figure 8: Observed and expected upper limits on $\sigma(pp \rightarrow b\bar{b}\phi) \times \mathcal{B}(\phi \rightarrow b\bar{b})$ at 95% C.L. as a function of the Higgs boson mass in 27.8 fb^{-1} of pp collision data at $\sqrt{s} = 13 \text{ TeV}$.

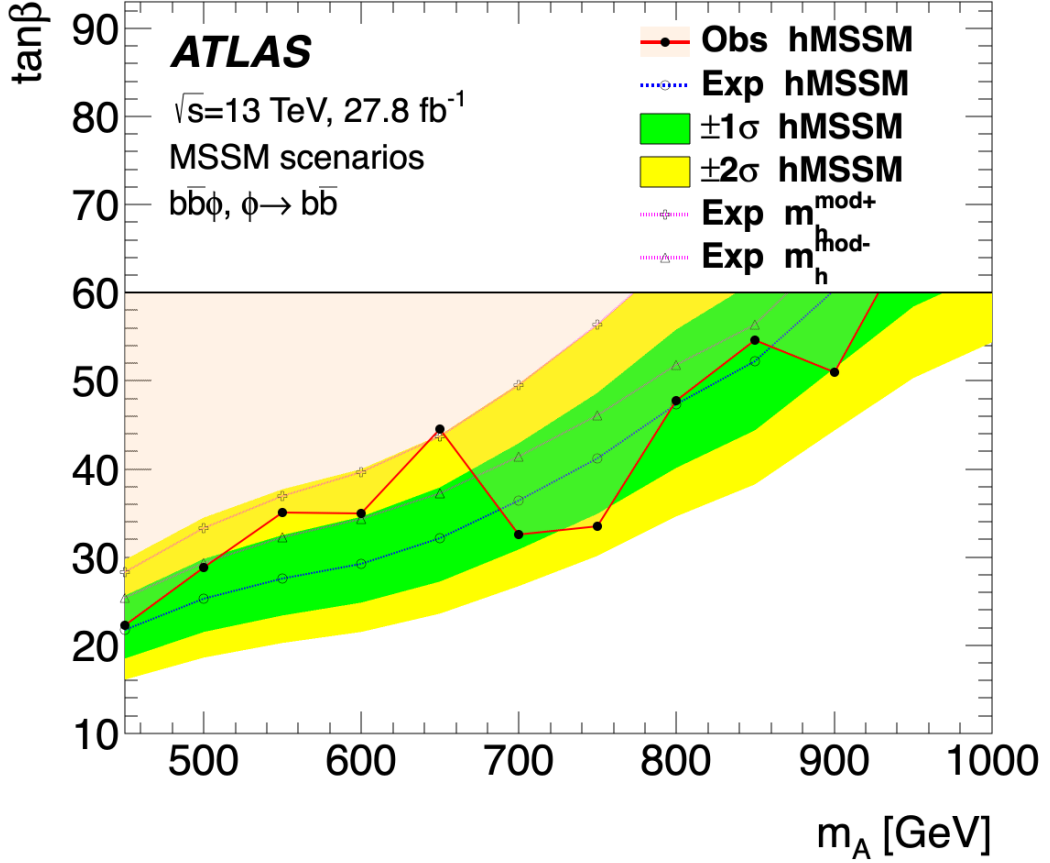


Figure 9: Observed and expected 95% C.L. exclusion limits for the hMSSM scenario as a function of m_A . The expected sensitivities for the $m_h^{\text{mod}+}$ and $m_h^{\text{mod}-}$ scenarios are also shown. The observed 95% C.L. limits for the $m_h^{\text{mod}+}$ and $m_h^{\text{mod}-}$ scenarios follow the same pattern with respect to their expected limits as the hMSSM observed limits. Limits are not shown for $\tan\beta > 60$ since the Higgs boson coupling becomes nonperturbative for very large values of $\tan\beta$ in the considered models.

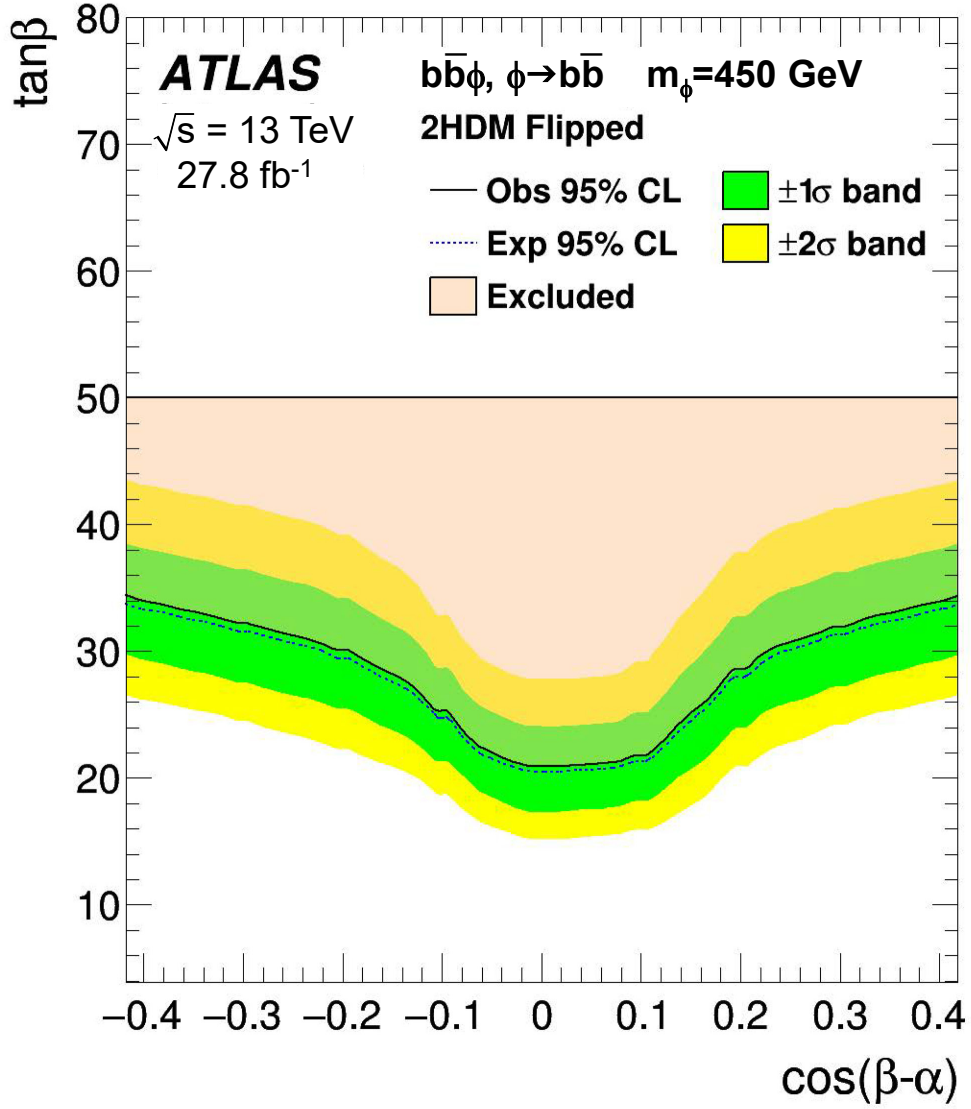


Figure 10: Observed and expected 95% C.L. exclusion limits for the flipped 2HDM scenario at $m_\phi = 450 \text{ GeV}$ as a function of $\cos(\beta - \alpha)$. Limits are not shown for $\tan\beta > 50$ since the Higgs boson coupling becomes nonperturbative for very large values of $\tan\beta$ in this model.

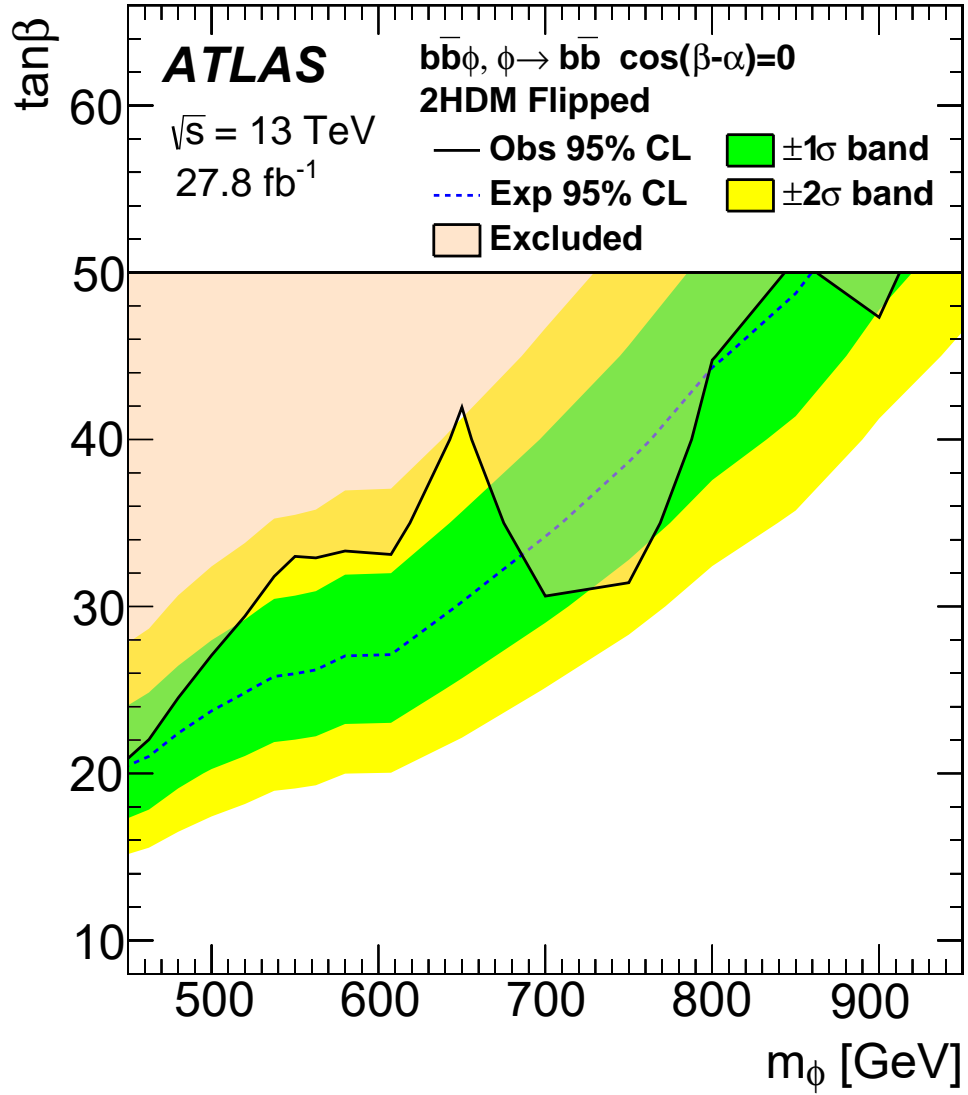


Figure 11: Observed and expected 95% C.L. exclusion limits for the flipped 2HDM scenario in the alignment limit as a function of m_ϕ . Limits are not shown for $\tan\beta > 50$ since the Higgs boson coupling becomes nonperturbative for very large values of $\tan\beta$ in this model.

8 Conclusions

A search for heavy neutral Higgs bosons produced in association with at least one b -quark and decaying into a pair of b -quarks was performed using 27.8 fb^{-1} of 13 TeV pp collision data recorded by the ATLAS detector at the LHC in 2015 and 2016. The data are compatible with SM expectations, yielding no significant excess of events in the mass range 450–1400 GeV. Upper limits on the cross section times branching ratio were derived as a function of the mass of the heavy Higgs boson. The 95% C.L. upper limits are in the range 0.6–4.0 pb. Compared to heavy neutral Higgs boson searches utilizing $\phi \rightarrow \tau^+\tau^-$ or $A \rightarrow Zh$ decays, these limits expand the excluded Type Y (flipped) 2HDM parameter space into regions with $|\cos(\beta - \alpha)| \approx 0$ and $\tan\beta \gtrsim 20$.

Acknowledgments

We thank CERN for the very successful operation of the LHC, as well as the support staff from our institutions without whom ATLAS could not be operated efficiently.

We acknowledge the support of ANPCyT, Argentina; YerPhI, Armenia; ARC, Australia; BMWFW and FWF, Austria; ANAS, Azerbaijan; SSTC, Belarus; CNPq and FAPESP, Brazil; NSERC, NRC and CFI, Canada; CERN; CONICYT, Chile; CAS, MOST and NSFC, China; COLCIENCIAS, Colombia; MSMT CR, MPO CR and VSC CR, Czech Republic; DNRF and DNSRC, Denmark; IN2P3-CNRS and CEA-DRF/IRFU, France; SRNSFG, Georgia; BMBF, HGF and MPG, Germany; GSRT, Greece; RGC and Hong Kong SAR, China; ISF and Benoziyo Center, Israel; INFN, Italy; MEXT and JSPS, Japan; CNRST, Morocco; NWO, Netherlands; RCN, Norway; MNiSW and NCN, Poland; FCT, Portugal; MNE/IFA, Romania; MES of Russia and NRC KI, Russia Federation; JINR; MESTD, Serbia; MSSR, Slovakia; ARRS and MIZŠ, Slovenia; DST/NRF, South Africa; MICINN, Spain; SRC and Wallenberg Foundation, Sweden; SERI, SNSF and Cantons of Bern and Geneva, Switzerland; MOST, Taiwan; TAEK, Turkey; STFC, United Kingdom; DOE and NSF, United States of America. In addition, individual groups and members have received support from BCKDF, CANARIE, Compute Canada and CRC, Canada; ERC, ERDF, Horizon 2020, Marie Skłodowska-Curie Actions and COST, European Union; Investissements d’Avenir Labex, Investissements d’Avenir Idex and ANR, France; DFG and AvH Foundation, Germany; Herakleitos, Thales and Aristeia programmes co-financed by EU-ESF and the Greek NSRF, Greece; BSF-NSF and GIF, Israel; La Caixa Banking Foundation, CERCA Programme Generalitat de Catalunya and PROMETEO and GenT Programmes Generalitat Valenciana, Spain; Göran Gustafssons Stiftelse, Sweden; The Royal Society and Leverhulme Trust, United Kingdom.

The crucial computing support from all WLCG partners is acknowledged gratefully, in particular from CERN, the ATLAS Tier-1 facilities at TRIUMF (Canada), NDGF (Denmark, Norway, Sweden), CC-IN2P3 (France), KIT/GridKA (Germany), INFN-CNAF (Italy), NL-T1 (Netherlands), PIC (Spain), ASGC (Taiwan), RAL (UK) and BNL (USA), the Tier-2 facilities worldwide and large non-WLCG resource providers. Major contributors of computing resources are listed in Ref. [78].

References

- [1] ATLAS Collaboration, *Observation of a new particle in the search for the Standard Model Higgs boson with the ATLAS detector at the LHC*, *Phys. Lett. B* **716** (2012) 1, arXiv: [1207.7214 \[hep-ex\]](#).
- [2] CMS Collaboration, *Observation of a new boson at a mass of 125 GeV with the CMS experiment at the LHC*, *Phys. Lett. B* **716** (2012) 30, arXiv: [1207.7235 \[hep-ex\]](#).
- [3] F. Englert and R. Brout, *Broken Symmetry and the Mass of Gauge Vector Mesons*, *Phys. Rev. Lett.* **13** (1964) 321.
- [4] P. W. Higgs, *Broken symmetries, massless particles and gauge fields*, *Phys. Lett.* **12** (1964) 132.
- [5] P. W. Higgs, *Broken Symmetries and the Masses of Gauge Bosons*, *Phys. Rev. Lett.* **13** (1964) 508.
- [6] G. S. Guralnik, C. R. Hagen, and T. W. B. Kibble, *Global Conservation Laws and Massless Particles*, *Phys. Rev. Lett.* **13** (1964) 585.
- [7] G. C. Branco et al., *Theory and phenomenology of two-Higgs-doublet models*, *Phys. Rept.* **516** (2012) 1, arXiv: [1106.0034 \[hep-ph\]](#).
- [8] J. F. Gunion, H. E. Haber, G. L. Kane, and S. Dawson, *The Higgs Hunter's Guide*, *Front. Phys.* **80** (2000), URL: <https://cds.cern.ch/record/425736>.
- [9] D. M. Asner et al., *ILC Higgs White Paper*, 2013, arXiv: [1310.0763 \[hep-ph\]](#).
- [10] ALEPH, DELPHI, L3 and OPAL Collaborations, *Search for neutral MSSM Higgs bosons at LEP*, *Eur. Phys. J. C* **47** (2006) 547, arXiv: [hep-ex/0602042 \[hep-ex\]](#).
- [11] ATLAS Collaboration, *Search for additional heavy neutral Higgs and gauge bosons in the ditau final state produced in 36 fb^{-1} of pp collisions at $\sqrt{s} = 13 \text{ TeV}$ with the ATLAS detector*, *JHEP* **01** (2018) 055, arXiv: [1709.07242 \[hep-ex\]](#).
- [12] CMS Collaboration, *Search for additional neutral MSSM Higgs bosons in the $\tau\tau$ final state in proton-proton collisions at $\sqrt{s} = 13 \text{ TeV}$* , *JHEP* **09** (2018) 007, arXiv: [1803.06553 \[hep-ex\]](#).
- [13] M. Carena, S. Heinemeyer, C. E. M. Wagner, and G. Weiglein, *MSSM Higgs boson searches at the Tevatron and the LHC: Impact of different benchmark scenarios*, *Eur. Phys. J. C* **45** (2006) 797, arXiv: [hep-ph/0511023](#).
- [14] R. Harlander, M. Krämer, and M. Schumacher, *Bottom-quark associated Higgs-boson production: reconciling the four- and five-flavour scheme approach*, (2011), arXiv: [1112.3478 \[hep-ph\]](#).
- [15] CMS Collaboration, *Search for beyond the standard model Higgs bosons decaying into a $b\bar{b}$ pair in pp collisions at $\sqrt{s} = 13 \text{ TeV}$* , *JHEP* **08** (2018) 113, arXiv: [1805.12191 \[hep-ex\]](#).
- [16] ATLAS Collaboration, *The ATLAS Experiment at the CERN Large Hadron Collider*, *JINST* **3** (2008) S08003.
- [17] ATLAS Collaboration, *ATLAS Insertable B-Layer Technical Design Report*, ATLAS-TDR-19, 2010, URL: <https://cds.cern.ch/record/1291633>, *ATLAS Insertable B-Layer Technical Design Report Addendum*, ATLAS-TDR-19-ADD-1, 2012, URL: <https://cds.cern.ch/record/1451888>.
- [18] B. Abbott et al., *Production and integration of the ATLAS Insertable B-Layer*, *JINST* **13** (2018) T05008, arXiv: [1803.00844 \[physics.ins-det\]](#).
- [19] ATLAS Collaboration, *Performance of the ATLAS trigger system in 2015*, *Eur. Phys. J. C* **77** (2017) 317, arXiv: [1611.09661 \[hep-ex\]](#).

- [20] ATLAS Collaboration, *Performance of b -jet identification in the ATLAS experiment*, **JINST** **11** (2016) P04008, arXiv: [1512.01094 \[hep-ex\]](#).
- [21] ATLAS Collaboration, *Optimisation of the ATLAS b -tagging performance for the 2016 LHC Run*, ATLAS-PHYS-PUB-2016-012, 2016, URL: <https://cds.cern.ch/record/2160731>.
- [22] T. Gleisberg et al., *Event generation with SHERPA 1.1*, **JHEP** **02** (2009) 007, arXiv: [0811.4622 \[hep-ph\]](#).
- [23] R. D. Ball et al., *Parton distributions for the LHC run II*, **JHEP** **04** (2015) 040, arXiv: [1410.8849 \[hep-ph\]](#).
- [24] S. Heinemeyer, W. Hollik, and G. Weiglein, *FeynHiggs: A program for the calculation of the masses of the neutral CP-even Higgs bosons in the MSSM*, **Comput. Phys. Commun.** **124** (2000) 76, arXiv: [hep-ph/9812320](#).
- [25] ATLAS Collaboration, *The ATLAS Simulation Infrastructure*, **Eur. Phys. J. C** **70** (2010) 823, arXiv: [1005.4568 \[physics.ins-det\]](#).
- [26] S. Agostinelli et al., *GEANT4—A simulation toolkit*, **Nucl. Instrum. Meth. A** **506** (2003) 250.
- [27] T. Sjöstrand, S. Mrenna, and P. Z. Skands, *A brief introduction to PYTHIA 8.1*, **Comput. Phys. Commun.** **178** (2008) 852, arXiv: [0710.3820 \[hep-ph\]](#).
- [28] ATLAS Collaboration, *Summary of ATLAS Pythia 8 tunes*, ATL-PHYS-PUB-2012-003, 2012, URL: <https://cds.cern.ch/record/1474107>.
- [29] A. D. Martin, W. J. Stirling, R. S. Thorne, and G. Watt, *Parton distributions for the LHC*, **Eur. Phys. J. C** **63** (2009) 189, arXiv: [0901.0002 \[hep-ph\]](#).
- [30] P. Nason, *A New method for combining NLO QCD with shower Monte Carlo algorithms*, **JHEP** **11** (2004) 040, arXiv: [hep-ph/0409146](#).
- [31] S. Frixione, P. Nason, and C. Oleari, *Matching NLO QCD computations with Parton Shower simulations: the POWHEG method*, **JHEP** **11** (2007) 070, arXiv: [0709.2092 \[hep-ph\]](#).
- [32] S. Frixione, P. Nason, and G. Ridolfi, *A positive-weight next-to-leading-order Monte Carlo for heavy flavour hadroproduction*, **JHEP** **09** (2007) 126, arXiv: [0707.3088 \[hep-ph\]](#).
- [33] T. Sjöstrand, S. Mrenna, and P. Z. Skands, *PYTHIA 6.4 physics and manual*, **JHEP** **05** (2006) 026, arXiv: [hep-ph/0603175](#).
- [34] F. Maltoni and T. Stelzer, *MadEvent: automatic event generation with MadGraph*, **JHEP** **02** (2003) 027, arXiv: [hep-ph/0208156](#).
- [35] ATLAS Collaboration, *The simulation principle and performance of the ATLAS fast calorimeter simulation FastCaloSim*, ATL-PHYS-PUB-2010-013, 2010, URL: <https://cds.cern.ch/record/1300517>.
- [36] ATLAS Collaboration, *Reconstruction of primary vertices at the ATLAS experiment in Run 1 proton–proton collisions at the LHC*, **Eur. Phys. J. C** **77** (2017) 332, arXiv: [1611.10235 \[hep-ex\]](#).
- [37] M. Cacciari, G. P. Salam, and G. Soyez, *The anti- k_t jet clustering algorithm*, **JHEP** **04** (2008) 063, arXiv: [0802.1189 \[hep-ph\]](#).
- [38] ATLAS Collaboration, *Topological cell clustering in the ATLAS calorimeters and its performance in LHC Run 1*, **Eur. Phys. J. C** **77** (2017) 490, arXiv: [1603.02934 \[hep-ex\]](#).

- [39] ATLAS Collaboration, *Jet energy scale measurements and their systematic uncertainties in proton–proton collisions at $\sqrt{s} = 13$ TeV with the ATLAS detector*, *Phys. Rev. D* **96** (2017) 072002, arXiv: [1703.09665 \[hep-ex\]](#).
- [40] ATLAS Collaboration, *Performance of pile-up mitigation techniques for jets in pp collisions at $\sqrt{s} = 8$ TeV using the ATLAS detector*, *Eur. Phys. J. C* **76** (2016) 581, arXiv: [1510.03823 \[hep-ex\]](#).
- [41] ATLAS Collaboration, *Selection of jets produced in 13 TeV proton–proton collisions with the ATLAS detector*, ATLAS-CONF-2015-029, 2015, URL: <https://cds.cern.ch/record/2037702>.
- [42] ATLAS Collaboration, *Evidence for the $H \rightarrow b\bar{b}$ decay with the ATLAS detector*, *JHEP* **12** (2017) 024, arXiv: [1708.03299 \[hep-ex\]](#).
- [43] I. Jolliffe, *Principal Component Analysis*, in M. Lovric (Ed.), *International Encyclopedia of Statistical Science*. Springer, Berlin, Heidelberg, (2011).
- [44] B. Roe, *Probability and Statistics in Experimental Physics*, Springer-Verlag (2001) 264pp.
- [45] W. Verkerke and D. P. Kirkby, *The RooFit toolkit for data modeling*, 2003, arXiv: [physics/0306116](#).
- [46] K. Cranmer, G. Lewis, L. Moneta, A. Shibata, and W. Verkerke, *HistFactory: A tool for creating statistical models for use with RooFit and RooStats*, CERN-OPEN-2012-016, 2012, URL: <https://cds.cern.ch/record/1456844/>.
- [47] R. Barlow and C. Beeston, *Fitting using finite Monte Carlo samples*, *Comput. Phys. Commun.* **77** (1993) 219.
- [48] ATLAS Collaboration, *Measurements of b-jet tagging efficiency with the ATLAS detector using $t\bar{t}$ events at $\sqrt{s} = 13$ TeV*, *JHEP* **08** (2018) 089, arXiv: [1805.01845 \[hep-ex\]](#).
- [49] ATLAS Collaboration, *Measurement of b-tagging efficiency of c-jets in $t\bar{t}$ events using a likelihood approach with the ATLAS detector*, ATLAS-CONF-2018-001, 2018, URL: <https://cds.cern.ch/record/2306649>.
- [50] ATLAS Collaboration, *Calibration of light-flavour b-jet mistagging rates using ATLAS proton–proton collision data at $\sqrt{s} = 13$ TeV*, ATLAS-CONF-2018-006, 2018, URL: <https://cds.cern.ch/record/2314418>.
- [51] L. I. McClymont, “Searches for New Physics using Pairs of Jets Containing b-quarks at the ATLAS Detector,” PhD thesis: University College London, URL: <http://discovery.ucl.ac.uk/10052993/1/e-Thesis.pdf>.
- [52] ATLAS Collaboration, *Jet energy resolution in proton–proton collisions at $\sqrt{s} = 7$ TeV recorded in 2010 with the ATLAS detector*, *Eur. Phys. J. C* **73** (2013) 2306, arXiv: [1210.6210 \[hep-ex\]](#).
- [53] ATLAS Collaboration, *Luminosity determination in pp collisions at $\sqrt{s} = 8$ TeV using the ATLAS detector at the LHC*, *Eur. Phys. J. C* **76** (2016) 653, arXiv: [1608.03953 \[hep-ex\]](#).
- [54] G. Avoni et al., *The new LUCID-2 detector for luminosity measurement and monitoring in ATLAS*, *JINST* **13** (2018) P07017.
- [55] J. Alwall et al., *The automated computation of tree-level and next-to-leading order differential cross sections, and their matching to parton shower simulations*, *JHEP* **07** (2014) 079, arXiv: [1405.0301 \[hep-ph\]](#).
- [56] M. Wiesemann et al., *Higgs production in association with bottom quarks*, *JHEP* **02** (2015) 132, arXiv: [1409.5301 \[hep-ph\]](#).

- [57] G. Cowan, K. Cranmer, E. Gross, and O. Vitells, *Asymptotic formulae for likelihood-based tests of new physics*, *Eur. Phys. J. C* **71** (2011) 1554, arXiv: [1007.1727 \[hep-ex\]](#), Erratum: *Erratum to: Asymptotic formulae for likelihood-based tests of new physics*, *Eur. Phys. J. C* **73** (2013) 2501.
- [58] A. Djouadi et al., *The post-Higgs MSSM scenario: habemus MSSM?* *Eur. Phys. J. C* **73** (2013) 2650, arXiv: [1307.5205 \[hep-ph\]](#).
- [59] M. Carena, S. Heinemeyer, O. Stål, C. E. M. Wagner, and G. Weiglein, *MSSM Higgs boson searches at the LHC: benchmark scenarios after the discovery of a Higgs-like particle*, *Eur. Phys. J. C* **73** (2013) 2552, arXiv: [1302.7033 \[hep-ph\]](#).
- [60] D. de Florian et al., *Handbook of LHC Higgs Cross Sections: 4. Deciphering the nature of the Higgs sector*, CERN-2017-002-M (2017), arXiv: [1610.07922 \[hep-ph\]](#).
- [61] R. V. Harlander and W. B. Kilgore, *Higgs boson production in bottom quark fusion at next-to-next-to leading order*, *Phys. Rev. D* **68** (2003) 013001, arXiv: [hep-ph/0304035](#).
- [62] R. V. Harlander, S. Liebler, and H. Mantler, *SusHi: A program for the calculation of Higgs production in gluon fusion and bottom-quark annihilation in the Standard Model and the MSSM*, *Comput. Phys. Commun.* **184** (2013) 1605, arXiv: [1212.3249 \[hep-ph\]](#).
- [63] S. Dittmaier, M. Krämer, and M. Spira, *Higgs radiation off bottom quarks at the Fermilab Tevatron and the CERN LHC*, *Phys. Rev. D* **70** (2004) 074010, arXiv: [hep-ph/0309204](#).
- [64] S. Dawson, C. B. Jackson, L. Reina, and D. Wackerroth, *Exclusive Higgs boson production with bottom quarks at hadron colliders*, *Phys. Rev. D* **69** (2004) 074027, arXiv: [hep-ph/0311067](#).
- [65] A. Djouadi, J. Kalinowski, and M. Spira, *HDECAY: A Program for Higgs boson decays in the standard model and its supersymmetric extension*, *Comput. Phys. Commun.* **108** (1998) 56, arXiv: [hep-ph/9704448](#).
- [66] A. Djouadi, J. Kalinowski, M. Mühlleitner, and M. Spira, *HDECAY: Twenty++ years after*, *Comput. Phys. Commun.* **238** (2019) 214, arXiv: [1801.09506 \[hep-ph\]](#).
- [67] S. Heinemeyer, W. Hollik, and G. Weiglein, *The masses of the neutral CP-even Higgs bosons in the MSSM: Accurate analysis at the two loop level*, *Eur. Phys. J. C* **9** (1999) 343, arXiv: [hep-ph/9812472](#).
- [68] G. Degrandi, S. Heinemeyer, W. Hollik, P. Slavich, and G. Weiglein, *Towards high precision predictions for the MSSM Higgs sector*, *Eur. Phys. J. C* **28** (2003) 133, arXiv: [hep-ph/0212020](#).
- [69] M. Frank et al., *The Higgs boson masses and mixings of the complex MSSM in the Feynman-diagrammatic approach*, *JHEP* **02** (2007) 047, arXiv: [hep-ph/0611326](#).
- [70] T. Hahn, S. Heinemeyer, W. Hollik, H. Rzehak, and G. Weiglein, *High-Precision Predictions for the Light CP-Even Higgs Boson Mass of the Minimal Supersymmetric Standard Model*, *Phys. Rev. Lett.* **112** (2014) 141801, arXiv: [1312.4937 \[hep-ph\]](#).
- [71] A. Bredenstein, A. Denner, S. Dittmaier, and M. M. Weber, *Precise predictions for the Higgs-boson decay $H \rightarrow WW/ZZ \rightarrow 4$ leptons*, *Phys. Rev. D* **74** (2006) 013004, arXiv: [hep-ph/0604011](#).
- [72] A. Bredenstein, A. Denner, S. Dittmaier, and M. M. Weber, *Radiative corrections to the semileptonic and hadronic Higgs-boson decays $H \rightarrow WW/ZZ \rightarrow 4$ fermions*, *JHEP* **02** (2007) 080, arXiv: [hep-ph/0611234 \[hep-ph\]](#).
- [73] ATLAS Collaboration, *Search for charged Higgs bosons decaying via $H^\pm \rightarrow \tau^\pm \nu_\tau$ in the τ +jets and τ +lepton final states with 36 fb^{-1} of pp collision data recorded at $\sqrt{s} = 13 \text{ TeV}$ with the ATLAS experiment*, *JHEP* **09** (2018) 139, arXiv: [1807.07915 \[hep-ex\]](#).

- [74] CMS Collaboration, *Search for charged Higgs bosons in the $H^\pm \rightarrow \tau^\pm \nu_\tau$ decay channel in proton-proton collisions at $\sqrt{s} = 13$ TeV*, (2019), arXiv: [1903.04560 \[hep-ex\]](#).
- [75] D. Eriksson, J. Rathsman, and O. Stål, *2HDMC – two-Higgs-doublet model calculator*, *Comput. Phys. Commun.* **181** (2010) 189, arXiv: [0902.0851 \[hep-ph\]](#).
- [76] ATLAS Collaboration, *Search for heavy resonances decaying into a W or Z boson and a Higgs boson in final states with leptons and b-jets in 36fb^{-1} of $\sqrt{s} = 13$ TeV pp collisions with the ATLAS detector*, *JHEP* **03** (2018) 174, arXiv: [1712.06518 \[hep-ex\]](#), Erratum: *JHEP* **11** (2018) 051.
- [77] ATLAS Collaboration, *Search for a heavy Higgs boson decaying into a Z boson and another heavy Higgs boson in the $\ell\ell bb$ final state in pp collisions at $\sqrt{s} = 13$ TeV with the ATLAS detector*, *Phys. Lett. B* **783** (2018) 392, arXiv: [1804.01126 \[hep-ex\]](#).
- [78] ATLAS Collaboration, *ATLAS Computing Acknowledgements*, ATL-SOFT-PUB-2020-001, URL: <https://cds.cern.ch/record/2717821>.

The ATLAS Collaboration

G. Aad¹⁰², B. Abbott¹²⁹, D.C. Abbott¹⁰³, O. Abidinov^{13,*}, A. Abed Abud^{71a,71b}, K. Abeling⁵³, D.K. Abhayasinghe⁹⁴, S.H. Abidi¹⁶⁷, O.S. AbouZeid⁴⁰, N.L. Abraham¹⁵⁶, H. Abramowicz¹⁶¹, H. Abreu¹⁶⁰, Y. Abulaiti⁶, B.S. Acharya^{67a,67b,q}, B. Achkar⁵³, S. Adachi¹⁶³, L. Adam¹⁰⁰, C. Adam Bourdarios⁶⁵, L. Adamczyk^{84a}, L. Adamek¹⁶⁷, J. Adelman¹²¹, M. Adersberger¹¹⁴, A. Adiguzel^{12c,an}, S. Adorni⁵⁴, T. Adye¹⁴⁴, A.A. Affolder¹⁴⁶, Y. Afik¹⁶⁰, C. Agapopoulou⁶⁵, M.N. Agaras³⁸, A. Aggarwal¹¹⁹, C. Agheorghiesei^{27c}, J.A. Aguilar-Saavedra^{140f,140a,am}, F. Ahmadov⁸⁰, W.S. Ahmed¹⁰⁴, X. Ai¹⁸, G. Aielli^{74a,74b}, S. Akatsuka⁸⁶, T.P.A. Åkesson⁹⁷, E. Akilli⁵⁴, A.V. Akimov¹¹¹, K. Al Khoury⁶⁵, G.L. Alberghi^{23b,23a}, J. Albert¹⁷⁶, M.J. Alconada Verzini¹⁶¹, S. Alderweireldt³⁶, M. Aleksa³⁶, I.N. Aleksandrov⁸⁰, C. Alexa^{27b}, D. Alexandre¹⁹, T. Alexopoulos¹⁰, A. Alfonsi¹²⁰, M. Alhroob¹²⁹, B. Ali¹⁴², G. Alimonti^{69a}, J. Alison³⁷, S.P. Alkire¹⁴⁸, C. Allaire⁶⁵, B.M.M. Allbrooke¹⁵⁶, B.W. Allen¹³², P.P. Allport²¹, A. Aloisio^{70a,70b}, A. Alonso⁴⁰, F. Alonso⁸⁹, C. Alpigiani¹⁴⁸, A.A. Alshehri⁵⁷, M. Alvarez Estevez⁹⁹, D. Álvarez Piqueras¹⁷⁴, M.G. Alviggi^{70a,70b}, Y. Amaral Coutinho^{81b}, A. Ambler¹⁰⁴, L. Ambroz¹³⁵, C. Amelung²⁶, D. Amidei¹⁰⁶, S.P. Amor Dos Santos^{140a}, S. Amoroso⁴⁶, C.S. Amrouche⁵⁴, F. An⁷⁹, C. Anastopoulos¹⁴⁹, N. Andari¹⁴⁵, T. Andeen¹¹, C.F. Anders^{61b}, J.K. Anders²⁰, A. Andreazza^{69a,69b}, V. Andrei^{61a}, C.R. Anelli¹⁷⁶, S. Angelidakis³⁸, A. Angerami³⁹, A.V. Anisenkov^{122b,122a}, A. Annovi^{72a}, C. Antel^{61a}, M.T. Anthony¹⁴⁹, M. Antonelli⁵¹, D.J.A. Antrim¹⁷¹, F. Anulli^{73a}, M. Aoki⁸², J.A. Aparisi Pozo¹⁷⁴, L. Aperio Bella³⁶, G. Arabidze¹⁰⁷, J.P. Araque^{140a}, V. Araujo Ferraz^{81b}, R. Araujo Pereira^{81b}, C. Arcangeletti⁵¹, A.T.H. Arce⁴⁹, F.A. Arduh⁸⁹, J-F. Arguin¹¹⁰, S. Argyropoulos⁷⁸, J.-H. Arling⁴⁶, A.J. Armbruster³⁶, L.J. Armitage⁹³, A. Armstrong¹⁷¹, O. Arnæz¹⁶⁷, H. Arnold¹²⁰, A. Artamonov^{124,*}, G. Artoni¹³⁵, S. Artz¹⁰⁰, S. Asai¹⁶³, N. Asbah⁵⁹, E.M. Asimakopoulou¹⁷², L. Asquith¹⁵⁶, K. Assamagan²⁹, R. Astalos^{28a}, R.J. Atkin^{33a}, M. Atkinson¹⁷³, N.B. Atlay¹⁵¹, H. Atmani⁶⁵, K. Augsten¹⁴², G. Avolio³⁶, R. Avramidou^{60a}, M.K. Ayoub^{15a}, A.M. Azoulay^{168b}, G. Azeulov^{110,ba}, M.J. Baca²¹, H. Bachacou¹⁴⁵, K. Bachas^{68a,68b}, M. Backes¹³⁵, F. Backman^{45a,45b}, P. Bagnaia^{73a,73b}, M. Bahmani⁸⁵, H. Bahrasemani¹⁵², A.J. Bailey¹⁷⁴, V.R. Bailey¹⁷³, J.T. Baines¹⁴⁴, M. Bajic⁴⁰, C. Bakalis¹⁰, O.K. Baker¹⁸³, P.J. Bakker¹²⁰, D. Bakshi Gupta⁸, S. Balaji¹⁵⁷, E.M. Baldin^{122b,122a}, P. Balek¹⁸⁰, F. Balli¹⁴⁵, W.K. Balunas¹³⁵, J. Balz¹⁰⁰, E. Banas⁸⁵, A. Bandyopadhyay²⁴, Sw. Banerjee^{181,k}, A.A.E. Bannoura¹⁸², L. Barak¹⁶¹, W.M. Barbe³⁸, E.L. Barberio¹⁰⁵, D. Barberis^{55b,55a}, M. Barbero¹⁰², T. Barillari¹¹⁵, M-S. Barisits³⁶, J. Barkeloo¹³², T. Barklow¹⁵³, R. Barnea¹⁶⁰, S.L. Barnes^{60c}, B.M. Barnett¹⁴⁴, R.M. Barnett¹⁸, Z. Barnovska-Blenessy^{60a}, A. Baroncelli^{60a}, G. Barone²⁹, A.J. Barr¹³⁵, L. Barranco Navarro^{45a,45b}, F. Barreiro⁹⁹, J. Barreiro Guimarães da Costa^{15a}, S. Barsov¹³⁸, R. Bartoldus¹⁵³, G. Bartolini¹⁰², A.E. Barton⁹⁰, P. Bartos^{28a}, A. Basalae⁴⁶, A. Bassalat^{65,au}, R.L. Bates⁵⁷, S.J. Batista¹⁶⁷, S. Batlamous^{35e}, J.R. Batley³², B. Batool¹⁵¹, M. Battaglia¹⁴⁶, M. Baucé^{73a,73b}, F. Bauer¹⁴⁵, K.T. Bauer¹⁷¹, H.S. Bawa^{31,o}, J.B. Beacham⁴⁹, T. Beau¹³⁶, P.H. Beauchemin¹⁷⁰, F. Becherer⁵², P. Bechtel²⁴, H.C. Beck⁵³, H.P. Beck^{20,u}, K. Becker⁵², M. Becker¹⁰⁰, C. Becot⁴⁶, A. Beddall^{12d}, A.J. Beddall^{12a}, V.A. Bednyakov⁸⁰, M. Bedognetti¹²⁰, C.P. Bee¹⁵⁵, T.A. Beermann⁷⁷, M. Begalli^{81b}, M. Begel²⁹, A. Behera¹⁵⁵, J.K. Behr⁴⁶, F. Beisiegel²⁴, A.S. Bell⁹⁵, G. Bella¹⁶¹, L. Bellagamba^{23b}, A. Bellerive³⁴, P. Bellos⁹, K. Beloborodov^{122b,122a}, K. Belotskiy¹¹², N.L. Belyaev¹¹², D. Bencheekroun^{35a}, N. Benekos¹⁰, Y. Benhammou¹⁶¹, D.P. Benjamin⁶, M. Benoit⁵⁴, J.R. Bensinger²⁶, S. Bentvelsen¹²⁰, L. Beresford¹³⁵, M. Beretta⁵¹, D. Berge⁴⁶, E. Bergeaas Kuutmann¹⁷², N. Berger⁵, B. Bergmann¹⁴², L.J. Bergsten²⁶, J. Beringer¹⁸, S. Berlendis⁷, N.R. Bernard¹⁰³, G. Bernardi¹³⁶, C. Bernius¹⁵³, F.U. Bernlochner²⁴, T. Berry⁹⁴, P. Berta¹⁰⁰, C. Bertella^{15a}, I.A. Bertram⁹⁰, G.J. Besjes⁴⁰, O. Bessidskaia Bylund¹⁸², N. Besson¹⁴⁵, A. Bethani¹⁰¹, S. Bethke¹¹⁵, A. Betti²⁴, A.J. Bevan⁹³, J. Beyer¹¹⁵, R. Bi¹³⁹, R.M. Bianchi¹³⁹, O. Biebel¹¹⁴, D. Biedermann¹⁹, R. Bielski³⁶, K. Bierwagen¹⁰⁰, N.V. Biesuz^{72a,72b}, M. Biglietti^{75a}, T.R.V. Billoud¹¹⁰, M. Bindi⁵³,

A. Bingul^{12d}, C. Bini^{73a,73b}, S. Biondi^{23b,23a}, M. Birman¹⁸⁰, T. Bisanz⁵³, J.P. Biswal¹⁶¹, A. Bitadze¹⁰¹,
 C. Bittrich⁴⁸, K. Bjørke¹³⁴, K.M. Black²⁵, T. Blazek^{28a}, I. Bloch⁴⁶, C. Blocker²⁶, A. Blue⁵⁷,
 U. Blumenschein⁹³, G.J. Bobbink¹²⁰, V.S. Bobrovnikov^{122b,122a}, S.S. Bocchetta⁹⁷, A. Bocci⁴⁹,
 D. Boerner⁴⁶, D. Bogavac¹⁴, A.G. Bogdanchikov^{122b,122a}, C. Bohm^{45a}, V. Boisvert⁹⁴, P. Bokan^{53,172,53},
 T. Bold^{84a}, A.S. Boldyrev¹¹³, A.E. Bolz^{61b}, M. Bomben¹³⁶, M. Bona⁹³, J.S. Bonilla¹³², M. Boonekamp¹⁴⁵,
 H.M. Borecka-Bielska⁹¹, A. Borisov¹²³, G. Borissov⁹⁰, J. Bortfeldt³⁶, D. Bortoletto¹³⁵,
 V. Bortolotto^{74a,74b}, D. Boscherini^{23b}, M. Bosman¹⁴, J.D. Bossio Sola¹⁰⁴, K. Bouaouda^{35a}, J. Boudreau¹³⁹,
 E.V. Bouhova-Thacker⁹⁰, D. Boumediene³⁸, S.K. Boutle⁵⁷, A. Boveia¹²⁷, J. Boyd³⁶, D. Boye^{33c,av},
 I.R. Boyko⁸⁰, A.J. Bozson⁹⁴, J. Bracinik²¹, N. Brahimi¹⁰², G. Brandt¹⁸², O. Brandt^{61a}, F. Braren⁴⁶,
 B. Brau¹⁰³, J.E. Brau¹³², W.D. Breaden Madden⁵⁷, K. Brendlinger⁴⁶, L. Brenner⁴⁶, R. Brenner¹⁷²,
 S. Bressler¹⁸⁰, B. Brickwedde¹⁰⁰, D.L. Briglin²¹, D. Britton⁵⁷, D. Britzger¹¹⁵, I. Brock²⁴, R. Brock¹⁰⁷,
 G. Brooijmans³⁹, W.K. Brooks^{147d}, E. Brost¹²¹, J.H. Broughton²¹, P.A. Bruckman de Renstrom⁸⁵,
 D. Bruncko^{28b}, A. Bruni^{23b}, G. Bruni^{23b}, L.S. Bruni¹²⁰, S. Bruno^{74a,74b}, B.H. Brunt³², M. Bruschi^{23b},
 N. Bruscano¹³⁹, P. Bryant³⁷, L. Bryngemark⁹⁷, T. Buanes¹⁷, Q. Buat³⁶, P. Buchholz¹⁵¹, A.G. Buckley⁵⁷,
 I.A. Budagov⁸⁰, M.K. Bugge¹³⁴, F. Bühner⁵², O. Bulekov¹¹², T.J. Burch¹²¹, S. Burdin⁹¹, C.D. Burgard¹²⁰,
 A.M. Burger¹³⁰, B. Burghgrave⁸, J.T.P. Burr⁴⁶, J.C. Burzynski¹⁰³, V. Büscher¹⁰⁰, E. Buschmann⁵³,
 P.J. Bussey⁵⁷, J.M. Butler²⁵, C.M. Buttar⁵⁷, J.M. Butterworth⁹⁵, P. Butti³⁶, W. Buttinger³⁶, A. Buzatu¹⁵⁸,
 A.R. Buzykaev^{122b,122a}, G. Cabras^{23b,23a}, S. Cabrera Urbán¹⁷⁴, D. Caforio⁵⁶, H. Cai¹⁷³, V.M.M. Cairo¹⁵³,
 O. Cakir^{4a}, N. Calace³⁶, P. Calafiura¹⁸, A. Calandri¹⁰², G. Calderini¹³⁶, P. Calfayan⁶⁶, G. Callea⁵⁷,
 L.P. Caloba^{81b}, S. Calvente Lopez⁹⁹, D. Calvet³⁸, S. Calvet³⁸, T.P. Calvet¹⁵⁵, M. Calvetti^{72a,72b},
 R. Camacho Toro¹³⁶, S. Camarda³⁶, D. Camarero Munoz⁹⁹, P. Camarri^{74a,74b}, D. Cameron¹³⁴,
 R. Caminal Armadans¹⁰³, C. Camincher³⁶, S. Campana³⁶, M. Campanelli⁹⁵, A. Camplani⁴⁰,
 A. Campoverde¹⁵¹, V. Canale^{70a,70b}, A. Canesse¹⁰⁴, M. Cano Bret^{60c}, J. Cantero¹³⁰, T. Cao¹⁶¹, Y. Cao¹⁷³,
 M.D.M. Capeans Garrido³⁶, M. Capua^{41b,41a}, R. Cardarelli^{74a}, F. Cardillo¹⁴⁹, G. Carducci^{41b,41a},
 I. Carli¹⁴³, T. Carli³⁶, G. Carlino^{70a}, B.T. Carlson¹³⁹, L. Carminati^{69a,69b}, R.M.D. Carney^{45a,45b},
 S. Caron¹¹⁹, E. Carquin^{147d}, S. Carrá⁴⁶, J.W.S. Carter¹⁶⁷, M.P. Casado^{14,f}, A.F. Casha¹⁶⁷, D.W. Casper¹⁷¹,
 R. Castelijin¹²⁰, F.L. Castillo¹⁷⁴, V. Castillo Gimenez¹⁷⁴, N.F. Castro^{140a,140e}, A. Catinaccio³⁶,
 J.R. Catmore¹³⁴, A. Cattai³⁶, J. Caudron²⁴, V. Cavaliere²⁹, E. Cavallaro¹⁴, M. Cavalli-Sforza¹⁴,
 V. Cavasinni^{72a,72b}, E. Celebi^{12b}, F. Ceradini^{75a,75b}, L. Cerda Alberich¹⁷⁴, K. Cerny¹³¹, A.S. Cerqueira^{81a},
 A. Cerri¹⁵⁶, L. Cerrito^{74a,74b}, F. Cerutti¹⁸, A. Cervelli^{23b,23a}, S.A. Cetin^{12b}, Z. Chadi^{35a}, D. Chakraborty¹²¹,
 S.K. Chan⁵⁹, W.S. Chan¹²⁰, W.Y. Chan⁹¹, J.D. Chapman³², B. Chargeishvili^{159b}, D.G. Charlton²¹,
 T.P. Charman⁹³, C.C. Chau³⁴, S. Che¹²⁷, A. Chegwiddden¹⁰⁷, S. Chekanov⁶, S.V. Chekulaev^{168a},
 G.A. Chelkov^{80,as}, M.A. Chelstowska³⁶, B. Chen⁷⁹, C. Chen^{60a}, C.H. Chen⁷⁹, H. Chen²⁹, J. Chen^{60a},
 J. Chen³⁹, S. Chen¹³⁷, S.J. Chen^{15c}, X. Chen^{15b,az}, Y. Chen⁸³, Y-H. Chen⁴⁶, H.C. Cheng^{63a}, H.J. Cheng^{15a},
 A. Cheplakov⁸⁰, E. Cheremushkina¹²³, R. Cherkaoui El Moursli^{35e}, E. Cheu⁷, K. Cheung⁶⁴,
 T.J.A. Chevalérias¹⁴⁵, L. Chevalier¹⁴⁵, V. Chiarella⁵¹, G. Chiarelli^{72a}, G. Chiodini^{68a}, A.S. Chisholm^{36,21},
 A. Chitan^{27b}, I. Chiu¹⁶³, Y.H. Chiu¹⁷⁶, M.V. Chizhov⁸⁰, K. Choi⁶⁶, A.R. Chomont^{73a,73b}, S. Chouridou¹⁶²,
 Y.S. Chow¹²⁰, M.C. Chu^{63a}, X. Chu^{15a,15d}, J. Chudoba¹⁴¹, A.J. Chuinard¹⁰⁴, J.J. Chwastowski⁸⁵,
 L. Chytka¹³¹, K.M. Ciesla⁸⁵, D. Cinca⁴⁷, V. Cindro⁹², I.A. Cioară^{27b}, A. Ciocio¹⁸, F. Ciroto^{70a,70b},
 Z.H. Citron^{180,m}, M. Citterio^{69a}, D.A. Ciubotaru^{27b}, B.M. Ciungu¹⁶⁷, A. Clark⁵⁴, M.R. Clark³⁹,
 P.J. Clark⁵⁰, C. Clement^{45a,45b}, Y. Coadou¹⁰², M. Coba^{67a,67c}, A. Coccaro^{55b}, J. Cochran⁷⁹, H. Cohen¹⁶¹,
 A.E.C. Coimbra³⁶, L. Colasurdo¹¹⁹, B. Cole³⁹, A.P. Colijn¹²⁰, J. Collot⁵⁸, P. Conde Muñio^{140a,g},
 E. Coniavitis⁵², S.H. Connell^{33c}, I.A. Connelly⁵⁷, S. Constantinescu^{27b}, F. Conventi^{70a,bb},
 A.M. Cooper-Sarkar¹³⁵, F. Cormier¹⁷⁵, K.J.R. Cormier¹⁶⁷, L.D. Corpe⁹⁵, M. Corradi^{73a,73b},
 E.E. Corrigan⁹⁷, F. Corriveau^{104,ai}, M.J. Costa¹⁷⁴, F. Costanza⁵, D. Costanzo¹⁴⁹, G. Cowan⁹⁴,
 J.W. Cowley³², J. Crane¹⁰¹, K. Cranmer¹²⁵, S.J. Crawley⁵⁷, R.A. Creager¹³⁷, S. Crépe-Renaudin⁵⁸,
 F. Crescioli¹³⁶, M. Cristinziani²⁴, V. Croft¹²⁰, G. Crosetti^{41b,41a}, A. Cueto⁵, T. Cuhadar Donszelmann¹⁴⁹,

A.R. Cukierman¹⁵³, S. Czekerda⁸⁵, P. Czodrowski³⁶, M.J. Da Cunha Sargedas De Sousa^{60b},
 J.V. Da Fonseca Pinto^{81b}, C. Da Via¹⁰¹, W. Dabrowski^{84a}, T. Dado^{28a}, S. Dahbi^{35e}, T. Dai¹⁰⁶,
 C. Dallapiccola¹⁰³, M. Dam⁴⁰, G. D'amen^{23b,23a}, V. D'Amico^{75a,75b}, J. Damp¹⁰⁰, J.R. Dandoy¹³⁷,
 M.F. Daneri³⁰, N.P. Dang^{181,k}, N.S. Dann¹⁰¹, M. Danninger¹⁷⁵, V. Dao³⁶, G. Darbo^{55b}, O. Dartsi⁵,
 A. Dattagupta¹³², T. Daubney⁴⁶, S. D'Auria^{69a,69b}, W. Davey²⁴, C. David⁴⁶, T. Davidek¹⁴³, D.R. Davis⁴⁹,
 I. Dawson¹⁴⁹, K. De⁸, R. De Asmundis^{70a}, M. De Beurs¹²⁰, S. De Castro^{23b,23a}, S. De Cecco^{73a,73b},
 N. De Groot¹¹⁹, P. de Jong¹²⁰, H. De la Torre¹⁰⁷, A. De Maria^{15c}, D. De Pedis^{73a}, A. De Salvo^{73a},
 U. De Sanctis^{74a,74b}, M. De Santis^{74a,74b}, A. De Santo¹⁵⁶, K. De Vasconcelos Corga¹⁰²,
 J.B. De Vivie De Regie⁶⁵, C. Debenedetti¹⁴⁶, D.V. Dedovich⁸⁰, A.M. Deiana⁴², M. Del Gaudio^{41b,41a},
 J. Del Peso⁹⁹, Y. Delabat Diaz⁴⁶, D. Delgove⁶⁵, F. Deliot^{145,t}, C.M. Delitzsch⁷, M. Della Pietra^{70a,70b},
 D. Della Volpe⁵⁴, A. Dell'Acqua³⁶, L. Dell'Asta^{74a,74b}, M. Delmastro⁵, C. Delporte⁶⁵, P.A. Delsart⁵⁸,
 D.A. DeMarco¹⁶⁷, S. Demers¹⁸³, M. Demichev⁸⁰, G. Demontigny¹¹⁰, S.P. Denisov¹²³, D. Denysiuk¹²⁰,
 L. D'Eramo¹³⁶, D. Derendarz⁸⁵, J.E. Derkaoui^{35d}, F. Derue¹³⁶, P. Dervan⁹¹, K. Desch²⁴, C. Deterre⁴⁶,
 K. Dette¹⁶⁷, C. Deutsch²⁴, M.R. Devesa³⁰, P.O. Deviveiros³⁶, A. Dewhurst¹⁴⁴, S. Dhaliwal²⁶,
 F.A. Di Bello⁵⁴, A. Di Ciaccio^{74a,74b}, L. Di Ciaccio⁵, W.K. Di Clemente¹³⁷, C. Di Donato^{70a,70b},
 A. Di Girolamo³⁶, G. Di Gregorio^{72a,72b}, B. Di Micco^{75a,75b}, R. Di Nardo¹⁰³, K.F. Di Petrillo⁵⁹,
 R. Di Sipio¹⁶⁷, D. Di Valentino³⁴, C. Diaconu¹⁰², F.A. Dias⁴⁰, T. Dias Do Vale^{140a}, M.A. Diaz^{147a},
 J. Dickinson¹⁸, E.B. Diehl¹⁰⁶, J. Dietrich¹⁹, S. Díez Cornell⁴⁶, A. Dimitrievska¹⁸, W. Ding^{15b},
 J. Dingfelder²⁴, F. Dittus³⁶, F. Djama¹⁰², T. Djobava^{159b}, J.I. Djuvsland¹⁷, M.A.B. Do Vale^{81c},
 M. Dobre^{27b}, D. Dodsworth²⁶, C. Doglioni⁹⁷, J. Dolejsi¹⁴³, Z. Dolezal¹⁴³, M. Donadelli^{81d}, B. Dong^{60c},
 J. Donini³⁸, A. D'onofrio⁹³, M. D'Onofrio⁹¹, J. Dopke¹⁴⁴, A. Doria^{70a}, M.T. Dova⁸⁹, A.T. Doyle⁵⁷,
 E. Drechsler¹⁵², E. Dreyer¹⁵², T. Dreyer⁵³, A.S. Drobac¹⁷⁰, Y. Duan^{60b}, F. Dubinin¹¹¹, M. Dubovsky^{28a},
 A. Dubreuil⁵⁴, E. Duchovni¹⁸⁰, G. Duckeck¹¹⁴, A. Ducourthial¹³⁶, O.A. Ducu¹¹⁰, D. Duda¹¹⁵,
 A. Dudarev³⁶, A.C. Dudder¹⁰⁰, E.M. Duffield¹⁸, L. Dufflot⁶⁵, M. Dührssen³⁶, C. Dülsen¹⁸²,
 M. Dumancic¹⁸⁰, A.E. Dumitriu^{27b}, A.K. Duncan⁵⁷, M. Dunford^{61a}, A. Duperrin¹⁰², H. Duran Yildiz^{4a},
 M. Düren⁵⁶, A. Durglishvili^{159b}, D. Duschinger⁴⁸, B. Dutta⁴⁶, D. Duvnjak¹, G.I. Dyckes¹³⁷, M. Dyndal³⁶,
 S. Dysch¹⁰¹, B.S. Dziedzic⁸⁵, K.M. Ecker¹¹⁵, R.C. Edgar¹⁰⁶, T. Eifert³⁶, G. Eigen¹⁷, K. Einsweiler¹⁸,
 T. Ekelof¹⁷², H. El Jarrari^{35e}, M. El Kacimi^{35c}, R. El Kosseifi¹⁰², V. Ellajosyula¹⁷², M. Ellert¹⁷²,
 F. Ellinghaus¹⁸², A.A. Elliot⁹³, N. Ellis³⁶, J. Elmsheuser²⁹, M. Elsing³⁶, D. Emelianov¹⁴⁴, A. Emerman³⁹,
 Y. Enari¹⁶³, M.B. Epland⁴⁹, J. Erdmann⁴⁷, A. Ereditato²⁰, M. Errenst³⁶, M. Escalier⁶⁵, C. Escobar¹⁷⁴,
 O. Estrada Pastor¹⁷⁴, E. Etzion¹⁶¹, H. Evans⁶⁶, A. Ezhilov¹³⁸, F. Fabbri⁵⁷, L. Fabbri^{23b,23a}, V. Fabiani¹¹⁹,
 G. Facini⁹⁵, R.M. Faisca Rodrigues Pereira^{140a}, R.M. Fakhruddinov¹²³, S. Falciano^{73a}, P.J. Falke⁵,
 S. Falke⁵, J. Faltova¹⁴³, Y. Fang^{15a}, Y. Fang^{15a}, G. Fanourakis⁴⁴, M. Fanti^{69a,69b}, M. Faraj^{67a,67c,w},
 A. Farbin⁸, A. Farilla^{75a}, E.M. Farina^{71a,71b}, T. Farooque¹⁰⁷, S. Farrell¹⁸, S.M. Farrington⁵⁰, P. Farthouat³⁶,
 F. Fassi^{35e}, P. Fassnacht³⁶, D. Fassouliotis⁹, M. Fauci Giannelli⁵⁰, W.J. Fawcett³², L. Fayard⁶⁵,
 O.L. Fedin^{138,r}, W. Fedorko¹⁷⁵, M. Feickert⁴², S. Feigl¹³⁴, L. Feligioni¹⁰², A. Fell¹⁴⁹, C. Feng^{60b},
 E.J. Feng³⁶, M. Feng⁴⁹, M.J. Fenton⁵⁷, A.B. Fenyuk¹²³, J. Ferrando⁴⁶, A. Ferrante¹⁷³, A. Ferrari¹⁷²,
 P. Ferrari¹²⁰, R. Ferrari^{71a}, D.E. Ferreira de Lima^{61b}, A. Ferrer¹⁷⁴, D. Ferrere⁵⁴, C. Ferretti¹⁰⁶, F. Fiedler¹⁰⁰,
 A. Filipčič⁹², F. Filthaut¹¹⁹, K.D. Finelli²⁵, M.C.N. Fiolhais^{140a,140c,a}, L. Fiorini¹⁷⁴, F. Fischer¹¹⁴,
 W.C. Fisher¹⁰⁷, I. Fleck¹⁵¹, P. Fleischmann¹⁰⁶, R.R.M. Fletcher¹³⁷, T. Flick¹⁸², B.M. Flierl¹¹⁴, L. Flores¹³⁷,
 L.R. Flores Castillo^{63a}, F.M. Follega^{76a,76b}, N. Fomin¹⁷, J.H. Foo¹⁶⁷, G.T. Forcolin^{76a,76b}, A. Formica¹⁴⁵,
 F.A. Förster¹⁴, A.C. Forti¹⁰¹, A.G. Foster²¹, M.G. Foti¹³⁵, D. Fournier⁶⁵, H. Fox⁹⁰, P. Francavilla^{72a,72b},
 S. Francescato^{73a,73b}, M. Franchini^{23b,23a}, S. Franchino^{61a}, D. Francis³⁶, L. Franconi²⁰, M. Franklin⁵⁹,
 A.N. Fray⁹³, B. Freund¹¹⁰, W.S. Freund^{81b}, E.M. Freundlich⁴⁷, D.C. Frizzell¹²⁹, D. Froidevaux³⁶,
 J.A. Frost¹³⁵, C. Fukunaga¹⁶⁴, E. Fullana Torregrosa¹⁷⁴, E. Fumagalli^{55b,55a}, T. Fusayasu¹¹⁶, J. Fuster¹⁷⁴,
 A. Gabrielli^{23b,23a}, A. Gabrielli¹⁸, G.P. Gach^{84a}, S. Gadatsch⁵⁴, P. Gadow¹¹⁵, G. Gagliardi^{55b,55a},
 L.G. Gagnon¹¹⁰, C. Galea^{27b}, B. Galhardo^{140a}, G.E. Gallardo¹³⁵, E.J. Gallas¹³⁵, B.J. Gallop¹⁴⁴,

G. Galster⁴⁰, R. Gamboa Goni⁹³, K.K. Gan¹²⁷, S. Ganguly¹⁸⁰, J. Gao^{60a}, Y. Gao⁵⁰, Y.S. Gao^{31,o}, C. García¹⁷⁴, J.E. García Navarro¹⁷⁴, J.A. García Pascual^{15a}, C. Garcia-Argos⁵², M. Garcia-Sciveres¹⁸, R.W. Gardner³⁷, N. Garelli¹⁵³, S. Gargiulo⁵², V. Garonne¹³⁴, A. Gaudiello^{55b,55a}, G. Gaudio^{71a}, I.L. Gavrilenko¹¹¹, A. Gavriilyuk¹²⁴, C. Gay¹⁷⁵, G. Gaycken⁴⁶, E.N. Gazis¹⁰, A.A. Geanta^{27b}, C.N.P. Gee¹⁴⁴, J. Geisen⁵³, M. Geisen¹⁰⁰, M.P. Geisler^{61a}, C. Gemme^{55b}, M.H. Genest⁵⁸, C. Geng¹⁰⁶, S. Gentile^{73a,73b}, S. George⁹⁴, T. Geralis⁴⁴, L.O. Gerlach⁵³, P. Gessinger-Befurt¹⁰⁰, G. Gessner⁴⁷, S. Ghasemi¹⁵¹, M. Ghasemi Bostanabad¹⁷⁶, A. Ghosh⁶⁵, A. Ghosh⁷⁸, B. Giacobbe^{23b}, S. Giagu^{73a,73b}, N. Giangiacomi^{23b,23a}, P. Giannetti^{72a}, A. Giannini^{70a,70b}, S.M. Gibson⁹⁴, M. Gignac¹⁴⁶, D. Gillberg³⁴, G. Gilles¹⁸², D.M. Gingrich^{3,ba}, M.P. Giordani^{67a,67c}, F.M. Giorgi^{23b}, P.F. Giraud¹⁴⁵, G. Giugliarelli^{67a,67c}, D. Giugni^{69a}, F. Giuli^{74a,74b}, S. Gkaitatzis¹⁶², I. Gkialas^{9,i}, E.L. Gkoukousis¹⁴, P. Gkoutoumis¹⁰, L.K. Gladilin¹¹³, C. Glasman⁹⁹, J. Glatzer¹⁴, P.C.F. Glaysher⁴⁶, A. Glazov⁴⁶, M. Goblirsch-Kolb²⁶, S. Goldfarb¹⁰⁵, T. Golling⁵⁴, D. Golubkov¹²³, A. Gomes^{140a,140b}, R. Goncalves Gama⁵³, R. Gonçalves^{140a}, G. Gonella⁵², L. Gonella²¹, A. Gongadze⁸⁰, F. Gonnella²¹, J.L. Gonski⁵⁹, S. González de la Hoz¹⁷⁴, S. Gonzalez-Sevilla⁵⁴, G.R. Gonzalvo Rodriguez¹⁷⁴, L. Goossens³⁶, P.A. Gorbounov¹²⁴, H.A. Gordon²⁹, B. Gorini³⁶, E. Gorini^{68a,68b}, A. Gorišek⁹², A.T. Goshaw⁴⁹, M.I. Gostkin⁸⁰, C.A. Gottardo¹¹⁹, M. Goughri^{35b}, D. Goujdami^{35c}, A.G. Goussiou¹⁴⁸, N. Govender^{33c,b}, C. Goy⁵, E. Gozani¹⁶⁰, I. Grabowska-Bold^{84a}, E.C. Graham⁹¹, J. Gramling¹⁷¹, E. Gramstad¹³⁴, S. Grancagnolo¹⁹, M. Grandi¹⁵⁶, V. Gratchev¹³⁸, P.M. Gravila^{27f}, F.G. Gravili^{68a,68b}, C. Gray⁵⁷, H.M. Gray¹⁸, C. Grefe²⁴, K. Gregersen⁹⁷, I.M. Gregor⁴⁶, P. Grenier¹⁵³, K. Grevtsov⁴⁶, C. Grieco¹⁴, N.A. Grieser¹²⁹, J. Griffiths⁸, A.A. Grillo¹⁴⁶, K. Grimm^{31,n}, S. Grinstein^{14,ac}, J.-F. Grivaz⁶⁵, S. Groh¹⁰⁰, E. Gross¹⁸⁰, J. Grosse-Knetter⁵³, Z.J. Grout⁹⁵, C. Grud¹⁰⁶, A. Grummer¹¹⁸, L. Guan¹⁰⁶, W. Guan¹⁸¹, J. Guenther³⁶, A. Guerguichon⁶⁵, J.G.R. Guerrero Rojas¹⁷⁴, F. Guescini¹¹⁵, D. Guest¹⁷¹, R. Gugel⁵², T. Guillemin⁵, S. Guindon³⁶, U. Gul⁵⁷, J. Guo^{60c}, W. Guo¹⁰⁶, Y. Guo^{60a,v}, Z. Guo¹⁰², R. Gupta⁴⁶, S. Gurbuz^{12c}, G. Gustavino¹²⁹, P. Gutierrez¹²⁹, C. Gutschow⁹⁵, C. Guyot¹⁴⁵, C. Gwenlan¹³⁵, C.B. Gwilliam⁹¹, A. Haas¹²⁵, C. Haber¹⁸, H.K. Hadavand⁸, N. Haddad^{35e}, A. Hadeef^{60a}, S. Hageböck³⁶, M. Hagihara¹⁶⁹, M. Haleem¹⁷⁷, J. Haley¹³⁰, G. Halladjian¹⁰⁷, G.D. Hallelwell¹⁰², K. Hamacher¹⁸², P. Hamal¹³¹, K. Hamano¹⁷⁶, H. Hamdaoui^{35e}, G.N. Hamity¹⁴⁹, K. Han^{60a,ab}, L. Han^{60a}, S. Han^{15a}, K. Hanagaki^{82,z}, M. Hance¹⁴⁶, D.M. Handl¹¹⁴, B. Haney¹³⁷, R. Hankache¹³⁶, E. Hansen⁹⁷, J.B. Hansen⁴⁰, J.D. Hansen⁴⁰, M.C. Hansen²⁴, P.H. Hansen⁴⁰, E.C. Hanson¹⁰¹, K. Hara¹⁶⁹, A.S. Hard¹⁸¹, T. Harenberg¹⁸², S. Harkusha¹⁰⁸, P.F. Harrison¹⁷⁸, N.M. Hartmann¹¹⁴, Y. Hasegawa¹⁵⁰, A. Hasib⁵⁰, S. Hassani¹⁴⁵, S. Haug²⁰, R. Hauser¹⁰⁷, L.B. Havener³⁹, M. Havranek¹⁴², C.M. Hawkes²¹, R.J. Hawkins³⁶, D. Hayden¹⁰⁷, C. Hayes¹⁵⁵, R.L. Hayes¹⁷⁵, C.P. Hays¹³⁵, J.M. Hays⁹³, H.S. Hayward⁹¹, S.J. Haywood¹⁴⁴, F. He^{60a}, M.P. Heath⁵⁰, V. Hedberg⁹⁷, L. Heelan⁸, S. Heer²⁴, K.K. Heidegger⁵², W.D. Heidorn⁷⁹, J. Heilman³⁴, S. Heim⁴⁶, T. Heim¹⁸, B. Heinemann^{46,aw}, J.J. Heinrich¹³², L. Heinrich³⁶, C. Heinz⁵⁶, J. Hejbal¹⁴¹, L. Helary^{61b}, A. Held¹⁷⁵, S. Hellesund¹³⁴, C.M. Helling¹⁴⁶, S. Hellman^{45a,45b}, C. Helsen³⁶, R.C.W. Henderson⁹⁰, Y. Heng¹⁸¹, S. Henkelmann¹⁷⁵, A.M. Henriques Correia³⁶, G.H. Herbert¹⁹, H. Herde²⁶, V. Herget¹⁷⁷, Y. Hernández Jiménez^{33e}, H. Herr¹⁰⁰, M.G. Herrmann¹¹⁴, T. Herrmann⁴⁸, G. Herten⁵², R. Hertenberger¹¹⁴, L. Hervas³⁶, T.C. Herwig¹³⁷, G.G. Hesketh⁹⁵, N.P. Hessey^{168a}, A. Higashida¹⁶³, S. Higashino⁸², E. Higón-Rodríguez¹⁷⁴, K. Hildebrand³⁷, E. Hill¹⁷⁶, J.C. Hill³², K.K. Hill²⁹, K.H. Hiller⁴⁶, S.J. Hillier²¹, M. Hils⁴⁸, I. Hinchliffe¹⁸, F. Hinterkeuser²⁴, M. Hirose¹³³, S. Hirose⁵², D. Hirschbuehl¹⁸², B. Hiti⁹², O. Hladik¹⁴¹, D.R. Hlaluku^{33e}, X. Hoad⁵⁰, J. Hobbs¹⁵⁵, N. Hod¹⁸⁰, M.C. Hodgkinson¹⁴⁹, A. Hoecker³⁶, F. Hoenic¹¹⁴, D. Hohn⁵², D. Hohov⁶⁵, T.R. Holmes³⁷, M. Holzbock¹¹⁴, L.B.A.H. Hommels³², S. Honda¹⁶⁹, T. Honda⁸², T.M. Hong¹³⁹, A. Hönle¹¹⁵, B.H. Hooberman¹⁷³, W.H. Hopkins⁶, Y. Horii¹¹⁷, P. Horn⁴⁸, L.A. Horyn³⁷, A. Hostiuc¹⁴⁸, S. Hou¹⁵⁸, A. Hoummada^{35a}, J. Howarth¹⁰¹, J. Hoya⁸⁹, M. Hrabovsky¹³¹, J. Hrdinka⁷⁷, I. Hristova¹⁹, J. Hrivnac⁶⁵, A. Hrynevich¹⁰⁹, T. Hryn'ova⁵, P.J. Hsu⁶⁴, S.-C. Hsu¹⁴⁸, Q. Hu²⁹, S. Hu^{60c}, Y. Huang^{15a}, Z. Hubacek¹⁴², F. Hubaut¹⁰², M. Huebner²⁴, F. Huegging²⁴, T.B. Huffman¹³⁵, M. Huhtinen³⁶, R.F.H. Hunter³⁴, P. Huo¹⁵⁵, A.M. Hupe³⁴,

N. Huseynov^{80,ak}, J. Huston¹⁰⁷, J. Huth⁵⁹, R. Hyneman¹⁰⁶, S. Hyrych^{28a}, G. Iacobucci⁵⁴, G. Iakovidis²⁹, I. Ibragimov¹⁵¹, L. Iconomidou-Fayard⁶⁵, Z. Idrissi^{35e}, P. Inengo³⁶, R. Ignazzi⁴⁰, O. Igonkina^{120,ae,*}, R. Iguchi¹⁶³, T. Iizawa⁵⁴, Y. Ikegami⁸², M. Ikeno⁸², D. Iliadis¹⁶², N. Ilic^{119,167,ai}, F. Iltzsche⁴⁸, G. Introzzi^{71a,71b}, M. Iodice^{75a}, K. Iordanidou^{168a}, V. Ippolito^{73a,73b}, M.F. Isacson¹⁷², M. Ishino¹⁶³, M. Ishitsuka¹⁶⁵, W. Islam¹³⁰, C. Issever¹³⁵, S. Istin¹⁶⁰, F. Ito¹⁶⁹, J.M. Iturbe Ponce^{63a}, R. Iuppa^{76a,76b}, A. Ivina¹⁸⁰, H. Iwasaki⁸², J.M. Izen⁴³, V. Izzo^{70a}, P. Jacka¹⁴¹, P. Jackson¹, R.M. Jacobs²⁴, B.P. Jaeger¹⁵², V. Jain², G. Jäkel¹⁸², K.B. Jakobi¹⁰⁰, K. Jakobs⁵², S. Jakobsen⁷⁷, T. Jakoubek¹⁴¹, J. Jamieson⁵⁷, K.W. Janas^{84a}, R. Jansky⁵⁴, J. Janssen²⁴, M. Janus⁵³, P.A. Janus^{84a}, G. Jarlskog⁹⁷, N. Javadov^{80,ak}, T. Javûrek³⁶, M. Javurkova⁵², F. Jeanneau¹⁴⁵, L. Jeanty¹³², J. Jejelava^{159a,al}, A. Jelinskas¹⁷⁸, P. Jenni^{52,c}, J. Jeong⁴⁶, N. Jeong⁴⁶, S. Jézéquel⁵, H. Ji¹⁸¹, J. Jia¹⁵⁵, H. Jiang⁷⁹, Y. Jiang^{60a}, Z. Jiang^{153,s}, S. Jiggins⁵², F.A. Jimenez Morales³⁸, J. Jimenez Pena¹¹⁵, S. Jin^{15c}, A. Jinaru^{27b}, O. Jinnouchi¹⁶⁵, H. Jivan^{33e}, P. Johansson¹⁴⁹, K.A. Johns⁷, C.A. Johnson⁶⁶, K. Jon-And^{45a,45b}, R.W.L. Jones⁹⁰, S.D. Jones¹⁵⁶, S. Jones⁷, T.J. Jones⁹¹, J. Jongmanns^{61a}, P.M. Jorge^{140a}, J. Jovicevic³⁶, X. Ju¹⁸, J.J. Junggeburth¹¹⁵, A. Juste Rozas^{14,ac}, A. Kaczmarška⁸⁵, M. Kado^{73a,73b}, H. Kagan¹²⁷, M. Kagan¹⁵³, C. Kahra¹⁰⁰, T. Kaji¹⁷⁹, E. Kajomovitz¹⁶⁰, C.W. Kalderon⁹⁷, A. Kaluza¹⁰⁰, A. Kamenshchikov¹²³, L. Kanjir⁹², Y. Kano¹⁶³, V.A. Kantserov¹¹², J. Kanzaki⁸², L.S. Kaplan¹⁸¹, D. Kar^{33e}, M.J. Kareem^{168b}, E. Karentzos¹⁰, S.N. Karpov⁸⁰, Z.M. Karpova⁸⁰, V. Kartvelishvili⁹⁰, A.N. Karyukhin¹²³, L. Kashif¹⁸¹, R.D. Kass¹²⁷, A. Kastanas^{45a,45b}, Y. Kataoka¹⁶³, C. Kato^{60d,60c}, J. Katzy⁴⁶, K. Kawade⁸³, K. Kawagoe⁸⁸, T. Kawaguchi¹¹⁷, T. Kawamoto¹⁶³, G. Kawamura⁵³, E.F. Kay¹⁷⁶, V.F. Kazanin^{122b,122a}, R. Keeler¹⁷⁶, R. Kehoe⁴², J.S. Keller³⁴, E. Kellermann⁹⁷, D. Kelsey¹⁵⁶, J.J. Kempster²¹, J. Kendrick²¹, O. Kepka¹⁴¹, S. Kersten¹⁸², B.P. Kerševan⁹², S. Ketabchi Haghighat¹⁶⁷, M. Khader¹⁷³, F. Khalil-Zada¹³, M. Khandoga¹⁴⁵, A. Khanov¹³⁰, A.G. Kharlamov^{122b,122a}, T. Kharlamova^{122b,122a}, E.E. Khoda¹⁷⁵, A. Khodinov¹⁶⁶, T.J. Khoo⁵⁴, E. Khramov⁸⁰, J. Khubua^{159b}, S. Kido⁸³, M. Kiehn⁵⁴, C.R. Kilby⁹⁴, Y.K. Kim³⁷, N. Kimura⁹⁵, O.M. Kind¹⁹, B.T. King^{91,*}, D. Kirchmeier⁴⁸, J. Kirk¹⁴⁴, A.E. Kiryunin¹¹⁵, T. Kishimoto¹⁶³, D.P. Kisliuk¹⁶⁷, V. Kitali⁴⁶, O. Kivernyk⁵, E. Kladiva^{28b,*}, T. Klapdor-Kleingrothaus⁵², M. Klassen^{61a}, M.H. Klein¹⁰⁶, M. Klein⁹¹, U. Klein⁹¹, K. Kleinknecht¹⁰⁰, P. Klimek¹²¹, A. Klimentov²⁹, T. Klingl²⁴, T. Klioutchnikova³⁶, F.F. Klitzner¹¹⁴, P. Kluit¹²⁰, S. Kluth¹¹⁵, E. Kneringer⁷⁷, E.B.F.G. Knoop¹⁰², A. Knue⁵², D. Kobayashi⁸⁸, T. Kobayashi¹⁶³, M. Kobel⁴⁸, M. Kocian¹⁵³, P. Kodys¹⁴³, P.T. Koenig²⁴, T. Koffas³⁴, N.M. Köhler³⁶, T. Koi¹⁵³, M. Kolb^{61b}, I. Koletsou⁵, T. Komarek¹³¹, T. Kondo⁸², N. Kondrashova^{60c}, K. Köneke⁵², A.C. König¹¹⁹, T. Kono¹²⁶, R. Konoplich^{125,ar}, V. Konstantinides⁹⁵, N. Konstantinidis⁹⁵, B. Konya⁹⁷, R. Kopeliansky⁶⁶, S. Koperny^{84a}, K. Korcyl⁸⁵, K. Kordas¹⁶², G. Koren¹⁶¹, A. Korn⁹⁵, I. Korolkov¹⁴, E.V. Korolkova¹⁴⁹, N. Korotkova¹¹³, O. Kortner¹¹⁵, S. Kortner¹¹⁵, T. Kosek¹⁴³, V.V. Kostyukhin²⁴, A. Kotwal⁴⁹, A. Koulouris¹⁰, A. Kourkoumeli-Charalampidi^{71a,71b}, C. Kourkoumelis⁹, E. Kourlitis¹⁴⁹, V. Kouskoura²⁹, A.B. Kowalewska⁸⁵, R. Kowalewski¹⁷⁶, C. Kozakai¹⁶³, W. Kozanecki¹⁴⁵, A.S. Kozhin¹²³, V.A. Kramarenko¹¹³, G. Kramberger⁹², D. Krasnopevtsev^{60a}, M.W. Krasny¹³⁶, A. Krasznahorkay³⁶, D. Krauss¹¹⁵, J.A. Kremer^{84a}, J. Kretzschmar⁹¹, P. Krieger¹⁶⁷, F. Krieter¹¹⁴, A. Krishnan^{61b}, K. Krizka¹⁸, K. Kroeninger⁴⁷, H. Kroha¹¹⁵, J. Kroll¹⁴¹, J. Kroll¹³⁷, J. Krstic¹⁶, U. Kruchonak⁸⁰, H. Krüger²⁴, N. Krumnack⁷⁹, M.C. Kruse⁴⁹, J.A. Krzysiak⁸⁵, T. Kubota¹⁰⁵, O. Kuchinskaia¹⁶⁶, S. Kудay^{4b}, J.T. Kuechler⁴⁶, S. Kuehn³⁶, A. Kugel^{61a}, T. Kuhl⁴⁶, V. Kukhtin⁸⁰, R. Kukla¹⁰², Y. Kulchitsky^{108,ao}, S. Kuleshov^{147d}, Y.P. Kulinich¹⁷³, M. Kuna⁵⁸, T. Kunigo⁸⁶, A. Kupco¹⁴¹, T. Kupfer⁴⁷, O. Kuprash⁵², H. Kurashige⁸³, L.L. Kurchaninov^{168a}, Y.A. Kurochkin¹⁰⁸, A. Kurova¹¹², M.G. Kurth^{15a,15d}, E.S. Kuwertz³⁶, M. Kuze¹⁶⁵, A.K. Kvam¹⁴⁸, J. Kvita¹³¹, T. Kwan¹⁰⁴, A. La Rosa¹¹⁵, L. La Rotonda^{41b,41a}, F. La Ruffa^{41b,41a}, C. Lacasta¹⁷⁴, F. Lacava^{73a,73b}, D.P.J. Lack¹⁰¹, H. Lacker¹⁹, D. Lacour¹³⁶, E. Ladygin⁸⁰, R. Lafaye⁵, B. Laforge¹³⁶, T. Lagouri^{33e}, S. Lai⁵³, S. Lammers⁶⁶, W. Lampl⁷, C. Lampoudis¹⁶², E. Lançon²⁹, U. Landgraf⁵², M.P.J. Landon⁹³, M.C. Lanfermann⁵⁴, V.S. Lang⁴⁶, J.C. Lange⁵³, R.J. Langenberg³⁶, A.J. Lankford¹⁷¹, F. Lanni²⁹, K. Lantzscht²⁴, A. Lanza^{71a}, A. Lapertosa^{55b,55a}, S. Laplace¹³⁶, J.F. Laporte¹⁴⁵, T. Lari^{69a}, F. Lasagni Manghi^{23b,23a}, M. Lassnig³⁶,

T.S. Lau^{63a}, A. Laudrain⁶⁵, A. Laurier³⁴, M. Lavorgna^{70a,70b}, M. Lazzaroni^{69a,69b}, B. Le¹⁰⁵, E. Le Guirriec¹⁰², M. LeBlanc⁷, T. LeCompte⁶, F. Ledroit-Guillon⁵⁸, C.A. Lee²⁹, G.R. Lee¹⁷, L. Lee⁵⁹, S.C. Lee¹⁵⁸, S.J. Lee³⁴, B. Lefebvre^{168a}, M. Lefebvre¹⁷⁶, F. Legger¹¹⁴, C. Leggett¹⁸, K. Lehmann¹⁵², N. Lehmann¹⁸², G. Lehmann Miotto³⁶, W.A. Leight⁴⁶, A. Leisos^{162,aa}, M.A.L. Leite^{81d}, C.E. Leitgeb¹¹⁴, R. Leitner¹⁴³, D. Lellouch^{180,*}, K.J.C. Leney⁴², T. Lenz²⁴, B. Lenzi³⁶, R. Leone⁷, S. Leone^{72a}, C. Leonidopoulos⁵⁰, A. Leopold¹³⁶, G. Lerner¹⁵⁶, C. Leroy¹¹⁰, R. Les¹⁶⁷, C.G. Lester³², M. Levchenko¹³⁸, J. Levêque⁵, D. Levin¹⁰⁶, L.J. Levinson¹⁸⁰, D.J. Lewis²¹, B. Li^{15b}, B. Li¹⁰⁶, C-Q. Li^{60a}, F. Li^{60c}, H. Li^{60a}, H. Li^{60b}, J. Li^{60c}, K. Li¹⁵³, L. Li^{60c}, M. Li^{15a,15d}, Q. Li^{15a,15d}, Q.Y. Li^{60a}, S. Li^{60d,60c}, X. Li⁴⁶, Y. Li⁴⁶, Z. Li^{60b}, Z. Liang^{15a}, B. Liberti^{74a}, A. Liblong¹⁶⁷, K. Lie^{63c}, S. Liem¹²⁰, C.Y. Lin³², K. Lin¹⁰⁷, T.H. Lin¹⁰⁰, R.A. Linck⁶⁶, J.H. Lindon²¹, A.L. Lioni⁵⁴, E. Lipeles¹³⁷, A. Lipniacka¹⁷, M. Lisovyi^{61b}, T.M. Liss^{173,ay}, A. Lister¹⁷⁵, A.M. Litke¹⁴⁶, J.D. Little⁸, B. Liu^{79,ah}, B.L. Liu⁶, H.B. Liu²⁹, H. Liu¹⁰⁶, J.B. Liu^{60a}, J.K.K. Liu¹³⁵, K. Liu¹³⁶, M. Liu^{60a}, P. Liu¹⁸, Y. Liu^{15a,15d}, Y.L. Liu¹⁰⁶, Y.W. Liu^{60a}, M. Livan^{71a,71b}, A. Lleres⁵⁸, J. Llorente Merino^{15a}, S.L. Lloyd⁹³, C.Y. Lo^{63b}, F. Lo Sterzo⁴², E.M. Lobodzinska⁴⁶, P. Loch⁷, S. Loffredo^{74a,74b}, T. Lohse¹⁹, K. Lohwasser¹⁴⁹, M. Lokajicek¹⁴¹, J.D. Long¹⁷³, R.E. Long⁹⁰, L. Longo³⁶, K.A. Looper¹²⁷, J.A. Lopez^{147d}, I. Lopez Paz¹⁰¹, A. Lopez Solis¹⁴⁹, J. Lorenz¹¹⁴, N. Lorenzo Martinez⁵, M. Losada^{22a}, P.J. Lösel¹¹⁴, A. Lösle⁵², X. Lou⁴⁶, X. Lou^{15a}, A. Lounis⁶⁵, J. Love⁶, P.A. Love⁹⁰, J.J. Lozano Bahilo¹⁷⁴, M. Lu^{60a}, Y.J. Lu⁶⁴, H.J. Lubatti¹⁴⁸, C. Luci^{73a,73b}, A. Lucotte⁵⁸, C. Luedtke⁵², F. Luehring⁶⁶, I. Luise¹³⁶, L. Luminari^{73a}, B. Lund-Jensen¹⁵⁴, M.S. Lutz¹⁰³, D. Lynn²⁹, R. Lysak¹⁴¹, E. Lytken⁹⁷, F. Lyu^{15a}, V. Lyubushkin⁸⁰, T. Lyubushkina⁸⁰, H. Ma²⁹, L.L. Ma^{60b}, Y. Ma^{60b}, G. Maccarrone⁵¹, A. Macchiolo¹¹⁵, C.M. Macdonald¹⁴⁹, J. Machado Miguens¹³⁷, D. Madaffari¹⁷⁴, R. Madar³⁸, W.F. Mader⁴⁸, N. Madysa⁴⁸, J. Maeda⁸³, K. Maekawa¹⁶³, S. Maeland¹⁷, T. Maeno²⁹, M. Maerker⁴⁸, A.S. Maevskiy¹¹³, V. Magerl⁵², N. Magini⁷⁹, D.J. Mahon³⁹, C. Maidantchik^{81b}, T. Maier¹¹⁴, A. Maio^{140a,140b,140d}, K. Maj⁸⁵, O. Majersky^{28a}, S. Majewski¹³², Y. Makida⁸², N. Makovec⁶⁵, B. Malaescu¹³⁶, Pa. Malecki⁸⁵, V.P. Maleev¹³⁸, F. Malek⁵⁸, U. Mallik⁷⁸, D. Malon⁶, C. Malone³², S. Maltezos¹⁰, S. Malyukov⁸⁰, J. Mamuzic¹⁷⁴, G. Mancini⁵¹, I. Mandić⁹², L. Manhaes de Andrade Filho^{81a}, I.M. Maniatis¹⁶², J. Manjarres Ramos⁴⁸, K.H. Mankinen⁹⁷, A. Mann¹¹⁴, A. Manousos⁷⁷, B. Mansoulie¹⁴⁵, I. Manthos¹⁶², S. Manzoni¹²⁰, A. Marantis¹⁶², G. Marceca³⁰, L. Marchese¹³⁵, G. Marchiori¹³⁶, M. Marcisovsky¹⁴¹, C. Marcon⁹⁷, C.A. Marin Tobon³⁶, M. Marjanovic³⁸, Z. Marshall¹⁸, M.U.F. Martensson¹⁷², S. Marti-Garcia¹⁷⁴, C.B. Martin¹²⁷, T.A. Martin¹⁷⁸, V.J. Martin⁵⁰, B. Martin dit Latour¹⁷, L. Martinelli^{75a,75b}, M. Martinez^{14,ac}, V.I. Martinez Outschoorn¹⁰³, S. Martin-Haugh¹⁴⁴, V.S. Martoiu^{27b}, A.C. Martyniuk⁹⁵, A. Marzin³⁶, S.R. Maschek¹¹⁵, L. Masetti¹⁰⁰, T. Mashimo¹⁶³, R. Mashinistov¹¹¹, J. Masik¹⁰¹, A.L. Maslennikov^{122b,122a}, L.H. Mason¹⁰⁵, L. Massa^{74a,74b}, P. Massarotti^{70a,70b}, P. Mastrandrea^{72a,72b}, A. Mastroberardino^{41b,41a}, T. Masubuchi¹⁶³, D. Matakias¹⁰, A. Matic¹¹⁴, P. Mättig²⁴, J. Maurer^{27b}, B. Maček⁹², D.A. Maximov^{122b,122a}, R. Mazini¹⁵⁸, I. Maznas¹⁶², S.M. Mazza¹⁴⁶, S.P. Mc Kee¹⁰⁶, T.G. McCarthy¹¹⁵, L.I. McClymont⁹⁵, W.P. McCormack¹⁸, E.F. McDonald¹⁰⁵, J.A. Mcfayden³⁶, M.A. McKay⁴², K.D. McLean¹⁷⁶, S.J. McMahan¹⁴⁴, P.C. McNamara¹⁰⁵, C.J. McNicol¹⁷⁸, R.A. McPherson^{176,ai}, J.E. Mdhului^{33e}, Z.A. Meadows¹⁰³, S. Meehan¹⁴⁸, T. Megy⁵², S. Mehlhase¹¹⁴, A. Mehta⁹¹, T. Meideck⁵⁸, B. Meirose⁴³, D. Melini¹⁷⁴, B.R. Mellado Garcia^{33e}, J.D. Mellenthin⁵³, M. Melo^{28a}, F. Meloni⁴⁶, A. Melzer²⁴, S.B. Menary¹⁰¹, E.D. Mendes Gouveia^{140a,140e}, L. Meng³⁶, X.T. Meng¹⁰⁶, S. Menke¹¹⁵, E. Meoni^{41b,41a}, S. Mergelmeyer¹⁹, S.A.M. Merkt¹³⁹, C. Merlassino²⁰, P. Mermod⁵⁴, L. Merola^{70a,70b}, C. Meroni^{69a}, O. Meshkov^{113,111}, J.K.R. Meshreki¹⁵¹, A. Messina^{73a,73b}, J. Metcalfe⁶, A.S. Mete¹⁷¹, C. Meyer⁶⁶, J. Meyer¹⁶⁰, J-P. Meyer¹⁴⁵, H. Meyer Zu Theenhausen^{61a}, F. Miano¹⁵⁶, M. Michetti¹⁹, R.P. Middleton¹⁴⁴, L. Mijović⁵⁰, G. Mikenberg¹⁸⁰, M. Mikestikova¹⁴¹, M. Mikuš⁹², H. Mildner¹⁴⁹, M. Milesi¹⁰⁵, A. Milic¹⁶⁷, D.A. Millar⁹³, D.W. Miller³⁷, A. Milov¹⁸⁰, D.A. Milstead^{45a,45b}, R.A. Mina^{153,s}, A.A. Minaenko¹²³, M. Miñano Moya¹⁷⁴, I.A. Minashvili^{159b}, A.I. Mincer¹²⁵, B. Mindur^{84a}, M. Mineev⁸⁰, Y. Minegishi¹⁶³, Y. Ming¹⁸¹, L.M. Mir¹⁴, A. Mirto^{68a,68b}, K.P. Mistry¹³⁷, T. Mitani¹⁷⁹, J. Mitrevski¹¹⁴,

V.A. Mitsou¹⁷⁴, M. Mittal^{60c}, A. Miucci²⁰, P.S. Miyagawa¹⁴⁹, A. Mizukami⁸², J.U. Mjörnmark⁹⁷, T. Mkrtchyan¹⁸⁴, M. Mlynarikova¹⁴³, T. Moa^{45a,45b}, K. Mochizuki¹¹⁰, P. Mogg⁵², S. Mohapatra³⁹, R. Moles-Valls²⁴, M.C. Mondragon¹⁰⁷, K. Mönig⁴⁶, J. Monk⁴⁰, E. Monnier¹⁰², A. Montalbano¹⁵², J. Montejó Berlingen³⁶, M. Montella⁹⁵, F. Monticelli⁸⁹, S. Monzani^{69a}, N. Morange⁶⁵, D. Moreno^{22a}, M. Moreno Llácer³⁶, C. Moreno Martínez¹⁴, P. Morettini^{55b}, M. Morgenstern¹²⁰, S. Morgenstern⁴⁸, D. Mori¹⁵², M. Morii⁵⁹, M. Morinaga¹⁷⁹, V. Morisbak¹³⁴, A.K. Morley³⁶, G. Mornacchi³⁶, A.P. Morris⁹⁵, L. Morvaj¹⁵⁵, P. Moschovakos³⁶, B. Moser¹²⁰, M. Mosidze^{159b}, T. Moskalets¹⁴⁵, H.J. Moss¹⁴⁹, J. Moss^{31,p}, K. Motohashi¹⁶⁵, E. Mountricha³⁶, E.J.W. Moyse¹⁰³, S. Muanza¹⁰², J. Mueller¹³⁹, R.S.P. Mueller¹¹⁴, D. Muenstermann⁹⁰, G.A. Mullier⁹⁷, J.L. Muñoz Martínez¹⁴, F.J. Muñoz Sánchez¹⁰¹, P. Murin^{28b}, W.J. Murray^{178,144}, A. Murrone^{69a,69b}, M. Muškinja¹⁸, C. Mwewa^{33a}, A.G. Myagkov^{123,as}, J. Myers¹³², M. Myska¹⁴², B.P. Nachman¹⁸, O. Nackenhorst⁴⁷, A.Nag Nag⁴⁸, K. Nagai¹³⁵, K. Nagano⁸², Y. Nagasaka⁶², M. Nagel⁵², E. Nagy¹⁰², A.M. Nairz³⁶, Y. Nakahama¹¹⁷, K. Nakamura⁸², T. Nakamura¹⁶³, I. Nakano¹²⁸, H. Nanjo¹³³, F. Napolitano^{61a}, R.F. Naranjo García⁴⁶, R. Narayan⁴², I. Naryshkin¹³⁸, T. Naumann⁴⁶, G. Navarro^{22a}, H.A. Neal^{106,*}, P.Y. Nechaeva¹¹¹, F. Nechansky⁴⁶, T.J. Neep²¹, A. Negri^{71a,71b}, M. Negrini^{23b}, C. Nellist⁵³, M.E. Nelson¹³⁵, S. Nemecek¹⁴¹, P. Nemethy¹²⁵, M. Nessi^{36,e}, M.S. Neubauer¹⁷³, M. Neumann¹⁸², P.R. Newman²¹, Y.S. Ng¹⁹, Y.W.Y. Ng¹⁷¹, H.D.N. Nguyen¹⁰², T. Nguyen Manh¹¹⁰, E. Nibigira³⁸, R.B. Nickerson¹³⁵, R. Nicolaidou¹⁴⁵, D.S. Nielsen⁴⁰, J. Nielsen¹⁴⁶, N. Nikiforou¹¹, V. Nikolaenko^{123,as}, I. Nikolic-Audit¹³⁶, K. Nikolopoulos²¹, P. Nilsson²⁹, H.R. Nindhito⁵⁴, Y. Ninomiya⁸², A. Nisati^{73a}, N. Nishu^{60c}, R. Nisius¹¹⁵, I. Nitsche⁴⁷, T. Nitta¹⁷⁹, T. Nobe¹⁶³, Y. Noguchi⁸⁶, I. Nomidis¹³⁶, M.A. Nomura²⁹, M. Nordberg³⁶, N. Norjoharuddeen¹³⁵, T. Novak⁹², O. Novgorodova⁴⁸, R. Novotny¹⁴², L. Nozka¹³¹, K. Ntekas¹⁷¹, E. Nurse⁹⁵, F.G. Oakham^{34,ba}, H. Oberlack¹¹⁵, J. Ocariz¹³⁶, A. Ochi⁸³, I. Ochoa³⁹, J.P. Ochoa-Ricoux^{147a}, K. O'Connor²⁶, S. Oda⁸⁸, S. Odaka⁸², S. Oerdek⁵³, A. Ogrodnik^{84a}, A. Oh¹⁰¹, S.H. Oh⁴⁹, C.C. Ohm¹⁵⁴, H. Oide^{55b,55a}, M.L. Ojeda¹⁶⁷, H. Okawa¹⁶⁹, Y. Okazaki⁸⁶, Y. Okumura¹⁶³, T. Okuyama⁸², A. Olariu^{27b}, L.F. Oleiro Seabra^{140a}, S.A. Olivares Pino^{147a}, D. Oliveira Damazio²⁹, J.L. Oliver¹, M.J.R. Olsson¹⁷¹, A. Olszewski⁸⁵, J. Olszowska⁸⁵, D.C. O'Neil¹⁵², A. Onofre^{140a,140e}, K. Onogi¹¹⁷, P.U.E. Onyisi¹¹, H. Oppen¹³⁴, M.J. Oreglia³⁷, G.E. Orellana⁸⁹, D. Orestano^{75a,75b}, N. Orlando¹⁴, R.S. Orr¹⁶⁷, V. O'Shea⁵⁷, R. Ospanov^{60a}, G. Otero y Garzon³⁰, H. Otono⁸⁸, P.S. Ott^{61a}, M. Ouchrif^{35d}, J. Ouellette²⁹, F. Ould-Saada¹³⁴, A. Ouraou¹⁴⁵, Q. Ouyang^{15a}, M. Owen⁵⁷, R.E. Owen²¹, V.E. Ozcan^{12c}, N. Ozturk⁸, J. Pacalt¹³¹, H.A. Pacey³², K. Pachal⁴⁹, A. Pacheco Pages¹⁴, C. Padilla Aranda¹⁴, S. Pagan Griso¹⁸, M. Paganini¹⁸³, G. Palacino⁶⁶, S. Palazzo⁵⁰, S. Palestini³⁶, M. Palka^{84b}, D. Pallin³⁸, I. Panagoulas¹⁰, C.E. Pandini³⁶, J.G. Panduro Vazquez⁹⁴, P. Pani⁴⁶, G. Panizzo^{67a,67c}, L. Paolozzi⁵⁴, C. Papadatos¹¹⁰, K. Papageorgiou^{9,i}, A. Paramonov⁶, D. Paredes Hernandez^{63b}, S.R. Paredes Saenz¹³⁵, B. Parida¹⁶⁶, T.H. Park¹⁶⁷, A.J. Parker⁹⁰, M.A. Parker³², F. Parodi^{55b,55a}, E.W. Parrish¹²¹, J.A. Parsons³⁹, U. Parzefall⁵², L. Pascual Dominguez¹³⁶, V.R. Pascuzzi¹⁶⁷, J.M.P. Pasner¹⁴⁶, E. Pasqualucci^{73a}, S. Passaggio^{55b}, F. Pastore⁹⁴, P. Pasuwan^{45a,45b}, S. Pataria¹⁰⁰, J.R. Pater¹⁰¹, A. Pathak¹⁸¹, T. Pauly³⁶, B. Pearson¹¹⁵, M. Pedersen¹³⁴, L. Pedraza Diaz¹¹⁹, R. Pedro^{140a}, T. Peiffer⁵³, S.V. Peleganchuk^{122b,122a}, O. Penc¹⁴¹, H. Peng^{60a}, B.S. Peralva^{81a}, M.M. Perego⁶⁵, A.P. Pereira Peixoto^{140a}, D.V. Perepelitsa²⁹, F. Peri¹⁹, L. Perini^{69a,69b}, H. Pernegger³⁶, S. Perrella^{70a,70b}, K. Peters⁴⁶, R.F.Y. Peters¹⁰¹, B.A. Petersen³⁶, T.C. Petersen⁴⁰, E. Petit¹⁰², A. Petridis¹, C. Petridou¹⁶², P. Petroff⁶⁵, M. Petrov¹³⁵, F. Petrucci^{75a,75b}, M. Pettee¹⁸³, N.E. Pettersson¹⁰³, K. Petukhova¹⁴³, A. Peyaud¹⁴⁵, R. Pezoa^{147d}, L. Pezzotti^{71a,71b}, T. Pham¹⁰⁵, F.H. Phillips¹⁰⁷, P.W. Phillips¹⁴⁴, M.W. Phipps¹⁷³, G. Piacquadio¹⁵⁵, E. Pianori¹⁸, A. Picazio¹⁰³, R.H. Pickles¹⁰¹, R. Piegaia³⁰, D. Pietreanu^{27b}, J.E. Pilcher³⁷, A.D. Pilkington¹⁰¹, M. Pinamonti^{74a,74b}, J.L. Pinfold³, M. Pitt¹⁸⁰, L. Pizzimento^{74a,74b}, M.-A. Pleier²⁹, V. Pleskot¹⁴³, E. Plotnikova⁸⁰, P. Podberezko^{122b,122a}, R. Poettgen⁹⁷, R. Poggi⁵⁴, L. Poggioli⁶⁵, I. Pogrebnyak¹⁰⁷, D. Pohl²⁴, I. Pokharel⁵³, G. Polesello^{71a}, A. Poley¹⁸, A. Policicchio^{73a,73b}, R. Polifka¹⁴³, A. Polini^{23b}, C.S. Pollard⁴⁶, V. Polychronakos²⁹, D. Ponomarenko¹¹², L. Pontecorvo³⁶, S. Popa^{27a}, G.A. Popeneciu^{27d}, D.M. Portillo Quintero⁵⁸,

S. Pospisil¹⁴², K. Potamianos⁴⁶, I.N. Potrap⁸⁰, C.J. Potter³², H. Potti¹¹, T. Poulsen⁹⁷, J. Poveda³⁶, T.D. Powell¹⁴⁹, G. Pownall⁴⁶, M.E. Pozo Astigarraga³⁶, P. Pralavorio¹⁰², S. Prell⁷⁹, D. Price¹⁰¹, M. Primavera^{68a}, S. Prince¹⁰⁴, M.L. Proffitt¹⁴⁸, N. Proklova¹¹², K. Prokofiev^{63c}, F. Prokoshin⁸⁰, S. Protopopescu²⁹, J. Proudfoot⁶, M. Przybycien^{84a}, D. Pudzha¹³⁸, A. Puri¹⁷³, P. Puzo⁶⁵, J. Qian¹⁰⁶, Y. Qin¹⁰¹, A. Quadt⁵³, M. Queitsch-Maitland⁴⁶, A. Qureshi¹, P. Rados¹⁰⁵, F. Ragusa^{69a,69b}, G. Rahal⁹⁸, J.A. Raine⁵⁴, S. Rajagopalan²⁹, A. Ramirez Morales⁹³, K. Ran^{15a,15d}, T. Rashid⁶⁵, S. Raspopov⁵, D.M. Rauch⁴⁶, F. Rauscher¹¹⁴, S. Rave¹⁰⁰, B. Ravina¹⁴⁹, I. Ravinovich¹⁸⁰, J.H. Rawling¹⁰¹, M. Raymond³⁶, A.L. Read¹³⁴, N.P. Readioff⁵⁸, M. Reale^{68a,68b}, D.M. Rebuzzi^{71a,71b}, A. Redelbach¹⁷⁷, G. Redlinger²⁹, K. Reeves⁴³, L. Rehnisch¹⁹, J. Reichert¹³⁷, D. Reikher¹⁶¹, A. Reiss¹⁰⁰, A. Rej¹⁵¹, C. Rembser³⁶, M. Renda^{27b}, M. Rescigno^{73a}, S. Resconi^{69a}, E.D. Resseguie¹³⁷, S. Rettie¹⁷⁵, E. Reynolds²¹, O.L. Rezanova^{122b,122a}, P. Reznicek¹⁴³, E. Ricci^{76a,76b}, R. Richter¹¹⁵, S. Richter⁴⁶, E. Richter-Was^{84b}, O. Ricken²⁴, M. Ridel¹³⁶, P. Rieck¹¹⁵, C.J. Riegel¹⁸², O. Rifki⁴⁶, M. Rijssenbeek¹⁵⁵, A. Rimoldi^{71a,71b}, M. Rimoldi⁴⁶, L. Rinaldi^{23b}, G. Ripellino¹⁵⁴, B. Ristic⁹⁰, I. Riu¹⁴, J.C. Rivera Vergara¹⁷⁶, F. Rizatdinova¹³⁰, E. Rizvi⁹³, C. Rizzi³⁶, R.T. Roberts¹⁰¹, S.H. Robertson^{104,ai}, M. Robin⁴⁶, D. Robinson³², J.E.M. Robinson⁴⁶, C.M. Robles Gajardo^{147d}, A. Robson⁵⁷, E. Rocco¹⁰⁰, C. Roda^{72a,72b}, S. Rodriguez Bosca¹⁷⁴, A. Rodriguez Perez¹⁴, D. Rodriguez Rodriguez¹⁷⁴, A.M. Rodríguez Vera^{168b}, S. Roe³⁶, O. Røhne¹³⁴, R. Röhrig¹¹⁵, C.P.A. Roland⁶⁶, J. Roloff⁵⁹, A. Romaniouk¹¹², M. Romano^{23b,23a}, N. Rompotis⁹¹, M. Ronzani¹²⁵, L. Roos¹³⁶, S. Rosati^{73a}, K. Rosbach⁵², G. Rosin¹⁰³, B.J. Rosser¹³⁷, E. Rossi⁴⁶, E. Rossi^{75a,75b}, E. Rossi^{70a,70b}, L.P. Rossi^{55b}, L. Rossini^{69a,69b}, R. Rosten¹⁴, M. Rotaru^{27b}, J. Rothberg¹⁴⁸, D. Rousseau⁶⁵, G. Rovelli^{71a,71b}, A. Roy¹¹, D. Roy^{33e}, A. Rozanov¹⁰², Y. Rozen¹⁶⁰, X. Ruan^{33e}, F. Rubbo¹⁵³, F. Rühr⁵², A. Ruiz-Martinez¹⁷⁴, A. Rummeler³⁶, Z. Rurikova⁵², N.A. Rusakovich⁸⁰, H.L. Russell¹⁰⁴, L. Rustige^{38,47}, J.P. Rutherford⁷, E.M. Rüttinger^{46,1}, M. Rybar³⁹, G. Rybkin⁶⁵, E.B. Rye¹³⁴, A. Ryzhov¹²³, G.F. Rzehorz⁵³, P. Sabatini⁵³, G. Sabato¹²⁰, S. Sacerdoti⁶⁵, H.F.W. Sadrozinski¹⁴⁶, R. Sadykov⁸⁰, F. Safai Tehrani^{73a}, B. Safarzadeh Samani¹⁵⁶, P. Saha¹²¹, S. Saha¹⁰⁴, M. Sahinsoy^{61a}, A. Sahu¹⁸², M. Saimpert⁴⁶, M. Saito¹⁶³, T. Saito¹⁶³, H. Sakamoto¹⁶³, A. Sakharov^{125,ar}, D. Salamani⁵⁴, G. Salamanna^{75a,75b}, J.E. Salazar Loyola^{147d}, P.H. Sales De Bruin¹⁷², A. Salmikov¹⁵³, J. Salt¹⁷⁴, D. Salvatore^{41b,41a}, F. Salvatore¹⁵⁶, A. Salvucci^{63a,63b,63c}, A. Salzburger³⁶, J. Samarati³⁶, D. Sammel⁵², D. Sampsonidis¹⁶², D. Sampsonidou¹⁶², J. Sánchez¹⁷⁴, A. Sanchez Pineda^{67a,67c}, H. Sandaker¹³⁴, C.O. Sander⁴⁶, I.G. Sanderswood⁹⁰, M. Sandhoff¹⁸², C. Sandoval^{22a}, D.P.C. Sankey¹⁴⁴, M. Sannino^{55b,55a}, Y. Sano¹¹⁷, A. Sansoni⁵¹, C. Santoni³⁸, H. Santos^{140a,140b}, S.N. Santpur¹⁸, A. Santra¹⁷⁴, A. Saprnov⁸⁰, J.G. Saraiva^{140a,140d}, O. Sasaki⁸², K. Sato¹⁶⁹, E. Sauvan⁵, P. Savard^{167,ba}, N. Savic¹¹⁵, R. Sawada¹⁶³, C. Sawyer¹⁴⁴, L. Sawyer^{96,ap}, C. Sbarra^{23b}, A. Sbrizzi^{23a}, T. Scanlon⁹⁵, J. Schaarschmidt¹⁴⁸, P. Schacht¹¹⁵, B.M. Schachtner¹¹⁴, D. Schaefer³⁷, L. Schaefer¹³⁷, J. Schaeffer¹⁰⁰, S. Schaepe³⁶, U. Schäfer¹⁰⁰, A.C. Schaffer⁶⁵, D. Schaile¹¹⁴, R.D. Schamberger¹⁵⁵, N. Scharmberg¹⁰¹, V.A. Schegelsky¹³⁸, D. Scheirich¹⁴³, F. Schenck¹⁹, M. Schernau¹⁷¹, C. Schiavi^{55b,55a}, S. Schier¹⁴⁶, L.K. Schildgen²⁴, Z.M. Schillaci²⁶, E.J. Schioppa³⁶, M. Schioppa^{41b,41a}, K.E. Schleicher⁵², S. Schlenker³⁶, K.R. Schmidt-Sommerfeld¹¹⁵, K. Schmieden³⁶, C. Schmitt¹⁰⁰, S. Schmitt⁴⁶, S. Schmitz¹⁰⁰, J.C. Schmoedel⁴⁶, U. Schnoor⁵², L. Schoeffel¹⁴⁵, A. Schoening^{61b}, P.G. Scholer⁵², E. Schopf¹³⁵, M. Schott¹⁰⁰, J.F.P. Schouwenberg¹¹⁹, J. Schovancova³⁶, S. Schramm⁵⁴, F. Schroeder¹⁸², A. Schulte¹⁰⁰, H-C. Schultz-Coulon^{61a}, M. Schumacher⁵², B.A. Schumm¹⁴⁶, Ph. Schune¹⁴⁵, A. Schwartzman¹⁵³, T.A. Schwarz¹⁰⁶, Ph. Schwemling¹⁴⁵, R. Schwienhorst¹⁰⁷, A. Sciandra¹⁴⁶, G. Sciolla²⁶, M. Scodreggio⁴⁶, M. Scornajenghi^{41b,41a}, F. Scuri^{72a}, F. Scutti¹⁰⁵, L.M. Scyboz¹¹⁵, C.D. Sebastiani^{73a,73b}, P. Seema¹⁹, S.C. Seidel¹¹⁸, A. Seiden¹⁴⁶, T. Seiss³⁷, J.M. Seixas^{81b}, G. Sekhniaidze^{70a}, K. Sekhon¹⁰⁶, S.J. Sekula⁴², N. Semprini-Cesari^{23b,23a}, S. Sen⁴⁹, S. Senkin³⁸, C. Serfon⁷⁷, L. Serin⁶⁵, L. Serkin^{67a,67b}, M. Sessa^{60a}, H. Severini¹²⁹, T. Šfiligoj⁹², F. Sforza¹⁷⁰, A. Sfyrla⁵⁴, E. Shabalina⁵³, J.D. Shahinian¹⁴⁶, N.W. Shaikh^{45a,45b}, D. Shaked Renous¹⁸⁰, L.Y. Shan^{15a}, R. Shang¹⁷³, J.T. Shank²⁵, M. Shapiro¹⁸, A. Sharma¹³⁵, A.S. Sharma¹, P.B. Shatalov¹²⁴, K. Shaw¹⁵⁶, S.M. Shaw¹⁰¹, A. Shcherbakova¹³⁸,

Y. Shen¹²⁹, N. Sherafati³⁴, A.D. Sherman²⁵, P. Sherwood⁹⁵, L. Shi^{158,ax}, S. Shimizu⁸², C.O. Shimmin¹⁸³,
 Y. Shimogama¹⁷⁹, M. Shimojima¹¹⁶, I.P.J. Shipsey¹³⁵, S. Shirabe⁸⁸, M. Shiyakova^{80,af}, J. Shlomi¹⁸⁰,
 A. Shmeleva¹¹¹, M.J. Shochet³⁷, J. Shojaii¹⁰⁵, D.R. Shope¹²⁹, S. Shrestha¹²⁷, E.M. Shrif^{33e}, E. Shulga¹⁸⁰,
 P. Sicho¹⁴¹, A.M. Sickles¹⁷³, P.E. Sidebo¹⁵⁴, E. Sideras Haddad^{33e}, O. Sidiropoulou³⁶, A. Sidoti^{23b,23a},
 F. Siegert⁴⁸, Dj. Sijacki¹⁶, M.Jr. Silva¹⁸¹, M.V. Silva Oliveira^{81a}, S.B. Silverstein^{45a}, S. Simion⁶⁵,
 E. Simioni¹⁰⁰, R. Simoniello¹⁰⁰, S. Simsek^{12b}, P. Sinervo¹⁶⁷, V. Sinetckii^{113,111}, N.B. Sinev¹³²,
 M. Sioli^{23b,23a}, I. Siral¹⁰⁶, S.Yu. Sivoklov¹¹³, J. Sjölin^{45a,45b}, E. Skorda⁹⁷, P. Skubic¹²⁹, M. Slawinska⁸⁵,
 K. Sliwa¹⁷⁰, R. Slovak¹⁴³, V. Smakhtin¹⁸⁰, B.H. Smart¹⁴⁴, J. Smiesko^{28a}, N. Smirnov¹¹²,
 S.Yu. Smirnov¹¹², Y. Smirnov¹¹², L.N. Smirnova^{113,x}, O. Smirnova⁹⁷, J.W. Smith⁵³, M. Smizanska⁹⁰,
 K. Smolek¹⁴², A. Smykiewicz⁸⁵, A.A. Snesarev¹¹¹, H.L. Snoek¹²⁰, I.M. Snyder¹³², S. Snyder²⁹,
 R. Sobie^{176,ai}, A.M. Soffa¹⁷¹, A. Soffer¹⁶¹, A. Søggaard⁵⁰, F. Sohns⁵³, C.A. Solans Sanchez³⁶,
 E.Yu. Soldatov¹¹², U. Soldevila¹⁷⁴, A.A. Solodkov¹²³, A. Soloshenko⁸⁰, O.V. Solovyanov¹²³,
 V. Solovyev¹³⁸, P. Sommer¹⁴⁹, H. Son¹⁷⁰, W. Song¹⁴⁴, W.Y. Song^{168b}, A. Sopczak¹⁴², F. Sopkova^{28b},
 C.L. Sotiropoulou^{72a,72b}, S. Sottocornola^{71a,71b}, R. Soualah^{67a,67c,h}, A.M. Soukharev^{122b,122a}, D. South⁴⁶,
 S. Spagnolo^{68a,68b}, M. Spalla¹¹⁵, M. Spangenberg¹⁷⁸, F. Spanò⁹⁴, D. Sperlich⁵², T.M. Spieker^{61a},
 R. Spighi^{23b}, G. Spigo³⁶, M. Spina¹⁵⁶, D.P. Spiteri⁵⁷, M. Spousta¹⁴³, A. Stabile^{69a,69b}, B.L. Stamas¹²¹,
 R. Stamen^{61a}, M. Stamenkovic¹²⁰, E. Stanecka⁸⁵, R.W. Stanek⁶, B. Stanislaus¹³⁵, M.M. Stanitzki⁴⁶,
 M. Stankaityte¹³⁵, B. Stapf¹²⁰, E.A. Starchenko¹²³, G.H. Stark¹⁴⁶, J. Stark⁵⁸, S.H. Stark⁴⁰, P. Staroba¹⁴¹,
 P. Starovoitov^{61a}, S. Stärz¹⁰⁴, R. Staszewski⁸⁵, G. Stavropoulos⁴⁴, M. Stegler⁴⁶, P. Steinberg²⁹,
 A.L. Steinhebel¹³², B. Stelzer¹⁵², H.J. Stelzer¹³⁹, O. Stelzer-Chilton^{168a}, H. Stenzel⁵⁶, T.J. Stevenson¹⁵⁶,
 G.A. Stewart³⁶, M.C. Stockton³⁶, G. Stoicea^{27b}, M. Stolarski^{140a}, P. Stolte⁵³, S. Stonjek¹¹⁵,
 A. Straessner⁴⁸, J. Strandberg¹⁵⁴, S. Strandberg^{45a,45b}, M. Strauss¹²⁹, P. Strizenec^{28b}, R. Ströhmer¹⁷⁷,
 D.M. Strom¹³², R. Stroynowski⁴², A. Strubig⁵⁰, S.A. Stucci²⁹, B. Stugu¹⁷, J. Stupak¹²⁹, N.A. Styles⁴⁶,
 D. Su¹⁵³, S. Sucheck^{61a}, V.V. Sulin¹¹¹, M.J. Sullivan⁹¹, D.M.S. Sultan⁵⁴, S. Sultansoy^{4c}, T. Sumida⁸⁶,
 S. Sun¹⁰⁶, X. Sun³, K. Suruliz¹⁵⁶, C.J.E. Suster¹⁵⁷, M.R. Sutton¹⁵⁶, S. Suzuki⁸², M. Svatos¹⁴¹,
 M. Swiatlowski³⁷, S.P. Swift², T. Swirski¹⁷⁷, A. Sydorenko¹⁰⁰, I. Sykora^{28a}, M. Sykora¹⁴³, T. Sykora¹⁴³,
 D. Ta¹⁰⁰, K. Tackmann^{46,ad}, J. Taenzer¹⁶¹, A. Taffard¹⁷¹, R. Tafirout^{168a}, H. Takai²⁹, R. Takashima⁸⁷,
 K. Takeda⁸³, T. Takeshita¹⁵⁰, E.P. Takeva⁵⁰, Y. Takubo⁸², M. Talby¹⁰², A.A. Talyshev^{122b,122a},
 N.M. Tamir¹⁶¹, J. Tanaka¹⁶³, M. Tanaka¹⁶⁵, R. Tanaka⁶⁵, S. Tapia Araya¹⁷³, S. Tapprogge¹⁰⁰,
 A. Tarek Abouelfadl Mohamed¹³⁶, S. Tarem¹⁶⁰, G. Tarna^{27b,d}, G.F. Tartarelli^{69a}, P. Tas¹⁴³, M. Tasevsky¹⁴¹,
 T. Tashiro⁸⁶, E. Tassi^{41b,41a}, A. Tavares Delgado^{140a,140b}, Y. Tayalati^{35e}, A.J. Taylor⁵⁰, G.N. Taylor¹⁰⁵,
 W. Taylor^{168b}, A.S. Tee⁹⁰, R. Teixeira De Lima¹⁵³, P. Teixeira-Dias⁹⁴, H. Ten Kate³⁶, J.J. Teoh¹²⁰,
 S. Terada⁸², K. Terashi¹⁶³, J. Terron⁹⁹, S. Terzo¹⁴, M. Testa⁵¹, R.J. Teuscher^{167,ai}, S.J. Thais¹⁸³,
 T. Theveneaux-Pelzer⁴⁶, F. Thiele⁴⁰, D.W. Thomas⁹⁴, J.O. Thomas⁴², J.P. Thomas²¹, A.S. Thompson⁵⁷,
 P.D. Thompson²¹, L.A. Thomsen¹⁸³, E. Thomson¹³⁷, E.J. Thorpe⁹³, Y. Tian³⁹, R.E. Ticse Torres⁵³,
 V.O. Tikhomirov^{111,at}, Yu.A. Tikhonov^{122b,122a}, S. Timoshenko¹¹², P. Tipton¹⁸³, S. Tisserant¹⁰²,
 K. Todome^{23b,23a}, S. Todorova-Nova⁵, S. Todt⁴⁸, J. Tojo⁸⁸, S. Tokár^{28a}, K. Tokushuku⁸², E. Tolley¹²⁷,
 K.G. Tomiwa^{33e}, M. Tomoto¹¹⁷, L. Tompkins^{153,s}, B. Tong⁵⁹, P. Tornambe¹⁰³, E. Torrence¹³², H. Torres⁴⁸,
 E. Torró Pastor¹⁴⁸, C. Tosciri¹³⁵, J. Toth^{102,ag}, D.R. Tovey¹⁴⁹, A. Traeet¹⁷, C.J. Treado¹²⁵, T. Trefzger¹⁷⁷,
 F. Tresoldi¹⁵⁶, A. Tricoli²⁹, I.M. Trigger^{168a}, S. Trincaz-Duvoid¹³⁶, W. Trischuk¹⁶⁷, B. Trocme⁵⁸,
 A. Trofymov¹⁴⁵, C. Troncon^{69a}, M. Trovatelli¹⁷⁶, F. Trovato¹⁵⁶, L. Truong^{33c}, M. Trzebinski⁸⁵,
 A. Trzupek⁸⁵, F. Tsai⁴⁶, J.C.-L. Tseng¹³⁵, P.V. Tsiareshka^{108,ao}, A. Tsirigotis¹⁶², N. Tsirintanis⁹,
 V. Tsiskaridze¹⁵⁵, E.G. Tskhadadze^{159a}, M. Tsopoulou¹⁶², I.I. Tsukerman¹²⁴, V. Tsulaia¹⁸, S. Tsuno⁸²,
 D. Tsybychev¹⁵⁵, Y. Tu^{63b}, A. Tudorache^{27b}, V. Tudorache^{27b}, T.T. Tulbure^{27a}, A.N. Tuna⁵⁹,
 S. Turchikhin⁸⁰, D. Turgeman¹⁸⁰, I. Turk Cakir^{4b,y}, R.J. Turner²¹, R. Turra^{69a}, P.M. Tuts³⁹, S. Tzamarias¹⁶²,
 E. Tzovara¹⁰⁰, G. Uccielli⁴⁷, K. Uchida¹⁶³, I. Ueda⁸², M. Ughetto^{45a,45b}, F. Ukegawa¹⁶⁹, G. Unal³⁶,
 A. Undrus²⁹, G. Unel¹⁷¹, F.C. Ungaro¹⁰⁵, Y. Unno⁸², K. Uno¹⁶³, J. Urban^{28b}, P. Urquijo¹⁰⁵, G. Usai⁸,

J. Usui⁸², Z. Uysal^{12d}, L. Vacavant¹⁰², V. Vacek¹⁴², B. Vachon¹⁰⁴, K.O.H. Vadla¹³⁴, A. Vaidya⁹⁵,
 C. Valderanis¹¹⁴, E. Valdes Santurio^{45a,45b}, M. Valente⁵⁴, S. Valentinetti^{23b,23a}, A. Valero¹⁷⁴, L. Valéry⁴⁶,
 R.A. Vallance²¹, A. Vallier³⁶, J.A. Valls Ferrer¹⁷⁴, T.R. Van Daalen¹⁴, P. Van Gemmeren⁶,
 I. Van Vulpen¹²⁰, M. Vanadia^{74a,74b}, W. Vandelli³⁶, A. Vaniachine¹⁶⁶, D. Vannicola^{73a,73b}, R. Vari^{73a},
 E.W. Varnes⁷, C. Varni^{55b,55a}, T. Varol⁴², D. Varouchas⁶⁵, K.E. Varvell¹⁵⁷, M.E. Vasile^{27b},
 G.A. Vasquez¹⁷⁶, J.G. Vasquez¹⁸³, F. Vazeille³⁸, D. Vazquez Furelos¹⁴, T. Vazquez Schroeder³⁶,
 J. Veatch⁵³, V. Vecchio^{75a,75b}, M.J. Veen¹²⁰, L.M. Veloce¹⁶⁷, F. Veloso^{140a,140c}, S. Veneziano^{73a},
 A. Ventura^{68a,68b}, N. Venturi³⁶, A. Verbytskyi¹¹⁵, V. Vercesi^{71a}, M. Verducci^{72a,72b}, C.M. Vergel Infante⁷⁹,
 C. Vergis²⁴, W. Verkerke¹²⁰, A.T. Vermeulen¹²⁰, J.C. Vermeulen¹²⁰, M.C. Vetterli^{152,ba},
 N. Viaux Maira^{147d}, M. Vicente Barreto Pinto⁵⁴, T. Vickey¹⁴⁹, O.E. Vickey Boeriu¹⁴⁹,
 G.H.A. Viehhauser¹³⁵, L. Vigani^{61b}, M. Villa^{23b,23a}, M. Villaplana Perez^{69a,69b}, E. Vilucchi⁵¹,
 M.G. Vinciter³⁴, V.B. Vinogradov⁸⁰, A. Vishwakarma⁴⁶, C. Vittori^{23b,23a}, I. Vivarelli¹⁵⁶, M. Vogel¹⁸²,
 P. Vokac¹⁴², S.E. von Buddenbrock^{33e}, E. Von Toerne²⁴, V. Vorobel¹⁴³, K. Vorobev¹¹², M. Vos¹⁷⁴,
 J.H. Vossebeld⁹¹, M. Vozak¹⁰¹, N. Vranjes¹⁶, M. Vranjes Milosavljevic¹⁶, V. Vrba¹⁴², M. Vreeswijk¹²⁰,
 R. Vuillermet³⁶, I. Vukotic³⁷, P. Wagner²⁴, W. Wagner¹⁸², J. Wagner-Kuhr¹¹⁴, S. Wahdan¹⁸²,
 H. Wahlberg⁸⁹, K. Wakamiya⁸³, V.M. Walbrecht¹¹⁵, J. Walder⁹⁰, R. Walker¹¹⁴, S.D. Walker⁹⁴,
 W. Walkowiak¹⁵¹, V. Wallangen^{45a,45b}, A.M. Wang⁵⁹, C. Wang^{60c}, C. Wang^{60b}, F. Wang¹⁸¹, H. Wang¹⁸,
 H. Wang³, J. Wang¹⁵⁷, J. Wang^{61b}, P. Wang⁴², Q. Wang¹²⁹, R.-J. Wang¹⁰⁰, R. Wang^{60a}, R. Wang⁶,
 S.M. Wang¹⁵⁸, W.T. Wang^{60a}, W. Wang^{15c,aj}, W.X. Wang^{60a,aj}, Y. Wang^{60a,aq}, Z. Wang^{60c},
 C. Wanotayaroj⁴⁶, A. Warburton¹⁰⁴, C.P. Ward³², D.R. Wardrope⁹⁵, N. Warrack⁵⁷, A. Washbrook⁵⁰,
 A.T. Watson²¹, M.F. Watson²¹, G. Watts¹⁴⁸, B.M. Waugh⁹⁵, A.F. Webb¹¹, S. Webb¹⁰⁰, C. Weber¹⁸³,
 M.S. Weber²⁰, S.A. Weber³⁴, S.M. Weber^{61a}, A.R. Weidberg¹³⁵, J. Weingarten⁴⁷, M. Weirich¹⁰⁰,
 C. Weiser⁵², P.S. Wells³⁶, T. Wenaus²⁹, T. Wengler³⁶, S. Wenig³⁶, N. Wermes²⁴, M.D. Werner⁷⁹,
 M. Wessels^{61a}, T.D. Weston²⁰, K. Whalen¹³², N.L. Whallon¹⁴⁸, A.M. Wharton⁹⁰, A.S. White¹⁰⁶,
 A. White⁸, M.J. White¹, D. Whiteson¹⁷¹, B.W. Whitmore⁹⁰, W. Wiedenmann¹⁸¹, M. Wielers¹⁴⁴,
 N. Wieseotte¹⁰⁰, C. Wiglesworth⁴⁰, L.A.M. Wiik-Fuchs⁵², F. Wilk¹⁰¹, H.G. Wilkens³⁶, L.J. Wilkins⁹⁴,
 H.H. Williams¹³⁷, S. Williams³², C. Willis¹⁰⁷, S. Willocq¹⁰³, J.A. Wilson²¹, I. Wingerter-Seez⁵,
 E. Winkels¹⁵⁶, F. Winklmeier¹³², O.J. Winston¹⁵⁶, B.T. Winter⁵², M. Wittgen¹⁵³, M. Wobisch⁹⁶,
 A. Wolf¹⁰⁰, T.M.H. Wolf¹²⁰, R. Wolff¹⁰², R. Wölker¹³⁵, J. Wollrath⁵², M.W. Wolter⁸⁵, H. Wolters^{140a,140c},
 V.W.S. Wong¹⁷⁵, N.L. Woods¹⁴⁶, S.D. Worm²¹, B.K. Wosiek⁸⁵, K.W. Woźniak⁸⁵, K. Wraight⁵⁷,
 S.L. Wu¹⁸¹, X. Wu⁵⁴, Y. Wu^{60a}, T.R. Wyatt¹⁰¹, B.M. Wynne⁵⁰, S. Xella⁴⁰, Z. Xi¹⁰⁶, L. Xia¹⁷⁸, D. Xu^{15a},
 H. Xu^{60a,d}, L. Xu²⁹, T. Xu¹⁴⁵, W. Xu¹⁰⁶, Z. Xu^{60b}, Z. Xu¹⁵³, B. Yabsley¹⁵⁷, S. Yacoub^{33a}, K. Yajima¹³³,
 D.P. Yallup⁹⁵, D. Yamaguchi¹⁶⁵, Y. Yamaguchi¹⁶⁵, A. Yamamoto⁸², F. Yamane⁸³, M. Yamatani¹⁶³,
 T. Yamazaki¹⁶³, Y. Yamazaki⁸³, Z. Yan²⁵, H.J. Yang^{60c,60d}, H.T. Yang¹⁸, S. Yang⁷⁸, X. Yang^{60b,58},
 Y. Yang¹⁶³, W.-M. Yao¹⁸, Y.C. Yap⁴⁶, Y. Yasu⁸², E. Yatsenko^{60c,60d}, J. Ye⁴², S. Ye²⁹, I. Yeletsikh⁸⁰,
 M.R. Yexley⁹⁰, E. Yigitbasi²⁵, K. Yorita¹⁷⁹, K. Yoshihara¹³⁷, C.J.S. Young³⁶, C. Young¹⁵³, J. Yu⁷⁹,
 R. Yuan^{60b,j}, X. Yue^{61a}, S.P.Y. Yuen²⁴, B. Zabinski⁸⁵, G. Zacharis¹⁰, E. Zaffaroni⁵⁴, J. Zahreddine¹³⁶,
 A.M. Zaitsev^{123,as}, T. Zakareishvili^{159b}, N. Zakharchuk³⁴, S. Zambito⁵⁹, D. Zanzi³⁶, D.R. Zaripovas⁵⁷,
 S.V. Zeißner⁴⁷, C. Zeitnitz¹⁸², G. Zemaityte¹³⁵, J.C. Zeng¹⁷³, O. Zenin¹²³, T. Ženiš^{28a}, D. Zerwas⁶⁵,
 M. Zgubic¹³⁵, D.F. Zhang^{15b}, F. Zhang¹⁸¹, G. Zhang^{60a}, G. Zhang^{15b}, H. Zhang^{15c}, J. Zhang⁶, L. Zhang^{15c},
 L. Zhang^{60a}, M. Zhang¹⁷³, R. Zhang^{60a}, R. Zhang²⁴, X. Zhang^{60b}, Y. Zhang^{15a,15d}, Z. Zhang^{63a},
 Z. Zhang⁶⁵, P. Zhao⁴⁹, Y. Zhao^{60b}, Z. Zhao^{60a}, A. Zhemchugov⁸⁰, Z. Zheng¹⁰⁶, D. Zhong¹⁷³, B. Zhou¹⁰⁶,
 C. Zhou¹⁸¹, M.S. Zhou^{15a,15d}, M. Zhou¹⁵⁵, N. Zhou^{60c}, Y. Zhou⁷, C.G. Zhu^{60b}, H.L. Zhu^{60a}, H. Zhu^{15a},
 J. Zhu¹⁰⁶, Y. Zhu^{60a}, X. Zhuang^{15a}, K. Zhukov¹¹¹, V. Zhulanov^{122b,122a}, D. Zieminska⁶⁶, N.I. Zimine⁸⁰,
 S. Zimmermann⁵², Z. Zinonos¹¹⁵, M. Ziolkowski¹⁵¹, L. Živković¹⁶, G. Zoernig¹⁸¹, A. Zoccoli^{23b,23a},
 K. Zoch⁵³, T.G. Zorbas¹⁴⁹, R. Zou³⁷, L. Zwalinski³⁶.

- ¹Department of Physics, University of Adelaide, Adelaide; Australia.
- ²Physics Department, SUNY Albany, Albany NY; United States of America.
- ³Department of Physics, University of Alberta, Edmonton AB; Canada.
- ⁴(^a)Department of Physics, Ankara University, Ankara; (^b)Istanbul Aydin University, Application and Research Center for Advanced Studies, Istanbul; (^c)Division of Physics, TOBB University of Economics and Technology, Ankara; Turkey.
- ⁵LAPP, Université Grenoble Alpes, Université Savoie Mont Blanc, CNRS/IN2P3, Annecy; France.
- ⁶High Energy Physics Division, Argonne National Laboratory, Argonne IL; United States of America.
- ⁷Department of Physics, University of Arizona, Tucson AZ; United States of America.
- ⁸Department of Physics, University of Texas at Arlington, Arlington TX; United States of America.
- ⁹Physics Department, National and Kapodistrian University of Athens, Athens; Greece.
- ¹⁰Physics Department, National Technical University of Athens, Zografou; Greece.
- ¹¹Department of Physics, University of Texas at Austin, Austin TX; United States of America.
- ¹²(^a)Bahcesehir University, Faculty of Engineering and Natural Sciences, Istanbul; (^b)Istanbul Bilgi University, Faculty of Engineering and Natural Sciences, Istanbul; (^c)Department of Physics, Bogazici University, Istanbul; (^d)Department of Physics Engineering, Gaziantep University, Gaziantep; Turkey.
- ¹³Institute of Physics, Azerbaijan Academy of Sciences, Baku; Azerbaijan.
- ¹⁴Institut de Física d'Altes Energies (IFAE), Barcelona Institute of Science and Technology, Barcelona; Spain.
- ¹⁵(^a)Institute of High Energy Physics, Chinese Academy of Sciences, Beijing; (^b)Physics Department, Tsinghua University, Beijing; (^c)Department of Physics, Nanjing University, Nanjing; (^d)University of Chinese Academy of Science (UCAS), Beijing; China.
- ¹⁶Institute of Physics, University of Belgrade, Belgrade; Serbia.
- ¹⁷Department for Physics and Technology, University of Bergen, Bergen; Norway.
- ¹⁸Physics Division, Lawrence Berkeley National Laboratory and University of California, Berkeley CA; United States of America.
- ¹⁹Institut für Physik, Humboldt Universität zu Berlin, Berlin; Germany.
- ²⁰Albert Einstein Center for Fundamental Physics and Laboratory for High Energy Physics, University of Bern, Bern; Switzerland.
- ²¹School of Physics and Astronomy, University of Birmingham, Birmingham; United Kingdom.
- ²²(^a)Facultad de Ciencias y Centro de Investigaciones, Universidad Antonio Nariño, Bogotá; (^b)Departamento de Física, Universidad Nacional de Colombia, Bogotá, Colombia; Colombia.
- ²³(^a)INFN Bologna and Università di Bologna, Dipartimento di Fisica; (^b)INFN Sezione di Bologna; Italy.
- ²⁴Physikalisches Institut, Universität Bonn, Bonn; Germany.
- ²⁵Department of Physics, Boston University, Boston MA; United States of America.
- ²⁶Department of Physics, Brandeis University, Waltham MA; United States of America.
- ²⁷(^a)Transilvania University of Brasov, Brasov; (^b)Horia Hulubei National Institute of Physics and Nuclear Engineering, Bucharest; (^c)Department of Physics, Alexandru Ioan Cuza University of Iasi, Iasi; (^d)National Institute for Research and Development of Isotopic and Molecular Technologies, Physics Department, Cluj-Napoca; (^e)University Politehnica Bucharest, Bucharest; (^f)West University in Timisoara, Timisoara; Romania.
- ²⁸(^a)Faculty of Mathematics, Physics and Informatics, Comenius University, Bratislava; (^b)Department of Subnuclear Physics, Institute of Experimental Physics of the Slovak Academy of Sciences, Kosice; Slovak Republic.
- ²⁹Physics Department, Brookhaven National Laboratory, Upton NY; United States of America.
- ³⁰Departamento de Física, Universidad de Buenos Aires, Buenos Aires; Argentina.
- ³¹California State University, CA; United States of America.

- ³²Cavendish Laboratory, University of Cambridge, Cambridge; United Kingdom.
- ^{33(a)}Department of Physics, University of Cape Town, Cape Town;^(b)iThemba Labs, Western Cape;^(c)Department of Mechanical Engineering Science, University of Johannesburg, Johannesburg;^(d)University of South Africa, Department of Physics, Pretoria;^(e)School of Physics, University of the Witwatersrand, Johannesburg; South Africa.
- ³⁴Department of Physics, Carleton University, Ottawa ON; Canada.
- ^{35(a)}Faculté des Sciences Ain Chock, Réseau Universitaire de Physique des Hautes Energies - Université Hassan II, Casablanca;^(b)Faculté des Sciences, Université Ibn-Tofail, Kénitra;^(c)Faculté des Sciences Semlalia, Université Cadi Ayyad, LPHEA-Marrakech;^(d)Faculté des Sciences, Université Mohamed Premier and LPTPM, Oujda;^(e)Faculté des sciences, Université Mohammed V, Rabat; Morocco.
- ³⁶CERN, Geneva; Switzerland.
- ³⁷Enrico Fermi Institute, University of Chicago, Chicago IL; United States of America.
- ³⁸LPC, Université Clermont Auvergne, CNRS/IN2P3, Clermont-Ferrand; France.
- ³⁹Nevis Laboratory, Columbia University, Irvington NY; United States of America.
- ⁴⁰Niels Bohr Institute, University of Copenhagen, Copenhagen; Denmark.
- ^{41(a)}Dipartimento di Fisica, Università della Calabria, Rende;^(b)INFN Gruppo Collegato di Cosenza, Laboratori Nazionali di Frascati; Italy.
- ⁴²Physics Department, Southern Methodist University, Dallas TX; United States of America.
- ⁴³Physics Department, University of Texas at Dallas, Richardson TX; United States of America.
- ⁴⁴National Centre for Scientific Research "Demokritos", Agia Paraskevi; Greece.
- ^{45(a)}Department of Physics, Stockholm University;^(b)Oskar Klein Centre, Stockholm; Sweden.
- ⁴⁶Deutsches Elektronen-Synchrotron DESY, Hamburg and Zeuthen; Germany.
- ⁴⁷Lehrstuhl für Experimentelle Physik IV, Technische Universität Dortmund, Dortmund; Germany.
- ⁴⁸Institut für Kern- und Teilchenphysik, Technische Universität Dresden, Dresden; Germany.
- ⁴⁹Department of Physics, Duke University, Durham NC; United States of America.
- ⁵⁰SUPA - School of Physics and Astronomy, University of Edinburgh, Edinburgh; United Kingdom.
- ⁵¹INFN e Laboratori Nazionali di Frascati, Frascati; Italy.
- ⁵²Physikalisches Institut, Albert-Ludwigs-Universität Freiburg, Freiburg; Germany.
- ⁵³II. Physikalisches Institut, Georg-August-Universität Göttingen, Göttingen; Germany.
- ⁵⁴Département de Physique Nucléaire et Corpusculaire, Université de Genève, Genève; Switzerland.
- ^{55(a)}Dipartimento di Fisica, Università di Genova, Genova;^(b)INFN Sezione di Genova; Italy.
- ⁵⁶II. Physikalisches Institut, Justus-Liebig-Universität Giessen, Giessen; Germany.
- ⁵⁷SUPA - School of Physics and Astronomy, University of Glasgow, Glasgow; United Kingdom.
- ⁵⁸LPSC, Université Grenoble Alpes, CNRS/IN2P3, Grenoble INP, Grenoble; France.
- ⁵⁹Laboratory for Particle Physics and Cosmology, Harvard University, Cambridge MA; United States of America.
- ^{60(a)}Department of Modern Physics and State Key Laboratory of Particle Detection and Electronics, University of Science and Technology of China, Hefei;^(b)Institute of Frontier and Interdisciplinary Science and Key Laboratory of Particle Physics and Particle Irradiation (MOE), Shandong University, Qingdao;^(c)School of Physics and Astronomy, Shanghai Jiao Tong University, KLPPAC-MoE, SKLPPC, Shanghai;^(d)Tsung-Dao Lee Institute, Shanghai; China.
- ^{61(a)}Kirchhoff-Institut für Physik, Ruprecht-Karls-Universität Heidelberg, Heidelberg;^(b)Physikalisches Institut, Ruprecht-Karls-Universität Heidelberg, Heidelberg; Germany.
- ⁶²Faculty of Applied Information Science, Hiroshima Institute of Technology, Hiroshima; Japan.
- ^{63(a)}Department of Physics, Chinese University of Hong Kong, Shatin, N.T., Hong Kong;^(b)Department of Physics, University of Hong Kong, Hong Kong;^(c)Department of Physics and Institute for Advanced Study, Hong Kong University of Science and Technology, Clear Water Bay, Kowloon, Hong Kong; China.

- ⁶⁴Department of Physics, National Tsing Hua University, Hsinchu; Taiwan.
- ⁶⁵IJCLab, Université Paris-Saclay, CNRS/IN2P3, 91405, Orsay; France.
- ⁶⁶Department of Physics, Indiana University, Bloomington IN; United States of America.
- ⁶⁷(^a)INFN Gruppo Collegato di Udine, Sezione di Trieste, Udine; (^b)ICTP, Trieste; (^c)Dipartimento Politecnico di Ingegneria e Architettura, Università di Udine, Udine; Italy.
- ⁶⁸(^a)INFN Sezione di Lecce; (^b)Dipartimento di Matematica e Fisica, Università del Salento, Lecce; Italy.
- ⁶⁹(^a)INFN Sezione di Milano; (^b)Dipartimento di Fisica, Università di Milano, Milano; Italy.
- ⁷⁰(^a)INFN Sezione di Napoli; (^b)Dipartimento di Fisica, Università di Napoli, Napoli; Italy.
- ⁷¹(^a)INFN Sezione di Pavia; (^b)Dipartimento di Fisica, Università di Pavia, Pavia; Italy.
- ⁷²(^a)INFN Sezione di Pisa; (^b)Dipartimento di Fisica E. Fermi, Università di Pisa, Pisa; Italy.
- ⁷³(^a)INFN Sezione di Roma; (^b)Dipartimento di Fisica, Sapienza Università di Roma, Roma; Italy.
- ⁷⁴(^a)INFN Sezione di Roma Tor Vergata; (^b)Dipartimento di Fisica, Università di Roma Tor Vergata, Roma; Italy.
- ⁷⁵(^a)INFN Sezione di Roma Tre; (^b)Dipartimento di Matematica e Fisica, Università Roma Tre, Roma; Italy.
- ⁷⁶(^a)INFN-TIFPA; (^b)Università degli Studi di Trento, Trento; Italy.
- ⁷⁷Institut für Astro- und Teilchenphysik, Leopold-Franzens-Universität, Innsbruck; Austria.
- ⁷⁸University of Iowa, Iowa City IA; United States of America.
- ⁷⁹Department of Physics and Astronomy, Iowa State University, Ames IA; United States of America.
- ⁸⁰Joint Institute for Nuclear Research, Dubna; Russia.
- ⁸¹(^a)Departamento de Engenharia Elétrica, Universidade Federal de Juiz de Fora (UFJF), Juiz de Fora; (^b)Universidade Federal do Rio De Janeiro COPPE/EE/IF, Rio de Janeiro; (^c)Universidade Federal de São João del Rei (UFSJ), São João del Rei; (^d)Instituto de Física, Universidade de São Paulo, São Paulo; Brazil.
- ⁸²KEK, High Energy Accelerator Research Organization, Tsukuba; Japan.
- ⁸³Graduate School of Science, Kobe University, Kobe; Japan.
- ⁸⁴(^a)AGH University of Science and Technology, Faculty of Physics and Applied Computer Science, Krakow; (^b)Marian Smoluchowski Institute of Physics, Jagiellonian University, Krakow; Poland.
- ⁸⁵Institute of Nuclear Physics Polish Academy of Sciences, Krakow; Poland.
- ⁸⁶Faculty of Science, Kyoto University, Kyoto; Japan.
- ⁸⁷Kyoto University of Education, Kyoto; Japan.
- ⁸⁸Research Center for Advanced Particle Physics and Department of Physics, Kyushu University, Fukuoka ; Japan.
- ⁸⁹Instituto de Física La Plata, Universidad Nacional de La Plata and CONICET, La Plata; Argentina.
- ⁹⁰Physics Department, Lancaster University, Lancaster; United Kingdom.
- ⁹¹Oliver Lodge Laboratory, University of Liverpool, Liverpool; United Kingdom.
- ⁹²Department of Experimental Particle Physics, Jožef Stefan Institute and Department of Physics, University of Ljubljana, Ljubljana; Slovenia.
- ⁹³School of Physics and Astronomy, Queen Mary University of London, London; United Kingdom.
- ⁹⁴Department of Physics, Royal Holloway University of London, Egham; United Kingdom.
- ⁹⁵Department of Physics and Astronomy, University College London, London; United Kingdom.
- ⁹⁶Louisiana Tech University, Ruston LA; United States of America.
- ⁹⁷Fysiska institutionen, Lunds universitet, Lund; Sweden.
- ⁹⁸Centre de Calcul de l'Institut National de Physique Nucléaire et de Physique des Particules (IN2P3), Villeurbanne; France.
- ⁹⁹Departamento de Física Teórica C-15 and CIAFF, Universidad Autónoma de Madrid, Madrid; Spain.
- ¹⁰⁰Institut für Physik, Universität Mainz, Mainz; Germany.
- ¹⁰¹School of Physics and Astronomy, University of Manchester, Manchester; United Kingdom.

- ¹⁰²CPPM, Aix-Marseille Université, CNRS/IN2P3, Marseille; France.
- ¹⁰³Department of Physics, University of Massachusetts, Amherst MA; United States of America.
- ¹⁰⁴Department of Physics, McGill University, Montreal QC; Canada.
- ¹⁰⁵School of Physics, University of Melbourne, Victoria; Australia.
- ¹⁰⁶Department of Physics, University of Michigan, Ann Arbor MI; United States of America.
- ¹⁰⁷Department of Physics and Astronomy, Michigan State University, East Lansing MI; United States of America.
- ¹⁰⁸B.I. Stepanov Institute of Physics, National Academy of Sciences of Belarus, Minsk; Belarus.
- ¹⁰⁹Research Institute for Nuclear Problems of Byelorussian State University, Minsk; Belarus.
- ¹¹⁰Group of Particle Physics, University of Montreal, Montreal QC; Canada.
- ¹¹¹P.N. Lebedev Physical Institute of the Russian Academy of Sciences, Moscow; Russia.
- ¹¹²National Research Nuclear University MEPhI, Moscow; Russia.
- ¹¹³D.V. Skobeltsyn Institute of Nuclear Physics, M.V. Lomonosov Moscow State University, Moscow; Russia.
- ¹¹⁴Fakultät für Physik, Ludwig-Maximilians-Universität München, München; Germany.
- ¹¹⁵Max-Planck-Institut für Physik (Werner-Heisenberg-Institut), München; Germany.
- ¹¹⁶Nagasaki Institute of Applied Science, Nagasaki; Japan.
- ¹¹⁷Graduate School of Science and Kobayashi-Maskawa Institute, Nagoya University, Nagoya; Japan.
- ¹¹⁸Department of Physics and Astronomy, University of New Mexico, Albuquerque NM; United States of America.
- ¹¹⁹Institute for Mathematics, Astrophysics and Particle Physics, Radboud University Nijmegen/Nikhef, Nijmegen; Netherlands.
- ¹²⁰Nikhef National Institute for Subatomic Physics and University of Amsterdam, Amsterdam; Netherlands.
- ¹²¹Department of Physics, Northern Illinois University, DeKalb IL; United States of America.
- ¹²²(^a)Budker Institute of Nuclear Physics and NSU, SB RAS, Novosibirsk; (^b)Novosibirsk State University Novosibirsk; Russia.
- ¹²³Institute for High Energy Physics of the National Research Centre Kurchatov Institute, Protvino; Russia.
- ¹²⁴Institute for Theoretical and Experimental Physics named by A.I. Alikhanov of National Research Centre "Kurchatov Institute", Moscow; Russia.
- ¹²⁵Department of Physics, New York University, New York NY; United States of America.
- ¹²⁶Ochanomizu University, Otsuka, Bunkyo-ku, Tokyo; Japan.
- ¹²⁷Ohio State University, Columbus OH; United States of America.
- ¹²⁸Faculty of Science, Okayama University, Okayama; Japan.
- ¹²⁹Homer L. Dodge Department of Physics and Astronomy, University of Oklahoma, Norman OK; United States of America.
- ¹³⁰Department of Physics, Oklahoma State University, Stillwater OK; United States of America.
- ¹³¹Palacký University, RCPTM, Joint Laboratory of Optics, Olomouc; Czech Republic.
- ¹³²Institute for Fundamental Science, University of Oregon, Eugene, OR; United States of America.
- ¹³³Graduate School of Science, Osaka University, Osaka; Japan.
- ¹³⁴Department of Physics, University of Oslo, Oslo; Norway.
- ¹³⁵Department of Physics, Oxford University, Oxford; United Kingdom.
- ¹³⁶LPNHE, Sorbonne Université, Université de Paris, CNRS/IN2P3, Paris; France.
- ¹³⁷Department of Physics, University of Pennsylvania, Philadelphia PA; United States of America.
- ¹³⁸Konstantinov Nuclear Physics Institute of National Research Centre "Kurchatov Institute", PNPI, St. Petersburg; Russia.
- ¹³⁹Department of Physics and Astronomy, University of Pittsburgh, Pittsburgh PA; United States of

America.

^{140(a)}Laboratório de Instrumentação e Física Experimental de Partículas - LIP, Lisboa;^(b)Departamento de Física, Faculdade de Ciências, Universidade de Lisboa, Lisboa;^(c)Departamento de Física, Universidade de Coimbra, Coimbra;^(d)Centro de Física Nuclear da Universidade de Lisboa, Lisboa;^(e)Departamento de Física, Universidade do Minho, Braga;^(f)Departamento de Física Teórica y del Cosmos, Universidad de Granada, Granada (Spain);^(g)Dep Física and CEFITEC of Faculdade de Ciências e Tecnologia, Universidade Nova de Lisboa, Caparica;^(h)Instituto Superior Técnico, Universidade de Lisboa, Lisboa; Portugal.

¹⁴¹Institute of Physics of the Czech Academy of Sciences, Prague; Czech Republic.

¹⁴²Czech Technical University in Prague, Prague; Czech Republic.

¹⁴³Charles University, Faculty of Mathematics and Physics, Prague; Czech Republic.

¹⁴⁴Particle Physics Department, Rutherford Appleton Laboratory, Didcot; United Kingdom.

¹⁴⁵IRFU, CEA, Université Paris-Saclay, Gif-sur-Yvette; France.

¹⁴⁶Santa Cruz Institute for Particle Physics, University of California Santa Cruz, Santa Cruz CA; United States of America.

^{147(a)}Departamento de Física, Pontificia Universidad Católica de Chile, Santiago;^(b)Universidad Andres Bello, Department of Physics, Santiago;^(c)Instituto de Alta Investigación, Universidad de Tarapacá;^(d)Departamento de Física, Universidad Técnica Federico Santa María, Valparaíso; Chile.

¹⁴⁸Department of Physics, University of Washington, Seattle WA; United States of America.

¹⁴⁹Department of Physics and Astronomy, University of Sheffield, Sheffield; United Kingdom.

¹⁵⁰Department of Physics, Shinshu University, Nagano; Japan.

¹⁵¹Department Physik, Universität Siegen, Siegen; Germany.

¹⁵²Department of Physics, Simon Fraser University, Burnaby BC; Canada.

¹⁵³SLAC National Accelerator Laboratory, Stanford CA; United States of America.

¹⁵⁴Physics Department, Royal Institute of Technology, Stockholm; Sweden.

¹⁵⁵Departments of Physics and Astronomy, Stony Brook University, Stony Brook NY; United States of America.

¹⁵⁶Department of Physics and Astronomy, University of Sussex, Brighton; United Kingdom.

¹⁵⁷School of Physics, University of Sydney, Sydney; Australia.

¹⁵⁸Institute of Physics, Academia Sinica, Taipei; Taiwan.

^{159(a)}E. Andronikashvili Institute of Physics, Iv. Javakhishvili Tbilisi State University, Tbilisi;^(b)High Energy Physics Institute, Tbilisi State University, Tbilisi; Georgia.

¹⁶⁰Department of Physics, Technion, Israel Institute of Technology, Haifa; Israel.

¹⁶¹Raymond and Beverly Sackler School of Physics and Astronomy, Tel Aviv University, Tel Aviv; Israel.

¹⁶²Department of Physics, Aristotle University of Thessaloniki, Thessaloniki; Greece.

¹⁶³International Center for Elementary Particle Physics and Department of Physics, University of Tokyo, Tokyo; Japan.

¹⁶⁴Graduate School of Science and Technology, Tokyo Metropolitan University, Tokyo; Japan.

¹⁶⁵Department of Physics, Tokyo Institute of Technology, Tokyo; Japan.

¹⁶⁶Tomsk State University, Tomsk; Russia.

¹⁶⁷Department of Physics, University of Toronto, Toronto ON; Canada.

^{168(a)}TRIUMF, Vancouver BC;^(b)Department of Physics and Astronomy, York University, Toronto ON; Canada.

¹⁶⁹Division of Physics and Tomonaga Center for the History of the Universe, Faculty of Pure and Applied Sciences, University of Tsukuba, Tsukuba; Japan.

¹⁷⁰Department of Physics and Astronomy, Tufts University, Medford MA; United States of America.

¹⁷¹Department of Physics and Astronomy, University of California Irvine, Irvine CA; United States of

America.

¹⁷²Department of Physics and Astronomy, University of Uppsala, Uppsala; Sweden.

¹⁷³Department of Physics, University of Illinois, Urbana IL; United States of America.

¹⁷⁴Instituto de Física Corpuscular (IFIC), Centro Mixto Universidad de Valencia - CSIC, Valencia; Spain.

¹⁷⁵Department of Physics, University of British Columbia, Vancouver BC; Canada.

¹⁷⁶Department of Physics and Astronomy, University of Victoria, Victoria BC; Canada.

¹⁷⁷Fakultät für Physik und Astronomie, Julius-Maximilians-Universität Würzburg, Würzburg; Germany.

¹⁷⁸Department of Physics, University of Warwick, Coventry; United Kingdom.

¹⁷⁹Waseda University, Tokyo; Japan.

¹⁸⁰Department of Particle Physics, Weizmann Institute of Science, Rehovot; Israel.

¹⁸¹Department of Physics, University of Wisconsin, Madison WI; United States of America.

¹⁸²Fakultät für Mathematik und Naturwissenschaften, Fachgruppe Physik, Bergische Universität Wuppertal, Wuppertal; Germany.

¹⁸³Department of Physics, Yale University, New Haven CT; United States of America.

¹⁸⁴Yerevan Physics Institute, Yerevan; Armenia.

^a Also at Borough of Manhattan Community College, City University of New York, New York NY; United States of America.

^b Also at Centre for High Performance Computing, CSIR Campus, Rosebank, Cape Town; South Africa.

^c Also at CERN, Geneva; Switzerland.

^d Also at CPPM, Aix-Marseille Université, CNRS/IN2P3, Marseille; France.

^e Also at Département de Physique Nucléaire et Corpusculaire, Université de Genève, Genève; Switzerland.

^f Also at Departament de Física de la Universitat Autònoma de Barcelona, Barcelona; Spain.

^g Also at Departamento de Física, Instituto Superior Técnico, Universidade de Lisboa, Lisboa; Portugal.

^h Also at Department of Applied Physics and Astronomy, University of Sharjah, Sharjah; United Arab Emirates.

ⁱ Also at Department of Financial and Management Engineering, University of the Aegean, Chios; Greece.

^j Also at Department of Physics and Astronomy, Michigan State University, East Lansing MI; United States of America.

^k Also at Department of Physics and Astronomy, University of Louisville, Louisville, KY; United States of America.

^l Also at Department of Physics and Astronomy, University of Sheffield, Sheffield; United Kingdom.

^m Also at Department of Physics, Ben Gurion University of the Negev, Beer Sheva; Israel.

ⁿ Also at Department of Physics, California State University, East Bay; United States of America.

^o Also at Department of Physics, California State University, Fresno; United States of America.

^p Also at Department of Physics, California State University, Sacramento; United States of America.

^q Also at Department of Physics, King's College London, London; United Kingdom.

^r Also at Department of Physics, St. Petersburg State Polytechnical University, St. Petersburg; Russia.

^s Also at Department of Physics, Stanford University, Stanford CA; United States of America.

^t Also at Department of Physics, University of Adelaide, Adelaide; Australia.

^u Also at Department of Physics, University of Fribourg, Fribourg; Switzerland.

^v Also at Department of Physics, University of Michigan, Ann Arbor MI; United States of America.

^w Also at Dipartimento di Matematica, Informatica e Fisica, Università di Udine, Udine; Italy.

^x Also at Faculty of Physics, M.V. Lomonosov Moscow State University, Moscow; Russia.

^y Also at Giresun University, Faculty of Engineering, Giresun; Turkey.

^z Also at Graduate School of Science, Osaka University, Osaka; Japan.

^{aa} Also at Hellenic Open University, Patras; Greece.

- ab* Also at IJCLab, Université Paris-Saclay, CNRS/IN2P3, 91405, Orsay; France.
- ac* Also at Institutio Catalana de Recerca i Estudis Avancats, ICREA, Barcelona; Spain.
- ad* Also at Institut für Experimentalphysik, Universität Hamburg, Hamburg; Germany.
- ae* Also at Institute for Mathematics, Astrophysics and Particle Physics, Radboud University Nijmegen/Nikhef, Nijmegen; Netherlands.
- af* Also at Institute for Nuclear Research and Nuclear Energy (INRNE) of the Bulgarian Academy of Sciences, Sofia; Bulgaria.
- ag* Also at Institute for Particle and Nuclear Physics, Wigner Research Centre for Physics, Budapest; Hungary.
- ah* Also at Institute of High Energy Physics, Chinese Academy of Sciences, Beijing; China.
- ai* Also at Institute of Particle Physics (IPP), Vancouver; Canada.
- aj* Also at Institute of Physics, Academia Sinica, Taipei; Taiwan.
- ak* Also at Institute of Physics, Azerbaijan Academy of Sciences, Baku; Azerbaijan.
- al* Also at Institute of Theoretical Physics, Iliia State University, Tbilisi; Georgia.
- am* Also at Instituto de Fisica Teorica, IFT-UAM/CSIC, Madrid; Spain.
- an* Also at Istanbul University, Dept. of Physics, Istanbul; Turkey.
- ao* Also at Joint Institute for Nuclear Research, Dubna; Russia.
- ap* Also at Louisiana Tech University, Ruston LA; United States of America.
- aq* Also at LPNHE, Sorbonne Université, Université de Paris, CNRS/IN2P3, Paris; France.
- ar* Also at Manhattan College, New York NY; United States of America.
- as* Also at Moscow Institute of Physics and Technology State University, Dolgoprudny; Russia.
- at* Also at National Research Nuclear University MEPhI, Moscow; Russia.
- au* Also at Physics Department, An-Najah National University, Nablus; Palestine.
- av* Also at Physics Dept, University of South Africa, Pretoria; South Africa.
- aw* Also at Physikalisches Institut, Albert-Ludwigs-Universität Freiburg, Freiburg; Germany.
- ax* Also at School of Physics, Sun Yat-sen University, Guangzhou; China.
- ay* Also at The City College of New York, New York NY; United States of America.
- az* Also at The Collaborative Innovation Center of Quantum Matter (CICQM), Beijing; China.
- ba* Also at TRIUMF, Vancouver BC; Canada.
- bb* Also at Università di Napoli Parthenope, Napoli; Italy.
- * Deceased